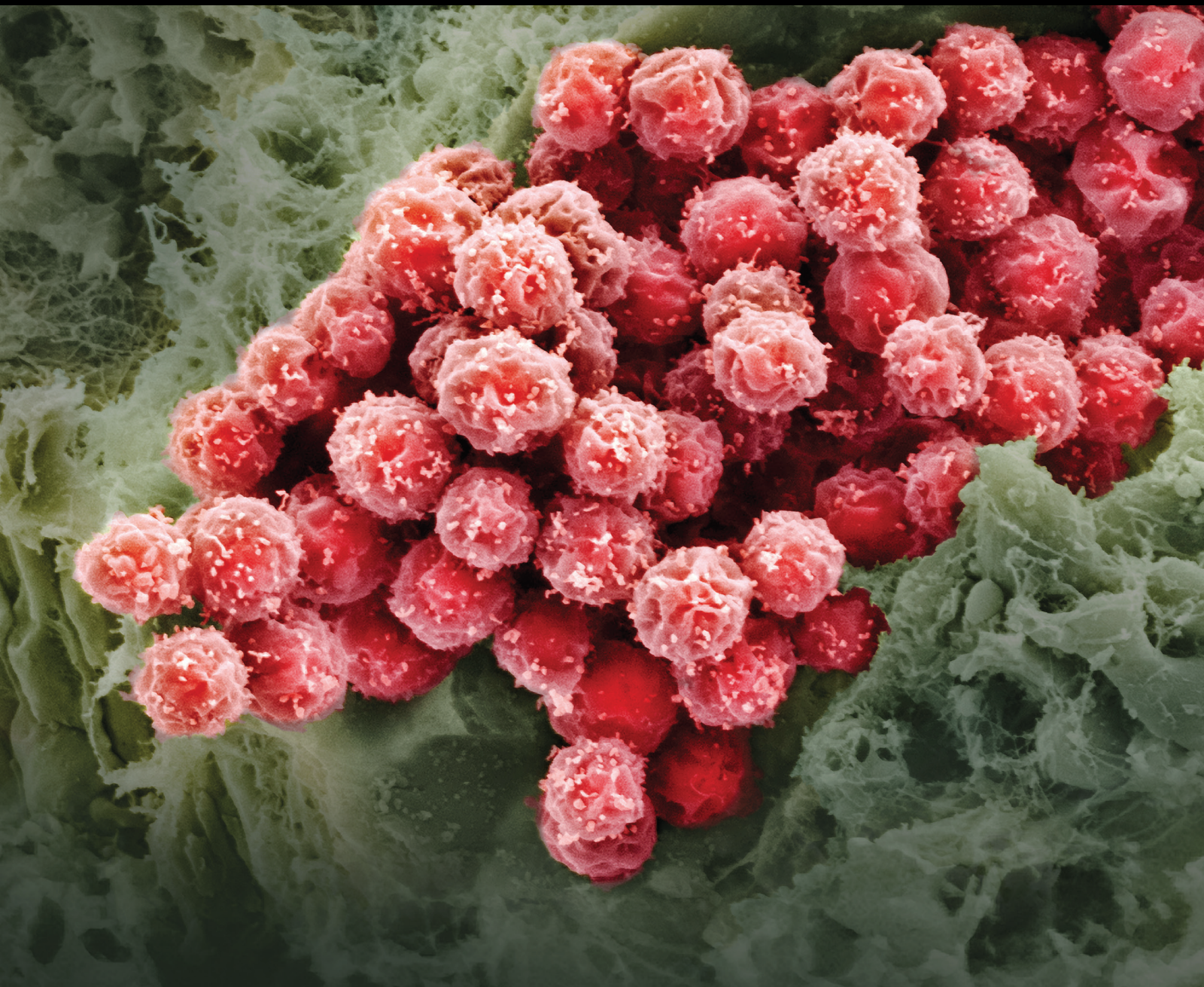


Current Status and Perspectives of Cartilage Regeneration

Lead Guest Editor: Quanyi Guo

Guest Editors: Giampiero La Rocca, Shuyun Liu, Zigang Ge, and Weimin Guo





Current Status and Perspectives of Cartilage Regeneration

Current Status and Perspectives of Cartilage Regeneration

Lead Guest Editor: Quanyi Guo

Guest Editors: Giampiero La Rocca, Shuyun Liu,
Zigang Ge, and Weimin Guo



Copyright © 2022 Hindawi Limited. All rights reserved.

This is a special issue published in “Stem Cells International.” All articles are open access articles distributed under the Creative Commons Attribution License, which permits unrestricted use, distribution, and reproduction in any medium, provided the original work is properly cited.

Chief Editor

Renke Li , Canada

Associate Editors

James Adjaye , Germany
Andrzej Lange, Poland
Tao-Sheng Li , Japan
Heinrich Sauer , Germany
Holm Zaehres , Germany

Academic Editors

Cinzia Allegrucci , United Kingdom
Eckhard U Alt, USA
Francesco Angelini , Italy
James A. Ankrum , USA
Stefan Arnhold , Germany
Marta Baiocchi, Italy
Julie Bejoy , USA
Philippe Bourin , France
Benedetta Bussolati, Italy
Leonora Buzanska , Poland
Stefania Cantore , Italy
Simona Ceccarelli , Italy
Alain Chapel , France
Sumanta Chatterjee, USA
Isotta Chimenti , Italy
Mahmood S. Choudhery , Pakistan
Pier Paolo Claudio , USA
Gerald A. Colvin , USA
Joery De Kock, Belgium
Valdo Jose Dias Da Silva , Brazil
Leonard M. Eisenberg , USA
Alessandro Faroni , United Kingdom
Ji-Dong Fu , USA
Marialucia Gallorini , Italy
Jacob H. Hanna , Israel
David A. Hart , Canada
Zhao Huang , China
Elena A. Jones , United Kingdom
Oswaldo Keith Okamoto , Brazil
Alexander Kleger , Germany
Laura Lasagni , Italy
Shinn-Zong Lin , Taiwan
Zhao-Jun Liu , USA
Valeria Lucchino, Italy
Risheng Ma, USA
Giuseppe Mandraffino , Italy

Katia Mareschi , Italy
Pasquale Marrazzo , Italy
Francesca Megiorni , Italy
Susanna Miettinen , Finland
Claudia Montero-Menei, France
Christian Morszeck, Germany
Patricia Murray , United Kingdom
Federico Mussano , Italy
Mustapha Najimi , Belgium
Norimasa Nakamura , Japan
Karim Nayernia, United Kingdom
Toru Ogasawara , Japan
Paulo J Palma Palma, Portugal
Zhaoji Pan , China
Gianpaolo Papaccio, Italy
Kishore B. S. Pasumarthi , Canada
Manash Paul , USA
Yuriy Petrenko , Czech Republic
Phuc Van Pham, Vietnam
Alessandra Pisciotta , Italy
Bruno P#ault, USA
Liren Qian , China
Md Shaifur Rahman, Bangladesh
Pranela Rameshwar , USA
Syed Shadab Raza Raza , India
Alessandro Rosa , Italy
Subhadeep Roy , India
Antonio Salgado , Portugal
Fermin Sanchez-Guijo , Spain
Arif Siddiqui , Saudi Arabia
Shimon Slavin, Israel
Sieghart Sopper , Austria
Valeria Sorrenti , Italy
Ann Steele, USA
Alexander Storch , Germany
Hirotaka Suga , Japan
Gareth Sullivan , Norway
Masatoshi Suzuki , USA
Daniele Torella , Italy
H M Arif Ullah , USA
Aijun Wang , USA
Darius Widera , United Kingdom
Wasco Wruck , Germany
Takao Yasuhara, Japan
Zhaohui Ye , USA



Shuiqiao Yuan , China
Dunfang Zhang , China
Ludovic Zimmerlin, USA
Ewa K. Zuba-Surma , Poland

Contents

Umbilical Cord Mesenchymal Stromal Cells for Cartilage Regeneration Applications

E. Russo , M. Caprnda , P. Kruzliak , P. G. Conaldi , C. V. Borlongan , and G. La Rocca 
Review Article (23 pages), Article ID 2454168, Volume 2022 (2022)

Characterization and miRNA Profiling of Extracellular Vesicles from Human Osteoarthritic Subchondral Bone Multipotential Stromal Cells (MSCs)

Clara Sanjurjo-Rodríguez , Rachel E. Crossland , Monica Reis , Hemant Pandit , Xiao-nong Wang , and Elena Jones 
Research Article (16 pages), Article ID 7232773, Volume 2021 (2021)

Chondrogenic Potential of Human Dental Pulp Stem Cells Cultured as Microtissues

Rubén Salvador-Clavell , José Javier Martín de Llano , Lara Milián , María Oliver , Manuel Mata , Carmen Carda , and María Sancho-Tello 
Research Article (11 pages), Article ID 7843798, Volume 2021 (2021)

Hydrostatic Pressure Modulates Intervertebral Disc Cell Survival and Extracellular Matrix Homeostasis via Regulating Hippo-YAP/TAZ Pathway

Yiyang Wang , Baoshuai Bai, Yanzhu Hu , Haoming Wang , Ningyuan Liu , Yibo Li , Pei Li , Guangdong Zhou , and Qiang Zhou 
Research Article (17 pages), Article ID 5626487, Volume 2021 (2021)

Review Article

Umbilical Cord Mesenchymal Stromal Cells for Cartilage Regeneration Applications

E. Russo ¹, M. Caprnda ², P. Kruzliak ³, P. G. Conaldi ⁴, C. V. Borlongan ⁵,
and G. La Rocca ¹

¹Section of Histology and Embryology, Department of Biomedicine, Neurosciences and Advanced Diagnostics, University of Palermo, Italy

²1st Department of Internal Medicine, Faculty of Medicine, Comenius University and University Hospital, Bratislava, Slovakia

³2nd Department of Surgery, Faculty of Medicine, Masaryk University and St. Anne's University Hospital, Brno, Czech Republic

⁴Department of Research, IRCCS ISMETT—Mediterranean Institute for Transplantation and Advanced Specialized Therapies, Palermo, Italy

⁵Department of Neurosurgery and Brain Repair, Morsani College of Medicine, University of South Florida, Tampa, FL, USA

Correspondence should be addressed to G. La Rocca; giampylr@hotmail.com

Received 18 June 2021; Revised 13 October 2021; Accepted 23 November 2021; Published 6 January 2022

Academic Editor: Andrea Ballini

Copyright © 2022 E. Russo et al. This is an open access article distributed under the Creative Commons Attribution License, which permits unrestricted use, distribution, and reproduction in any medium, provided the original work is properly cited.

Chondropathies are increasing worldwide, but effective treatments are currently lacking. Mesenchymal stromal cell (MSCs) transplantation represents a promising approach to counteract the degenerative and inflammatory environment characterizing those pathologies, such as osteoarthritis (OA) and rheumatoid arthritis (RA). Umbilical cord- (UC-) MSCs gained increasing interest due to their multilineage differentiation potential, immunomodulatory, and anti-inflammatory properties as well as higher proliferation rates, abundant supply along with no risks for the donor compared to adult MSCs. In addition, UC-MSCs are physiologically adapted to survive in an ischemic and nutrient-poor environment as well as to produce an extracellular matrix (ECM) similar to that of the cartilage. All these characteristics make UC-MSCs a pivotal source for a stem cell-based treatment of chondropathies. In this review, the regenerative potential of UC-MSCs for the treatment of cartilage diseases will be discussed focusing on *in vitro*, *in vivo*, and clinical studies.

1. Introduction

Chondropathies are a group of cartilage diseases that deviate from or interrupt the normal structure and function of cartilage, including osteoarthritis (OA), achondroplasia, spinal disc herniation (SDH), relapsing polychondritis, cartilage tumor (CT), and chondrocalcinosis [1]. There are over 100 types of arthritis. The most common forms are OA (degenerative joint disease) and rheumatoid arthritis (RA, autoimmune form of arthritis). OA is the most well-known chondropathy in the world, affecting the health of 343 million of people, while RA affects 14 million of people [2]. OA is a multifactorial and complex degenerative joint disease characterized by age-related “wear and tear,” chondrocytes’ poor response to growth factors, altered biomechanical properties of articular

cartilage, mitochondrial dysfunction, oxidative stress, and inflammation [3]. The degenerative lesions in cartilage are secondary to inflammation associated with hyperplasia and chondrocyte apoptosis [4]. Increasing age is linked to a reduction in subchondral blood vessels resulting in cartilage-related physiological and biochemical anomalies [5]. This pathological process results in secondary joint fibrosis, stiffness, pain, and decreased function, leading to a poor quality of life. Risk factors for chondropathies include trauma, genetics, age, sex, obesity, and degenerative pathology. The biological mechanisms of chondropathies remain largely unknown, and there is no effective way to treat the cartilage damage because of its nature.

Cartilage is a supportive connective tissue, and it has a dense and highly organized extracellular matrix (ECM) embedding chondrocytes [6]. Three types of cartilage tissue

are present throughout the body at various sites: hyaline, elastic, and fibrocartilaginous. Hyaline cartilage is the predominant form of cartilage and is present on the articular surfaces of synovial joints. Type II collagen is the main component in healthy articular cartilage. Other collagens of cartilage ECM are types III, VI, IX, X, XI, XII, and XIV. The main proteoglycan present in cartilage is aggrecan, but other proteoglycans found in cartilage include the syndecans, glypican, decorin, biglycan, fibromodulin, lumican, epiphygan, and perlecan. The chondrocytes are contained in cavities called lacunae embedded in the network of collagen fibrils and proteoglycans [6].

Cartilage has a decreased ability to self-repair because is avascular, resulting in a poor replicative capacity of chondrocytes. The lack of vascularity, along with the dense packing of ECM components, hinders the transport of drugs in the tissue, thus, challenging the treatments of cartilage diseases. In addition, cartilage also lacks nerve cells or endings and, therefore, cannot directly generate pain that is the main symptom of a chondropathy [7]. Therefore, symptoms usually occur only after the significant structural destruction of the cartilage ECM (with the damage affecting other tissues of the whole joint that do contain nociceptors), thus, making treatments difficult.

Current treatment of articular cartilage defects includes pharmacological management of pain, weight reduction, and exercises as well as intra-articular treatments with corticosteroid or hyaluronan and hylan derivatives injections [8]. Surgical options consist in bone marrow stimulation procedures such as subchondral drilling, microfracture, and abrasion arthroplasty, allowing endogenous mesenchymal stem cells (MSCs) to migrate into the lesion [9]. However, no treatment or procedure represents a cure for cartilaginous defects.

MSC-based therapy is beginning to show great potential in cartilage regeneration through several mechanisms including homing, angiogenesis, differentiation, and response to inflammatory condition. The most widely studied sources of MSCs are bone marrow (BM) and adipose tissue (AT). However, umbilical cord-derived MSCs (UC-MSCs) compared to AT- and BM-MSCs have many advantages such as higher proliferation rates, greater expansion ability, higher purity, and abundant supply along with no risks for the donor, since the UC is usually discarded after birth [10]. In Table 1 are listed the advantages and disadvantages of the different populations of stem/stromal cells used so far for cartilage regeneration purposes. UC-MSCs can be isolated from different regions of the UC stromal tissue called Wharton's Jelly (WJ), and three different populations of UC-MSCs have been obtained: perivascular (PV-MSCs), intermediate WJ (WJ-MSCs), and subamniotic stromal region or cord lining (CL-MSCs) [11]. Notably, ECM components in WJ share several features with cartilage ECM. To this regard, UC-MSCs express aggrecan, type II collagen, and SOX-9 [12]. In addition, UC-MSCs express growth factors, chemokines, and cytokines at similar levels to those of cartilage [12]. Finally, since UC relies on only two arteries and one vein to supply oxygen and nutrients, without any capillary circulation, UC-MSCs are physiologically adapted to survive in a relatively hypoxic environment leading to the potential advantage to survive in cartilage. These

results reinforce the concept of UC-MSCs as one of the best candidates for MSC-based therapy for cartilage regeneration.

2. Regeneration Mechanisms of UC-MSCs for Cartilage Diseases

There are two main concepts for UC-MSCs' contribution to cartilage repair: preventing the degradation of cartilage, through the secretion of bioactive factors, and/or the differentiative potential of UC-MSCs to become chondrocytes. Several *in vitro* and *in vivo* studies indicated that UC-MSCs can play crucial roles in cartilage repair and regeneration by several mechanisms including (i) migration and homing, (ii) adaptation to cartilage hypoxic and nutrient-poor environment, (iii) chondrogenesis differentiation potential and promotion of survival, proliferation and differentiation of endogenous MSCs, (iv) synthesis and prevention of cartilage ECM degradation, and (v) anti-inflammatory and immunomodulatory properties.

2.1. Homing and Migration. MSCs exhibit certain capabilities of the homing of local mature leukocytes to inflammatory sites, such as rolling and adhesion [13]. Migration and homing ability into injured sites are considered as the primary steps for tissue repair in regenerative medicine. Different molecules mediate cell retention or mobilization such as adhesion molecules (E and P-selectin), integrins (particularly $\alpha 4\beta 1$), stromal-derived factor 1 (SDF-1), and its receptor CXCR4 chemokine receptor 4 (CXCR4) [13]. In addition, other factors play a key role in damaged joints homing such as CXCR1 and CXCR2, CC chemokine receptor 1 (CCR1), and monocyte chemoattractant protein 1 (MCP-1) through its receptor CCR2, vascular endothelial growth factor receptor 1 (Flt-1), platelet-derived growth factor receptor α (PDGFR- α , CD140a), PDGFR- β (CD140b), and their respective ligands IL-8, macrophage inflammatory protein 1 α (MIP-1 α), placenta growth factor (PIGF), and PDGF [14]. In Table 2, we reported different proteins involved in homing and migration of UC-MSCs in comparison with those expressed by BM- and AT-MSCs. In particular, BM- and AT-MSCs show similar expression pattern. On the other hand, based on the quantitative data reported in literature, UC-MSCs express higher levels of different proteins than BM- and AT-MSCs such as HGF, IL-8, IL-1RA, IGF-1, ICAM-1, bFGF, MCP-1, MIP-1 β , PDGF-AA, PDGF-AB, PDGF-R, CXCR4, CCR2, VEGF-A, and VEGF-1. Interestingly, unlike cells from BM- and AT-MSCs, UC-MSCs express integrin $\alpha 4$ and MIP-1 β suggesting their strong ability in homing and migration. In addition, UC-MSCs show less hematopoietic effects than BM- and AT-MSCs (low levels of SDF-1 and VCAM-1).

Increased levels of SDF-1, MCP-1, IL-8, MIP-1 α , PIGF, and PDGF were found in synovial fluid of OA and RA patients [14]. Shen et al. demonstrated that UC-MSCs secrete growth factors and chemokines which may contribute to a chemoattractive environment such as SDF-1, MCP-1, hepatocyte growth factor (HGF), vascular cell adhesion protein-1 (VCAM-1), IL-8, insulin-like growth factor-1 (IGF-1), and vascular endothelial growth factor (VEGF) [15]. In addition, UC-MSCs express CXCR4, CCR2, and c-

TABLE 1: Comparative analysis of the advantages and disadvantages of different stem cell populations used for cartilage regeneration.

Source	Advantages	Disadvantages	Ref.
ESCs	Pluripotent Chondrocytes differentiation capacity Synthesis of cartilage ECM	Difficulty of controlling ESCs differentiation Ethical concerns Risk of immune rejection Risk of teratoma formation	[99]
iPSCs	Pluripotent Chondrocytes differentiation capacity Synthesis of cartilage ECM No ethical concerns	Complex and expensive iPSC generation procedures Risk of immune rejection Risk of teratoma formation	[100]
BM-MSCs	Multipotent Chondrocytes differentiation capacity Synthesis of cartilage ECM No ethical concerns Low immunogenicity	Invasive isolation procedure with risk of infection Low isolation yield (about 1×10^5 cells in the BM) Donor age affects initial yield of isolation and the proliferative and differentiation properties Sign of senescence from passage 4	[101]
AT-MSCs	Multipotent Chondrocytes differentiation capacity Synthesis of cartilage ECM No ethical concerns Low immunogenicity Isolation yield 500 times more than BM-MSCs Pluripotent without teratoma formation risk Chondrocytes differentiation capacity Synthesis of cartilage ECM No ethical concerns Low immunogenicity High isolation yield (about 1×10^4 cells from 1 cm of cord) No sign of senescence or abnormality over 16 passages 300 fold expansions reached within 6-7 passages	Invasive isolation procedure with risk of infection Heterogeneity of AT-MSCs extracted from different body sites Sign of senescence from passage 8	[101]
UC-MSCs	Multipotent High chondrogenic potential Multipotent Higher chondrogenic potential than BM-MSCs Higher colony-forming potential and proliferation rate than BM- and AT-MSCs	Limited knowledge about the UC-MSCs populations	[102]
IPFSCs	Multipotent High chondrogenic potential	Limited source of tissue (7.5 million cells from 5 g of tissue)	[103]
SD-MSCs	Multipotent Higher chondrogenic potential than BM-MSCs Higher colony-forming potential and proliferation rate than BM- and AT-MSCs	Limited source of tissue (knee: $10.5 \pm 8.1 \times 10^3$ cells/mg; hip: $3.1 \pm 2.2 \times 10^3$ cells/mg)	[104]

AT-MSCs: adipose tissue-derived mesenchymal stem cells (MSCs); BM-MSCs: bone marrow-derived MSCs; ESCs: embryonic stem cells; IPFSCs: infrapatellar fat pad-derived stem cells; iPSCs: induced pluripotent stem cells; UC-MSCs: umbilical cord-derived MSCs; SD-MSCs: synovium-derived MSCs.

TABLE 2: Expression analysis of different markers involved in homing and migration.

Marker	UC-MSCs	BM-MSCs	AT-MSCs	Ref.
Secreted factors				
COX-2	↑	↓	↓	[45]
bFGF (FGF-2)	↑↑	↓	↑	[45]
HGF	↑↑	↓	↓↓	[45, 105]
IGF-1	↑	↓	↓	[54]
IL-1 α	↑↑	↓	ND	[54]
IL-1?	↑↑	↓	↑	[54, 105, 106]
IL-6	↑	↓	↓	[105]
	↔	↔	↔	[45]
IL-8	↑	↓	↓	[105]
IL-1RA	↑	↓	↓	[105]
MCP-1 (CCL2)	↑	↓	↓	[45, 105]
	↔	↔	↔	[45]
MIP-1 α (CCL3)	↓	↑	+	[107, 108]
MIP-1? (CCL4)	+	-	-	[105]
OPN	↓	↑	↓	[109]
PDGF-AA	↑	↓	↓	[105, 107]
PDGF-AB	↑	↓	-	[107, 110]
PDGF-BB	-	↓	-	[105]
PGE2	↓	↓	↓	[106]
PIGF	↓	↓↓	↑	[105]
SDF-1	↑	↑	↓	[111, 112]
SDF-1 α	↔	↔	↔	[45]
TGF- β 1	↔	↔	↔	[105]
TGF- β 2	↑	↓	↓	[105]
VEGF-A	↑	↓	↓	[45]
VEGF-D	↑	↓	↓	[105, 107]
MMPs and TIMPS				
MMP-1	↑	↓	↑↑	[105]
MMP-2	↔	↑	↔	[113]
MMP-3	↓	↓	↑	[105]
MMP-7	↓	↑	-	[105]
MMP-8	-	↑	-	[105]
MMP-13	-	-	+	[105]
TIMP-1	↔	↔	↔	[113]
TIMP-2	↔	↔	↔	[113]
Adhesion molecules and receptors				
CCR2	↑	↓	↓	[54]
CXCR4	↑	↓	↓	[114]
Flt-1 (VEGFR1)	↑	↓	ND	[54]
ICAM-1	↑↑	↓	↑	[45]
Integrin α 4	↑↑	↓	-	[54]
PDGF-Ra	↔	↔		[107]
PDGF-Rb	↑	↓	↓	[107]
VCAM-1	↓	↑	↓	[45]
Immunoregulatory molecules				
B7-H3 (CD276)	+	+	+	[71]
CD200	↑	↓	↓↓	[54, 115]

TABLE 2: Continued.

Marker	UC-MSCs	BM-MSCs	AT-MSCs	Ref.
Galectin 1	↑	↑	↓	[113]
HLA-ABC	↔	↔	↔	[54, 116]
HLA-DR	↔	↔	↔	[54, 116]
HLA-G	↑	↓	↓	[54, 116]
HLA-E	↑	↓	↓	[54, 117]
HLA-F	↑	↓	-	[54, 117]
IDO	↔	↔	↔	[45]
	↑↑	↑	ND	[118]
IP-10	↑	↓	↓	[105]
LIF	↑	↓	↓	[54, 113]
PD-L1 (B7-H1)	↑	↓	+	[54, 119]
PD-L2 (B7-DC/CD273)	↑	↓	+	[54, 119]
RANTES (CCL5)	↑	↓	↓	[105]
TLR-1	↔	↔	↔	[106]
TLR-2	↔	↔	↔	[106]
TLR-3	↔	↔	↔	[106]
TLR-4	-	↔	↔	[106]
TLR-5	↔	↔	↔	[106]
TLR-6	↔	↔	↔	[106]
TLR-9	↔	↔	↔	[106]

Expression: ↑: higher; ↑↑: significantly higher; ↓: lower; ↓↓: significantly lower; ↔: similar; +: qualitatively expressed, but not quantified; -: not expressed; ND: not detected.

met receptors. Therefore, UC-MSCs are able to migrate *in vitro* and *in vivo* via the SDF-1/CXCR4 and MCP-1/CCR2 axes, and the secreted factors may induce the recruitment of cells from the surrounding tissues and promote regeneration of injured tissue [15]. To this regard, the SDF-1/CXCR4 axis has been shown to play a key role in endogenous and transplanted stem cell homing in the injured site promoting the regeneration of different tissues including cartilage [16, 17].

Another key player in cell adhesion is integrin $\alpha 4\beta 1$ (very late antigen-4, VLA-4). It has been demonstrated a crucial link between the CXCR4/SDF-1 homing axis and the VLA-4/VCAM-1 (vascular cell adhesion molecule-1, CD106) adhesion axis [18]. In particular, SDF-1 (through CXCR4) increases VLA-4 adhesion to VCAM-1. VLA-4 is an integrin dimer composed of $\alpha 4$ (CD49d) and $\beta 1$ (CD29) [19]. Although MSCs lack the expression of selectins, they express integrin $\beta 1$. Interestingly, in contrast to BM-MSCs, UC-MSCs express integrin $\alpha 4$, VCAM-1, and intercellular adhesion molecule-1 (ICAM-1; CD54) supporting their stronger potential in homing [20].

One more ligand of integrin $\beta 1$ is osteopontin (OPN), an osteogenic marker with several biological functions including migration, adhesion, and survival of MSCs [21]. On the other hand, OPN is also involved in regulation and propagation of inflammatory responses of macrophages, T-cells, and dendritic cells [22]. Notably, OPN is involved in different inflammatory pathologies including RA and OA pathogenesis [23, 24]. In a study of Schneider et al., UC-MSCs showed similar osteogenic and migration abilities compared

to BM-MSCs with the lesser expression of OPN and the major expression of matrix metalloproteinases (MMP)-1 and -2 [25].

Moreover, extensive evidence found that growth factors play an important role in homing and migration of MSCs, as seen for basic fibroblast growth factor (bFGF), VEGF, HGF, IGF-1, PDGF, and transforming growth factor $\beta 1$ (TGF- $\beta 1$) [26]. In particular, UC-MSCs are able to migrate *in vitro* and *in vivo*, in response to chemotactic factors such as EGF, FGF-2, HGF, IGF-1, PDGF-BB, TGF- β , and VEGF, along with SDF-1, MCP-1, and VCAM-1 [15].

2.2. Capacity of Adaptation to Cartilage Hypoxic Environment.

Because of the lack of vascularization, the physiological oxygen tension (physioxia) within human articular cartilage ranges between 2 and 5% [27]. Therefore, any MSC candidate for stem cell therapy of cartilage diseases should be able to adapt to a hypoxic environment with limited nutrient supply while maintaining its regenerative properties. Oxygen tension ranges from 1%-7% in bone marrow and from 10%-15% in adipose tissue [28, 29]. Regarding perinatal tissues such as the UC, oxygen tension within the mammalian female reproductive tract is low, between 1.5% and 8%, and lasts throughout the fetal development with dissolved oxygen in the fetal circulation rarely exceeding 5% [30]. Moreover, the UC is supplied by only two arteries and one vein and lacking in capillaries or lymphatics suggesting that UC-MSCs are physiologically adapted to survive in a hypoxic environment. It has been shown that low oxygen tension increases UC-MSC proliferation potential and matrix production and enhanced

chondrogenic marker expression in UC-MSCs [31, 32]. This increased chondrogenic differentiation can lead to hypoxia-inducible factor-1 alpha (HIF-1 α) and HIF-2 α increased expression, NOTCH signaling activation, and the subsequent Sox-9 induction [33]. In addition, the UC-MSCs cultured under hypoxic conditions showed increased expression of energy metabolism-associated genes including GLUT-1, LDH, and PDK1 suggesting a switching of cell metabolism from oxidative phosphorylation to anaerobic glycolysis [32]. The yield of lactate production from glucose, however, is significantly lower in UC-MSCs than it has been reported in BM- and AT-MSCs in both hypoxic and normoxic conditions [32]. This finding could be explained by our recent study [34]. We demonstrated that all the three UC-MSC populations (PV-, WJ-, and CL-MSCs) exhibit low levels of mitochondrial and glycolytic activities. Moreover, PV-, WJ-, and CL-MSCs showed comparable mitochondrial respiration parameters in both normal and oxygen and glucose deprivation followed by reperfusion (OGD/R) conditions maintaining their proliferation capacity. Interestingly, PV-MSCs showed the highest oxygen consumption rate and OGD/R affected their metabolism but not their viability suggesting a superior mitochondrial activity compared to the other UC-MSC populations. While CL-MSCs were the cells least affected suggesting their robust survival in ischemic environment. These evidences taken together suggest that UC-MSCs may be a pivotal source for stem cell-based therapy of ischemic pathologies including chondropathies, brain, heart, and lung diseases [35–38]. Further investigations are needed to better understand whether these slight but significant differences among the three UC-MSCs are due to the specific region's composition of different number of healthy mitochondria or improved adaptation of mitochondria to ischemic conditions.

2.3. Promotion of Survival, Proliferation, and Differentiation.

MSCs secrete growth factors that are involved in several biological processes such as homing and migration as well as promotion of survival, proliferation, and differentiation. Some of growth factors with a key role in cartilage repair are bone morphogenetic proteins (BMPs), epidermal growth factor (EGF), HGF, IGF, PDGF, VEGF, FGF, and TGF families and UC-MSCs are a rich source of them [39].

EGF is one of the ligands of EGF receptor (EGFR) that plays a key role in joint homeostasis. In particular, EGFR stimulates chondrocyte proliferation and survival as well as maintenance of cartilage in adulthood. On one hand, EGFR signaling promotes the lubrication of the articular surface by increasing the boundary lubricants Prg4 and HA from superficial chondrocytes [40]. On the other hand, EGFR signaling also can play a catabolic action by inhibiting the expression of the chondrogenic master transcription factor Sox9, thereby suppressing the synthesis of cartilage matrix proteins, such as type II collagen (Col II) and aggrecan, as well as by stimulating the expression of MMPs involved in cartilage degradation, such as MMP-13 [41]. Interestingly, Zhang et al. recently showed the UC-MSCs release EGFR ligands TGF- α and EGF attenuating OA progression via EGFR signaling pathway of cartilage superficial layer cells [42]. In addition, UC-MSCs inhibited the apoptosis of chondrocytes, increased the expres-

sion of chondrogenesis-related genes (Col-2, Sox9), and reduced the expression of cartilage catabolism-related genes (MMP-13, ADAMTS-5) *in vitro* and *in vivo* [42].

HGF is a multifunctional growth factor that affects cell survival and proliferation, matrix metabolism, inflammatory response, and neurotrophic action playing an important role in normal bone and cartilage turnover [43]. In particular, HGF and VEGF can reduce tissue injury, inhibit fibrotic remodeling and apoptosis, promote angiogenesis, stimulate stem cell recruitment and proliferation, and reduce oxidative stress [44]. A recent comparative study showed that the secretion of HGF was three times higher in UC-MSCs compared to AT-MSCs and around nine times higher than in BM-MSCs [45]. In contrast, UC-MSCs secreted the lower levels of VEGF-A. This is probably due to the fact that VEGF-A and HGF signaling pathways reciprocally modulate each other [46].

IGF1 has been implicated in promotion of chondrogenesis and accumulation of cartilage-specific ECM molecules [47]. In addition, the synergy between TGF- β 3 and IGF-1 promotes intervertebral disc regeneration [48]. WJ contains large amounts of IGF-I and IGF-I-binding proteins BP-3 and BP-1 suggesting a key role in stimulation of UC-MSCs to produce collagen and glycosaminoglycans (GAGs) in UC matrix as well as influencing the chondrogenic differentiation of these cells [49, 50].

TGF- β superfamily consists of about 30–35 different proteins including TGF- β proteins (TGF- β 1- β 2- β 3), Bone Morphogenetic Proteins (BMPs), and Growth Differentiation Factors (GDFs) involved in chondrogenic differentiation and production of cartilage extracellular matrix as well as stimulation of cartilage repair [51]. TGF- β 1, - β 2, and - β 3 play key roles in regulation of chondrocyte differentiation from early to terminal stages, including condensation, proliferation, terminal differentiation, and ECM synthesis as well as maintenance of articular chondrocytes [52]. All the three isoforms are expressed in mesenchymal condensations and secreted by UC-MSCs [53–55]. BMPs play important roles in bone and cartilage formation, including various aspects of embryonic development, such as skeletogenesis, and hematopoietic and epithelial cell differentiation [56]. Moreover, BMPs can induce protection against cartilage damage caused by inflammation or trauma, as well as stimulation of regenerative processes. BMPs are classified into subfamilies, including BMP subfamily (from BMP1 to BMP15), the osteogenic protein (OP) subfamily (OP1, OP2, and OP3 also known as BMP7, BMP8, and BMP8b, respectively), the GDF subfamily (GDF1, GDF2/BMP9, GDF3, GDF5/BMP14, GDF6/BMP13, GDF7/BMP12, GDF8, GDF9, GDF10, and GDF11/BMP11), and the cartilage-derived morphogenetic proteins (CDMP1/BMP14 and CDMP2/BMP13) [56]. BMP2, 4, 6, 7, and 9 have been reported to induce *in vitro* chondrogenesis of human MSCs [57]. UC-MSCs have been demonstrated to secrete BMP2 *in vitro* and to induce the increase of endogenous BMP4, 5, and 7 levels *in vivo* [58–60]. In addition, UC-MSCs induce overexpression of GDF5/BMP14/CDMP1, promoting chondrogenic differentiation in cocultures with fibroblast-like synoviocytes, thus, suggesting their potential in cartilage repair [61]. Moreover, UC-MSCs respond to

BMP6 via decapentaplegic homolog (SMAD) signaling (SMAD 1/4/5, BMPRI1A, and BMPRII2 receptors) enhancing osteogenic differentiation [62]. In particular, BMP-2 stimulates osteogenesis as well as matrix synthesis, promoting cartilage repair (by upregulation of tissue inhibitors of metalloproteinases-1, TIMP-1) and reversing chondrocyte dedifferentiation [63]. BMP-7 promotes cartilage matrix synthesis by acting synergistically with other anabolic growth factors and also inhibits catabolic factors, such as matrix metalloproteinase-1 (MMP-1), MMP-13, IL-1, IL-6, and IL-8 [64].

2.4. Cartilage Extracellular Matrix Repair. UC-MSCs can increase the ECM synthesis and inhibit the cartilage ECM destruction supporting the tissue repair. UC stromal tissue shares a number of features with cartilage ECM: UC-MSCs are able to synthesize aggrecan, type II collagen, and express SOX-9 transcription factor [12]. The deposition of ECM molecules and regulation of MMPs and their inhibitors (TIMPs) are the main mechanisms involved in cartilage ECM synthesis. MSCs secrete high levels of TIMP-1 and TIMP-2, which inhibit MMP-9 and MMP-2, respectively, thus, suppressing cartilage ECM resorption [65]. UC-MSCs secrete MMP-2, -8, -9, and -13 as well as TIMP-1 and TIMP-2 suggesting a balance between protection of ECM and antifibrotic activity (Table 2) [66–68]. In addition, UC-MSCs secrete growth factors such as HGF, IGF-1, and TGF- β superfamily members that stimulate cartilage ECM synthesis. In particular, HGF has been involved in inhibition of the fibrosis and apoptosis of chondrocytes and increase ECM synthesis [65]. IGF-I and IGF-I-BP-3 and -BP-1 stimulate UC-MSCs to produce collagen and glycosaminoglycans (GAGs) [49]. BMP-2 increases TIMP-1 expression while BMP-7 inhibits MMP-1 and MMP-13 suppressing the ECM degradation [63, 64].

2.5. Anti-Inflammatory and Immunomodulatory Properties. The microenvironment of damaged articular cartilage is particularly challenging, due to hypoxia, insufficient blood supply, and concurrent inflammation. The latter contributes to the degeneration of the joints because it hampers the proliferation of chondrocytes and the deposition of cartilage matrix, resulting in low efficiency of repair. Immunomodulatory and anti-inflammatory properties of UC-MSCs have been widely described (Table 2) [69]. In particular, UC-MSCs express MHC class I (HLA-ABC) at low levels and lack MHC class II (HLA-DR, -DP, and -DQ). Moreover, they express other molecules belonging to noncanonical type I MHC such as HLA-G, HLA-E, and HLA-F [70–72]. Interestingly, HLA-G interacts with Ig-like transcript (ILT) receptors (ILT-2, ILT-3, and ILT-4), which are expressed by T and B lymphocytes, as well as natural killer (NK) cells and mononuclear phagocytes [69]. Through this interaction, HLA-G displays relevant immune functions which physiologically contribute to maternal-fetal immunotolerance. In addition, UC-MSCs lack CD40/CD40L, CD80, CD86, and B7 costimulatory antigens implicated in the activation of T and B cell responses and express coinhibitory molecules including B7-H3/CD276, CD73, Indolamine 2,3-dioxygenase-1 (IDO-1), Galectin-1 (Gal-1), and leukemia inhibitory factor (LIF) [73]. WJ-MSCs

showed an immunosuppressive function by inhibiting the proliferative response of T helper cells (Th/CD4+) Type 1 (Th1) and Th17 and increasing Th2 and regulatory T cells (Tregs) [74]. UC-MSCs have been shown to be able to suppress the proliferation of both CD4 and CD8 cytotoxic T lymphocytes (Tc) and to decrease proinflammatory IFN- γ in activated peripheral blood mononuclear cells (PBMCs) [54, 75]. Moreover, secreted factors such as HGF and TGF- β 1 may function as mediators for T cell suppression [76, 77]. UC-MSCs are also able to inhibit B-cells and natural killer (NK) cell proliferation as well as regulate monocyte/macrophage system by reducing the infiltration of macrophages in injured tissues and shifting macrophages toward a M2 anti-inflammatory phenotype [78, 79].

In the synovia of OA patients, various immune cells have been identified including M1 macrophages, T cells Th1, Th17 and Tc, and B cells, leading to chronic inflammation, exacerbation of arthritis, and tissue damage [80]. UC-MSCs have been shown to reduce synovial inflammatory cells infiltration, such as CD4+ T cells and macrophages, as well as significantly decrease the expression of interleukin- (IL-) 1 β and tumor necrosis factor- α (TNF- α), while increasing anti-inflammatory factors TNF- α -induced protein 6 (TSG-6) and IL-1 receptor antagonist (IL-1RA) in rat OA models induced by monosodium iodoacetate (MIA) [81, 82]. In another study of MIA-induced OA in rabbits, UC-MSCs showed a prominent cartilage protective effect due to upregulation of growth factors FGF-2, TGF- β 1, and IGF-1, secretion of ECM molecules (collagen type-I alpha-1 chain, collagen type-II alpha-1 chain, and aggrecan), reduction of the expression levels of pro-inflammatory cytokines Tnf- α , IL-1 β , IL-6, and IL-17, and increase of anti-inflammatory cytokines TGF- β 1, IL-10, and IL-1RA [83]. Interestingly, our group and others showed that UC-MSCs keep their hypoimmunogenic and immunomodulatory properties even when they had undergone *in vitro* chondrocyte differentiation [50, 84].

RA is a chronic inflammatory autoimmune disease characterized by chronic proliferation of synovial cells and progressive joint damage [85]. Fibroblast-like synoviocytes (FLS) play an important role in thickening of the synovium determining arthritis and cartilage degradation as well as inflammation and degradation of the joints. UC-MSCs inhibit Cadherin 11 expression in RA FLS by secreting IL-10. This event precludes the ability of FLS from RA patients to migrate and erode cartilage of other joints, thereby improving arthritis [86].

3. Preclinical and Clinical Studies of UC-MSCs for the Treatment of Cartilaginous Diseases

Thanks to their chondrogenic potential and immunomodulatory and anti-inflammatory properties, as well as their ability to promote endogenous repair mechanisms, UC-MSCs have been regarded as potential therapeutic agents against cartilage degradation. In particular, early evidences that emerged from *in vitro* studies on cell cultures (summarized in Table 3) have been confirmed in several *in vivo* animal

TABLE 3: In vitro studies of UC-MSCs or their secretome.

Study type	Source	Aim	Culture system	Results	Ref.
	Human UC-MSCs	UC- and AT-MSC comparison	Cultured in CM supplemented with TGF β 3 and BMP-6	A more fibrous than hyaline cartilage phenotype in UC-MSCs compared to AT-MSCs	Hildner et al., 2010 [87]
	Human WJ-MSCs	Differentiation into NP-like cells	Coculture with NPCs	Increased expression of aggrecan, collagen II, and SRY-type HMG box-9 genes	Ruan et al., 2012 [88]
	Human UC-MSCs	Differentiation into NP-like cells	Cultured in a laminin-rich pseudo-3D culture system	GAGs, collagen II, laminin α 5, and laminin receptors (integrin α 3 and β 4) expression	Chon et al., 2013 [89]
	Human WJ-MSCs	Immunomodulatory properties test	Cultured in CM	Differentiated WJ-MSCs maintain their immune privilege	La Rocca et al., 2013 [50]
	Human UC-MSCs	Elastic cartilage differentiation	Seeded on PLGA nanofiber scaffolds with CM and CTGF	Increase of GAG/DNA ratio, collagen II, elastin mRNA and protein. No difference in collagen X or fibrillin mRNA	Caballero et al., 2013 [90]
	Human UC-MSCs	Tissue-engineered (TE) elastic cartilage from UC-MSCs and human cartilage comparison	Seeded onto PLGA nanofiber scaffolds with CM supplemented with CTGF	TE elastic cartilage from UC-MSCs expresses embryonic fibrillin III and similar levels of elastin, fibrillin I, collagens I and X when compared to native cartilage.	Pappa et al., 2014 [120]
Chondrogenic differentiation	Human and porcine UC-MSCs	Effects of periodic vibratory stimulus on UC-MSC differentiation	Cultured in chondrogenic or osteogenic medium and exposed to 1 or 100 Hz frequency vibrations	1 Hz stimulation resulted in a cartilage phenotype while 100 Hz stimulation resulted in a bone phenotype for both human and porcine UC-MSCs	Cashion et al. 2014 [121]
	Human UC-MSCs	UC-, BM-, and AT-MSC chondrogenesis comparison	Cultured in CM	Slightly differences in chondrogenesis between the MSCs. BM-MSCs showed the best chondrogenic potential	Danišović et al., 2016 [92]
	Human UC-MSCs	Effect of mechanical compression on UC-MSC chondrogenesis	Seeded in PVA-PCL scaffold with CM and subjected to dynamic compression	Increase in chondrogenic differentiation	Remya et al., 2016 [122]
	Human WJ-MSCs	Simulation of the articular cartilage microenvironment	Coculture of WJ-MSCs and primary ACs in ACECM- oriented scaffold	Chondrogenic differentiation of WJ-MSCs without any inducer, hyaline cartilage phenotype, and improved cytoactivity of ACs	Zhang et al., 2019a [96]
	Human UC-MSCs	Interactions between ACs and UC-MSCs.	Coculture with direct cell-cell contact	Enhanced differentiation of UC-MSCs and reduced dedifferentiation of chondrocytes	Li et al., 2019 [97]
	WJ-MSCs	Immunomodulatory properties test	Chondrogenic differentiation in Alg/HA scaffold	Differentiated WJ-MSCs inhibit T cell alloproliferation and maintain paracrine activity and functional immunomodulation	Voisin et al., 2020 [84]
Cartilage tissue engineering	Human UC-MSCs	PGA and PLLA scaffolds comparison	Seeded on nonwoven PGA or PLLA scaffolds in CM	Similar chondrogenic potential of UC-MSCs in PLLA and PGA scaffolds.	Zhao et al., 2010 [123]

TABLE 3: Continued.

Study type	Source	Aim	Culture system	Results	Ref.
	Human WJ-MSCs	WJ- and BM-MSCs chondrogenesis comparison	Seeded in PCL/Coll nanofibrous scaffolds in CM	Enhanced cell attachment, proliferation, and chondrogenesis of WJ-MSCs over BM-MSCs	Fong et al., 2012 [124]
	Human UC-MSCs	Chondrogenic differentiation	Embedded in collagen hydrogel scaffold with CM	Increased expressions of collagen II, aggrecan, COMP, and sox9	Chen et al., 2013 [125]
	Human UC-MSCs	Chondrogenic differentiation in PVA-PCL scaffolds	Seeded in PVA-PCL scaffolds with individual TGF β 1, TGF β 3, IGF, BMP2 and their combination with BMP2	SOX9, collagen II and aggrecan expression. The combination TGF- β 3 and BMP-2 was the more effective for chondrogenesis	Nirmal et al., 2013 [126]
	Human WJ-MSCs	Fabrication of a nonscaffold tissue-engineered cartilage	Pellet culture combined with RCCS	RCCS formed larger and denser cartilage-like tissue enriched of GAGs and collagen II than pellet culture	Liu et al., 2014 [12]
	Human WJ-MSCs	WJ- and BM-MSCs chondrogenesis in agarose hydrogel	Encapsulation of WJ-MSCs or BM-MSCs aggregates in agarose hydrogels	Both BM-MSCs and WJ-MSCs did better in matrix biosynthesis and chondrogenesis when in aggregates than in free cell suspension	Sridharan et al., 2015 [127]
	Human UC-MSCs	Chondrogenic differentiation in SF/HA scaffold	Seeded in different ratios of SF/HA with CM	Expression of collagen II, aggrecan, and Sox9. SF80 and SF70 scaffolds are the best for chondrogenesis	Jaipaw et al., 2016 [128]
	Human WJ-MSCs	Chondrogenesis of WJ-MSCs in PLLA-collagen nanofibers scaffold	Seeded on PLLA-collagen nanofibers scaffold with CM	PLLA-collagen nanofibers scaffold promotes the chondrogenic differentiation of WJ-MSCs	Wang et al., 2017 [129]
	Human WJ-MSCs	Chondrogenesis of WJ-MSCs in hyaluronic acid-based hydrogels	Seeded in hyaluronic acid-based hydrogels with CM	Increase of GAGs, collagen II and aggrecan,	Aleksander-Konert et al., 2016 [130]
	Human UC-MSC-ECM	Effect of decellularized UC-MSC-ECM on ACs	ACs seeded in culture plates coated with UC-MSC-ECM	Promotion of the proliferation and differentiation of chondrocytes	Zhang et al., 2019b [131]
Fibrocartilage tissue engineering	Human UC-MSCs	UC- and BM-MSCs chondrogenesis comparison	Seeded onto PGA scaffolds in chondrogenic medium	More GAGs, collagen I, and aggrecan and less collagen II in UC-MSCs than BM-MSCs	Wang et al., 2009a [132]
	Human UC-MSCs	Best density for UC-MSCs chondrogenesis	Seeded on nonwoven PGA scaffold in CM	More collagen I and II, aggrecan, GAGs, and mechanical integrity in high-density groups	Wang et al., 2009b [133]
Osteochondral tissue engineering	Human UC-MSCs	Chondrogenic and osteogenic differentiation	Seeded between chondrogenic and osteogenic PLLA constructs	Both chondrogenic and osteogenic differentiation of UC-MSCs in the respective sides of constructs	Wang et al., 2011 [134]
	Human UC-MSCs	Chondrogenic and osteogenic differentiation	Seeded in osteogenic scaffold and in Collagen I and III- or HA-based chondrogenic scaffolds in normoxic or hypoxic (8% O ₂) conditions.	Both chondrogenic and osteogenic differentiation of UC-MSCs. Hypoxia improved the expression of these chondrogenic markers	Marmotti et al., 2017 [31]

TABLE 3: Continued.

Study type	Source	Aim	Culture system	Results	Ref.
Orthopaedic tissue engineering	Human UC-MSCs	Multilineage differentiation	Cultured in adipogenic, osteogenic, chondrogenic, or myogenic medium	Multilineage differentiation potential toward bone, fat, cartilage, and muscle	Marmotti et al., 2012 [91]
	Human UC-MSCs	UC- and D-NP-MSCs comparison	Cultured with CM	D-NP-MSCs expressed lower expression levels of CD29 and CD105, reduced proliferation capability and differentiation potentials	Wu et al., 2017 [93]
	Human WJ-MSCs	Interactions between WJ-MSCs and degenerative NPCs	Coculture with or without direct cell-cell contact	NP-like cell differentiation of WJ-MSCs and biological status of degenerative NPCs restoration. The direct cell-cell contact yielded more favorable gene expressions	Han et al., 2018 [98]
IVD degeneration	Human UC-MSCs secretome	UC-MSC-conditioned medium (CM) effect on damaged NP-MSCs	Treatment of high glucose-induced degradation of NP-MSCs with UC-MSCs-CM	Reduction of apoptosis and ECM degradation via the p38 MAPK pathway	Qi 2019 et al., 2019 [135]
	Human UC-MSCs-ECM	Effect of UC-MSCs-ECM on IVD cells	IVD cells seeded on decellularized UC-MSCs-ECM	UC-MSCs-ECM improved the degenerated phenotype of human IVD cells affecting the expression of Sox2, Sox 9 and TRPS1	Penolazzi et al., 2020 [136]
OA	Human UC-MSCs secretome	Comparison of articular cartilage (AC), Hoffa's fat pad (HFP), synovial membrane (SM), and UC-MSC secretomes	Secretome analysis by mass spectrometry and effect on AC chondrogenesis and immunosuppressive and anti-inflammatory effects on PBMCs and macrophages	UC-MSCs-CM displayed superior anti-inflammatory, immunomodulatory and trophic effects compared to adult MSCs	Islam et al., 2019 [95]
RA	Human UC-MSCs	UC-MSCs effect on FLS	Coculture	Increase of FLS apoptosis, collagen II, and aggrecan; decrease of IL-1 β , IL-6 and CCL-2	Zeng et al., 2016 [61]
TMJ disorders	Human UC-MSCs	UC-MSCs and TMJ condylar chondrocytes comparison	Seeded in PGA scaffolds in CM	More collagen I and II, GAGs, and cellular density in UC-MSCs than TMJ construct	Bailey et al., 2007 [94]

AC: articular cartilage cells; ACECM: acellular cartilage extracellular matrix; Alg/HA: alginate enriched in hyaluronic acid; CTGF: connective tissue growth factor; CM: chondrogenic medium; D-NP-MSCs: NP stem/progenitor cells isolated from degenerated IVD; ECM: extracellular matrix; FLS: fibroblast-like synoviocytes; GAGs: glycosaminoglycans; n.a.: not applicable; IVD: intervertebral disc; NP: nucleus pulposus; NPCs: nucleus pulposus cells; OA: osteoarthritis; PCL/Coll: polycaprolactone/collagen; PGA: polyglycolic acid; PLGA: poly L-lactide/D-lactide/glycolide; PLLA: poly L-lactic acid; PMEF: pulsed electromagnetic field; PVA-PCL: polyvinyl alcohol-polycaprolactone; RA: rheumatoid arthritis; RCCS: rotary cell-culture system; SF/HA: silk fibroin/hyaluronic acid; TMJ: temporomandibular joint.

TABLE 4: In vivo studies of cartilage repair with UC-MSCs or their secretome.

Pathology	Source	Host	Study design	Results	Ref.
IVD degeneration	Human UC-MSCs	Rabbit	1×10^5 UC-MSCs injected into degenerated IVD	Increase in cellularity and a relative preservation of architecture	Leckie et al., 2013 [137]
	Human UC-MSCs	Rabbit	1×10^6 UC-MSCs or 1×10^6 UC-MSC-derived CPCs injected into degenerated IVD	Improvement in the histology, cellularity, ECM proteins, water, and GAGs contents and higher expression of NP specific markers SOX9, ACAN, COL2, FOXF1, and KRT19 with CPCs	Beeravolu et al., 2018 [138]
	Human UC-MSCs	Rabbit	1×10^6 UC-MSC-derived NPCs injected into degenerated IVD	Improvement in the histology, cellularity, sulfated GAGs, and water contents of the NP. Expression of SOX9, ACAN, COL2, FOXF1, KRT19, PAX6, CA12, and COMP	Perez-Cruet et al., 2019 [139]
	Human UC-MSCs	Rat	1×10^6 UC-MSCs or UC-MSC-derived CPCs injected into degenerated IVD	Expression of chondrogenic markers and downregulation of pain and inflammatory genes. Differentiation of transplanted UC-MSCs and CPCs in functional NPCs. Better survival, homing, and distribution in IVD with CPCs.	Ekram et al., 2021 [140]
	Equine UC-MSCs	Rabbit	Early (day 3) or delayed (day 15) intra-articular injection of $3.5 \cdot 10^6$ UC-MSCs	Early IA injection of UC-MSCs exerted better anti-inflammatory and anticytotoxic effects (reduction of MMPs -1, -3, -13, and TNF- α)	Saulnier et al., 2015 [141]
OA	AM/UC particulate	Rat	Intra-articular injection of 50 or 100 $\mu\text{g}/\mu\text{L}$ AM/UC particulate decellularized	Attenuation of cartilage destruction, significant increase in cartilage thickness and volume, significant decrease in total lesion area with high dose at 4 weeks postinjection	Raines et al., 2017 [142]
	Human UC-MSCs	Mouse	Intra-articular injection of 1×10^5 UC-MSCs	Regeneration and repair of cartilage, recovery from movement impairment, amelioration of cartilage apoptosis via caspase 3 pathway	Chang et al., 2018 [143]
	Canine UC-MSCs	Dog	Intra-articular injection of 1×10^6 UC-MSCs on days 1 and 3	Repair of cartilage and patella, improvement of the healing of the surrounding tissue, reduction of joint effusion and inflammation (reduction of TNF- α , IL-6, and IL-7 blood levels)	Zhang et al., 2018 [144]
	Canine UC-MSCs	Dog	Intra-articular injection of 7×10^6 UC-MSCs	Improvement of clinical signs related to OA in treated dogs	Kim et al., 2019 [145]
	Human UC-MSCs	Rabbit	Intra-articular injection of 1×10^5 , 5×10^5 or 1×10^6 UC-MSCs	Chondrogenesis induction, upregulation of the expression of growth factors, ECM markers, and anti-inflammatory cytokines, and reduced expression of proinflammatory cytokines. Medium dose exerted the best effects	Kim et al., 2019 [83]
Human UC-MSCs	Rat	Intra-articular injection of 1×10^7 UC-MSCs overexpressing miR-140-5p	UC-MSCs overexpressing miR-140-5p significantly enhanced articular cartilage self-repairing in comparison to normal UC-MSCs	Geng et al., 2019 [146]	

TABLE 4: Continued.

Pathology	Source	Host	Study design	Results	Ref.
	Human UC-MSCs	Minipig	Intra-articular injection of a UC-MSCs (5×10^6 cells) and HA composite (4%)	Significant gross and histological improvements in hyaline cartilage regeneration	Wu et al., 2019 [147]
	Equine UC-MSCs	Horse	1 or 2 intra-articular injections (at 1-month interval) of 10×10^6 UC-MSCs	Improvement of lameness and total clinical score. No apparent clinical benefit of repeated intra-articular administration	Magri et al., 2019 [148]
	Human UC-MSCs	Mouse	Intra-articular injection of 5×10^5 UC-MSCs at 3 or 6 weeks	Significantly reduction of the loss of joint space and no evidence of an inflammatory response	Perry et al., 2020 [149]
	Human UC-MSCs	Rat	Single (day 1) or three (on days 1, 7 and 14) intra-articular injections of 2.5×10^5 UC-MSCs	Amelioration of cartilage erosion, alleviation of inflammatory cells infiltration and hyperplasia of the synovium by repeated injections. Increase number of SFCs on the articular cartilage surface	Tong et al., 2020 [81]
	Human UC-MSCs	Rat	Intra-articular injection of 1×10^6 UC-MSCs in 100 μ L HA	Temporary effects that decelerate the progression of cartilage degeneration, but may not inhibit OA progression in the long-term.	Xing et al., 2020 [150]
	Human UC-MSCs	Mouse	Intra-articular injection of low-dose UC-MSCs or UC-MSC-loaded GMs (3×10^4 cells) or high-dose UC-MSCs (3×10^5 cells)	UC-MSC-GMs promoted cartilage regeneration and inhibited macrophage-mediated synovitis better than low-dose and similar to high-dose UC-MSCs	Zhang et al., 2021 [42]
	Human UC-MSCs	Rat	intra-articular injection of 2.5×10^5 UC-MSCs once a week for 3 weeks	UC-MSCs prevent cartilage degradation, restore the proliferation of chondrocytes, and inhibit the inflammatory response	Zhang et al., 2021 [82]
	Human UC-MSCs	Rabbit	Intra-articular injection of UC-MSCs with GO granular lubricant	UC-MSCs loaded with the GO granular lubricant reduce the inflammatory level and improve the level of biochemical environment in the joint	Wang et al., 2021 [151]
	Human UC-MSCs	Mouse	Intraperitoneal injection of 1×10^6 UC-MSCs each day for 5 days	Reduction of the severity of RA, reduced levels of proinflammatory cytokines and chemokines (TNF- α , IL-6, and MCP-1) and increased levels of the anti-inflammatory cytokine (IL-10), Th1/Th2 type responses shifting and Tregs induction	Liu et al., 2010 [152]
	Human UC-MSCs	Mouse	Intra-articular injection of 1×10^6 UC-MSCs and/or 100 μ g/mL TNF- α inhibitor	Inhibition of TNF- α decreases cartilage destruction by suppressing the immunogenicity of UC-MSCs	Wu et al., 2012 [153]
RA	Human UC-MSCs	Rat	Tail vein injection of 1×10^6 UC-MSCs	Markedly increased percentage of Tregs and antithrombin levels, decrease of IL-1, IL-17, TNF- α , VEGF, and tissue factor levels	Gu et al., 2015 [154]
	Human UC-MSCs	Mouse	Tail vein injection of 1×10^6 UC-MSCs or BM-MSCs or SHED	UC-MSCs exert the best therapeutic effect in reducing bone resorption, joint destruction, and inflammatory factor expression	Zhang et al. 2019 [155]
	Human UC-MSCs	Rat	Intravenous injection of 2×10^6 UC-MSCs	Improvement arthritis, delay of radiological progression, and inhibition of synovial hyperplasia by downregulation of RORyt and upregulation of Foxp3 expression, inhibition of IL-17 and promotion of TGF- β	Ma et al., 2019 [156]

TABLE 4: Continued.

Pathology	Source	Host	Study design	Results	Ref.
	Human UC-MSCs	Rat	Intraperitoneal injection of 2×10^6 UC-MSCs	expression, inhibition of proliferation and promotion of apoptosis in T lymphocytes and increased Tregs ratio Slow down the progression of disease activity and reversal of arthritic processes along with triggering of joint tissue repair mechanisms	Vohra et al., 2020 [157]
	Human UC-MSC-sEVs	Rat	ND	Ameliorate arthritis and inhibit synovial hyperplasia in a dose-dependent manner by inhibiting T lymphocyte proliferation and promoting their apoptosis, decreasing Th17 cell proportion and increasing that of Tregs, decreasing serum IL-17, and enhanced IL-10 and TGF- β expression, decreasing RORyt and increased FOXP3 expression	Xu et al., 2021 [158]
	Human WJ-ECM	Rabbit	1×10^6 rabbit chondrocytes seeded in decellularized WJ-ECM scaffold inserted into the cartilage defects	All defects were filled completely with repaired tissue, and most of which were hyaline cartilage compared to WJ-ECM alone in which the defects filled partially with repaired tissue	Zhao et al., 2018 [159]
	Human WJ-MSCs	Goat	1×10^6 WJ-MSCs seeded in ACECM-oriented scaffold implanted into the articular cartilage defect	The WJ-MSCs-ACECM scaffold complex achieved better quality repair and regeneration of hyaline cartilage compared to microfracture (predominant clinical treatment strategy for damaged cartilage)	Zhang et al., 2018 [160]
Cartilage defects	Human WJ-MSCs	Goat	1×10^7 WJ-MSCs and pACs mixed in 3 ratios: 100:0, 0:100 and 50:50 and seeded into ACECM-oriented scaffolds implanted into the articular cartilage defect	50:50 ratio was more similar to native cartilage and better integrated with the surrounding tissue, more abundant cartilage-specific content and significantly higher mechanical strength, no significant joint effusion or bone marrow edema signal. WJ-MSCs possessed low immunogenicity and escaped destruction by the immune system	Zhang et al., 2020 [161]
	Human UC-MSCs-Exosomes	Rabbit	Intra-articular injection of 1×10^{10} mL $^{-1}$ of 2D or 3D culture in hollow-fiber bioreactor of UC-MSCs exosomes	Enhanced gross appearance and attenuated cartilage defect; 3D-cultured exosomes showed a superior therapeutic effect	Yan et al., 2020 [162]
	Human UC-MSCs	Rat	WJ/CS composite scaffold loaded with UC-MSCs implanted into the articular cartilage defect	The composite scaffold loaded with UC-MSCs repaired cartilage defects better than did the WJ scaffold loaded with UC-MSCs. Both the scaffold and UC-MSCs showed low immunogenicity	Li et al., 2021 [163]
	Rabbit UC-MSCs	Rabbit	PLGA scaffold with a continuous gradient transition between TGF- β 1 and BMP-2 seeded with 3×10^5 UC-MSCs implanted into articular osteochondral defect	Beneficial effect for bone and cartilage regeneration	Domer et al., 2012 [164]
Osteochondral defects	Human WJ-MSCs	Rabbit	3×10^7 undifferentiated or chondrogenically induced WJ-MSCs seeded in ECM of swine cartilage-derived scaffolds	Tissues repair observed over 16 months, with a hyaline-like neocartilage layer and regenerated subchondral bone. No immune rejection. WJ-MSCs were superior to those differentiated	Liu et al., 2017 [165]

TABLE 4: Continued.

Pathology	Source	Host	Study design	Results	Ref.
			Rat: 25 $\mu\text{g}/\text{mL}$ of WJ-MSC exosomes injected in joint cavity (5 times, every 7 days) Rabbit: ACECM scaffold implanted into osteochondral defect with 25 $\mu\text{g}/\text{mL}$ of WJ-MSCs exosomes injected in joint cavity, 5 times every 7 days	WJ-MSC exosomes enhance the effect of the ACECM scaffold and promote osteochondral regeneration, regulate the microenvironment of the articular cavity promoting the polarization of macrophages toward the M2 phenotype and inhibiting the inflammatory response. WJ-MSC exosomes contain many miRNAs that can promote the regeneration of hyaline cartilage	Jiang et al., 2021 [166]

ACECM: acellular cartilage extracellular matrix; AM/UC: amniotic membrane/ umbilical cord; CPCs: chondroprogenitor cells; GMs: gelatin microcryogels; GO: graphene oxide; HA: hyaluronic acid; IVD: intervertebral disc; NP: nucleus pulposus; NPCs: NP-like cells; OA: osteoarthritis; PAC: primary cartilage cells; PLGA: poly(D,L-lactic-co-glycolic acid); RA: rheumatoid arthritis; sEVs: small extracellular vesicles; SFC: cartilage superficial; SHED: stem cells derived from human exfoliated deciduous teeth layer cells; WJ/CS: Wharton's jelly and chondroitin sulfate.

TABLE 5: Clinical trials of cartilage repair with UC-MSCs or their secretome.

Pathology	Source	Study design	Delivery mode	Patients (N ^o)	Results	Ref.
	Human UC-MSCs	Randomized, double-blind, controlled phase I/II	Intra-articular injection of 20×10^6 UC-MSCs once or twice vs. HA injection	29	Double injection group showed significant amelioration of pain and disability at 6 and 12 months of follow-up compared to HA group. No severe adverse events were reported.	Matas et al., 2019 [167]
OA	Human UC-MSCs	Open-label, single arm, phase I/II	Injection of 10×10^6 UC-MSCs in 2 mL secretome + 2 mL HA	29	Significant reduction of the pain and greatest improvement in knee function after 6th-month follow-up.	Dilogo et al., 2020 [168]
	AM/UC particulate	Single-center, investigator-initiated, retrospective study	Intra-articular injection of 100 mg of AM/UC particulate	42	Significant clinical improvement of pain and function in patients with moderate to severe knee OA, with the potential to delay total knee replacement for up to 12 months	Mead et al., 2020 [169]
	Human UC-MSCs	Prospective phase I/II study	Intravenous injection of 2×10^7 UC-MSCs	64	Lower levels of serological markers ESR, CRP, RF at 1 and 3 years and anti-CCP at 3 years after treatment. Decrease of health and joint function indexes 1 and 3 years after treatment.	Wang et al., 2019 [170]
RA	Human UC-MSCs	Phase I/II study	Intravenous drip of 4×10^7 UC-MSCs and intravenous injection of 24 mg of cervus and cucumis peptides	119	Significant reduction of serological markers ESR, CRP, RF, and anti-CCP and improvement of health index and joint function index 1 year after treatment	Qi et al., 2020 [171]
	Human UC-MSCs	Randomized, controlled phase I/2	Intravenous infusion of 1×10^6 cells/kg of body weight with or without a single intramuscular infusion of 1 million IU of IFN- γ	63	Efficacy and ACR20 response rates attained in 53.3% patients with UC-MSCs alone and in 93.3% patients with UC-MSCs combined with IFN- γ at 3-month follow-up. No new or unexpected safety issues in 1-year follow-up	He et al., 2020 [172]

ACR20: American College of Rheumatology 20; AM/UC: amniotic membrane/umbilical cord; CCP: cyclic citrullinated peptide (CCP) antibody; CRP: C-reactive protein; ESR: the erythrocyte sedimentation rate; HA: hyaluronic acid; OA: osteoarthritis; RA: rheumatoid arthritis; RF: rheumatoid factor.

models (listed in Table 4) and in recent clinical trials (reported in Table 5).

Preliminary *in vitro* studies investigated the chondrogenic potential of UC-MSCs, demonstrating their ability to achieve both hyaline, fibrous, and elastic cartilage phenotypes as well as nucleus pulposus-like cell differentiation capacity [87–90]. In addition, also the osteogenic, adipogenic, and myogenic differentiation potential have been reported suggesting UC-MSCs could be a pivotal stem cells source for tissue engineering applications in orthopaedics [91]. Comparative studies reported slightly differences in chondrogenesis between the UC-, BM-, and AT-MSCs. In particular, according to Danišovič et al., BM-MSCs showed the best chondrogenic potential while Hildner and coworkers showed that differentiated UC-MSCs present a more fibrous than hyaline cartilage phenotype compared to AT-MSCs suggesting their role in regeneration of fibrocartilage-like meniscus [87, 92]. Moreover, the results of Wu and coworkers indicate that, although nucleus pulposus stem/progenitor cells (D-NP-MSCs) isolated from degenerated intervertebral disc (IVD) shared the MSCs characteristics with UC-MSCs, the latter showed better proliferation capacity and differentiation potential, suggesting that UC-MSCs as a suitable source for regenerative therapy of IVD degeneration [93]. Furthermore, UC-MSCs may be an attractive alternative to condylar cartilage cells for temporomandibular joint tissue engineering applications [94]. Interestingly, UC-MSCs displayed superior anti-inflammatory, immunomodulatory, and trophic effects compared to adult MSCs including articular cartilage (AC), Hoffa's fat pad (HFP), synovial membrane (SM), and maintain their immunomodulatory and anti-inflammatory properties after differentiation [50, 84, 95]. Moreover, coculture experiments of UC-MSCs and articular cartilage cells (ACs), fibroblast-like synoviocytes (FLSs), and nucleus pulposus cells (NPCs) showed their suitability for the treatment of arthritis, synovitis, and IVD degeneration [61, 96–98]. Finally, there are several cartilage tissue engineering studies that demonstrated the osteochondral differentiation capacity of UC-MSCs in different scaffold constituted by acellular cartilage extracellular matrix (ACECM), alginate enriched in hyaluronic acid (Alg/HA), polycaprolactone/collagen (PCL/Coil), polyglycolic acid (PGA), poly L-lactide/D-lactide/glycolide (PLGA), poly-L-lactic acid (PLLA), polyvinyl alcohol-polycaprolactone (PVA-PCL), and silk fibroin/hyaluronic acid (SF/HA).

In vivo studies in different animal models from mice to horses confirmed *in vitro* studies showing the feasibility of using UC-MSCs for the treatment of IVD degeneration, OA, RA, and cartilage defects repair. UC-MSC transplantation promotes chondrogenesis and improves the histology, cellularity, and ECM proteins content along with reduction of inflammation in a preclinical model of IVD degeneration. In the same way, UC-MSCs induce regeneration and repair of cartilage reducing its destruction, promote recovery from movement impairment, and reduce joint effusion and inflammation slowing down the progression of OA animal models. In addition, preclinical studies on RA treatment showed that UC-MSCs exerted the best therapeutic effect in reducing bone resorption, joint destruction, and inflammatory factor expression compared to BM-MSCs. Interest-

ingly, several evidences support the regenerative potential of UC-MSCs in cartilage and osteochondral defects repair.

Following the promising *in vitro* and *in vivo* results, clinical applications have been attempted using UC-MSCs for the treatment of OA and RA (Table 5). In summary, clinical trials for the treatment of OA showed significant amelioration of pain and disability at 6 and 12 months of follow-up. No severe adverse events were reported. The main outcomes for RA patients treated with UC-MSCs were significant reduction of RA serological markers and improvement of health index and joint function index 1 year after treatment. No new or unexpected safety issues in 1-year follow-up. Despite the promising results of clinical trials, further basic and translational research investigations are needed to better understand the best stem cell candidate, scaffold materials, and/or best cellular derivatives which can be suitable for the different types of cartilage regeneration. In parallel, there is the need to increase the knowledge about underlying regenerative mechanisms. Finally, more research is needed to convert preclinical evidences obtained in animal models, to human-based clinical applications for cartilage regeneration. Consensus is still lacking in key points such as the methods to obtain the cell source, the use of scaffolds as well as bioactive molecules in parallel to the administration of stromal cells. As shown in the human studies reviewed so far, the achievement of amelioration of some parameters and confirmation of the safety of the overall procedure still needs more data generated on the interaction of the transplanted cells with the host tissue, their proper differentiation *in vivo*, as well as the long-term achievements of this cellular replacement strategy.

4. Conclusions

In conclusion, UC-MSCs represent a promising candidate for the therapy of chondropathies, as highlighted by the encouraging results emerged from *in vitro* and *in vivo* investigations and from the available results from clinical trials. UC-MSCs are characterized by several potential advantages such as a frank multilineage differentiation potential, immunomodulatory, and anti-inflammatory properties, as well as MSCs the ability to constitutively produce molecules that are involved in cartilage matrix biogenesis and in the trophic and reparative functions. In addition, UC-MSCs are able to migrate, home, and survive in an ischemic and nutrient-poor environment like cartilage as well as to produce an extracellular matrix (ECM) similar to that and induce endogenous repair mechanisms. We believe that these results warrant the need for further researches that can better define the criteria leading to the adoption of UC-MSCs in the stem cell-based therapy of cartilage diseases, as well as characterizing the mechanism of repair and increase the knowledge on the biomechanical properties of the regenerated cartilage tissue *in vivo*.

Conflicts of Interest

Prof. Giampiero La Rocca is member of the Scientific board of Auxocell Laboratories, Inc. The other authors report no conflicts.

Acknowledgments

GLR is a recipient of a PRIN 2017 fund by the Italian Ministry of University.

References

- [1] Y. Krishnan and A. J. Grodzinsky, "Cartilage diseases," *Matrix Biology*, vol. 71-72, pp. 51-69, 2018.
- [2] A. Cieza, K. Causey, K. Kamenov, S. W. Hanson, S. Chatterji, and T. Vos, "Global estimates of the need for rehabilitation based on the Global Burden of Disease study 2019: a systematic analysis for the Global Burden of Disease Study 2019," *The Lancet*, vol. 396, no. 10267, pp. 2006-2017, 2021.
- [3] Y. P. Li, X. C. Wei, J. M. Zhou, and L. Wei, "The age-related changes in cartilage and osteoarthritis," *BioMed Research International*, vol. 2013, Article ID 916530, 12 pages, 2013.
- [4] N. Arden and M. Nevitt, "Osteoarthritis: epidemiology," *Best Practice & Research. Clinical Rheumatology*, vol. 20, no. 1, pp. 3-25, 2006.
- [5] W. M. Hopman, M. B. Harrison, H. Coo, E. Friedberg, M. Buchanan, and E. G. VanDenKerkhof, "Associations between chronic disease, age and physical and mental health status," *Chronic Diseases in Canada*, vol. 29, no. 3, pp. 108-117, 2009.
- [6] D. Umlauf, S. Frank, T. Pap, and J. Bertrand, "Cartilage biology, pathology, and repair," *Cellular and Molecular Life Sciences*, vol. 67, no. 24, pp. 4197-4211, 2010.
- [7] T. W. O'Neill and D. T. Felson, "Mechanisms of osteoarthritis (OA) pain," *Current Osteoporosis Reports*, vol. 16, no. 5, pp. 611-616, 2018.
- [8] M. C. Reid, R. Shengelia, and S. J. Parker, "Pharmacologic management of osteoarthritis-related pain in older adults," *HSS Journal*, vol. 8, no. 2, pp. 159-164, 2012.
- [9] P. Orth, A. Rey-Rico, J. K. Venkatesan, H. Madry, and M. Cucchiari, "Current perspectives in stem cell research for knee cartilage repair," *Stem Cells Cloning*, vol. 7, pp. 1-17, 2014.
- [10] D. L. Troyer and M. L. Weiss, "Concise review: Wharton's jelly-derived cells are a primitive stromal cell population," *Stem Cells*, vol. 26, no. 3, pp. 591-599, 2008.
- [11] J. E. Davies, J. T. Walker, and A. Keating, "Concise review: Wharton's jelly: the rich, but enigmatic, source of mesenchymal stromal cells," *Stem Cells Translational Medicine*, vol. 6, no. 7, pp. 1620-1630, 2017.
- [12] S. Liu, K. D. Hou, M. Yuan et al., "Characteristics of mesenchymal stem cells derived from Wharton's jelly of human umbilical cord and for fabrication of non-scaffold tissue-engineered cartilage," *Journal of Bioscience and Bioengineering*, vol. 117, no. 2, pp. 229-235, 2014.
- [13] Y. Yin, X. Li, X. T. He, R. X. Wu, H. H. Sun, and F. M. Chen, "Leveraging stem cell homing for therapeutic regeneration," *Journal of Dental Research*, vol. 96, no. 6, pp. 601-609, 2017.
- [14] O. I. Eseonu and C. De Bari, "Homing of mesenchymal stem cells: mechanistic or stochastic? Implications for targeted delivery in arthritis," *Rheumatology*, vol. 54, no. 2, pp. 210-218, 2015.
- [15] C. Shen, P. Lie, T. Miao et al., "Conditioned medium from umbilical cord mesenchymal stem cells induces migration and angiogenesis," *Molecular Medicine Reports*, vol. 12, no. 1, pp. 20-30, 2015.
- [16] T. Kitaori, H. Ito, E. M. Schwarz et al., "Stromal cell-derived factor 1/CXCR4 signaling is critical for the recruitment of mesenchymal stem cells to the fracture site during skeletal repair in a mouse model," *Arthritis and Rheumatism*, vol. 60, no. 3, pp. 813-823, 2009.
- [17] W. Zhang, J. Chen, J. Tao et al., "The use of type 1 collagen scaffold containing stromal cell-derived factor-1 to create a matrix environment conducive to partial-thickness cartilage defects repair," *Biomaterials*, vol. 34, no. 3, pp. 713-723, 2013.
- [18] J. M. Petty, C. C. Lenox, D. J. Weiss, M. E. Poynter, and B. T. Suratt, "Crosstalk between CXCR4/Stromal Derived Factor-1 and VLA-4/VCAM-1 pathways regulates neutrophil retention in the bone marrow," *The Journal of Immunology*, vol. 182, no. 1, pp. 604-612, 2009.
- [19] D. Cox, M. Brennan, and N. Moran, "Integrins as therapeutic targets: lessons and opportunities," *Nature Reviews Drug Discovery*, vol. 9, no. 10, pp. 804-820, 2010.
- [20] N. L. Payne, G. Sun, C. McDonald et al., "Distinct immunomodulatory and migratory mechanisms underpin the therapeutic potential of human mesenchymal stem cells in autoimmune demyelination," *Cell Transplantation*, vol. 22, no. 8, pp. 1409-1425, 2013.
- [21] C. Zou, Q. Luo, J. Qin et al., "Osteopontin promotes mesenchymal stem cell migration and lessens cell stiffness via integrin $\beta 1$, FAK, and ERK pathways," *Cell Biochemistry and Biophysics*, vol. 65, no. 3, pp. 455-462, 2013.
- [22] S. A. Lund, C. M. Giachelli, and M. Scatena, "The role of osteopontin in inflammatory processes," *Journal of Cell Communication and Signaling*, vol. 3, no. 3-4, pp. 311-322, 2009.
- [23] F. Zhang, W. Luo, Y. Li, S. Gao, and G. Lei, "Role of osteopontin in rheumatoid arthritis," *Rheumatology International*, vol. 35, no. 4, pp. 589-595, 2015.
- [24] C. Cheng, S. Gao, and G. Lei, "Association of osteopontin with osteoarthritis," *Rheumatology International*, vol. 34, no. 12, pp. 1627-1631, 2014.
- [25] R. K. Schneider, A. Puellen, R. Kramann et al., "The osteogenic differentiation of adult bone marrow and perinatal umbilical mesenchymal stem cells and matrix remodelling in three-dimensional collagen scaffolds," *Biomaterials*, vol. 31, no. 3, pp. 467-480, 2010.
- [26] X. Fu, G. Liu, A. Halim, Y. Ju, Q. Luo, and G. Song, "Mesenchymal stem cell migration and tissue repair," *Cell*, vol. 8, no. 8, p. 784, 2019.
- [27] G. Pattappa, B. Johnstone, J. Zellner, D. Docheva, and P. Angele, "The importance of physioxia in mesenchymal stem cell chondrogenesis and the mechanisms controlling its response," *International Journal of Molecular Sciences*, vol. 20, no. 3, p. 484, 2019.
- [28] D. C. Chow, L. A. Wenning, W. M. Miller, and E. T. Papoutsakis, "Modeling pO₂ Distributions in the Bone Marrow Hematopoietic Compartment. I. Krogh's Model," *Biophysical Journal*, vol. 81, no. 2, pp. 675-684, 2001.
- [29] A. Bizzarri, H. Koehler, M. Cajlakovic et al., "Continuous oxygen monitoring in subcutaneous adipose tissue using microdialysis," *Analytica Chimica Acta*, vol. 573-574, pp. 48-56, 2006.
- [30] B. Fischer and B. D. Bavister, "Oxygen-tension in the oviduct and uterus of rhesus-monkeys, hamsters and rabbits," *Journal of Reproduction and Fertility*, vol. 99, no. 2, pp. 673-679, 1993.

- [31] A. Marmotti, S. Mattia, F. Castoldi et al., “Allogeneic umbilical cord-derived mesenchymal stem cells as a potential source for cartilage and bone regeneration: an in vitro study,” *Stem Cells International*, vol. 2017, Article ID 1732094, 16 pages, 2017.
- [32] A. Lavrentieva, I. Majore, C. Kasper, and R. Hass, “Effects of hypoxic culture conditions on umbilical cord-derived human mesenchymal stem cells,” *Cell Communication and Signaling: CCS*, vol. 8, no. 1, p. 18, 2010.
- [33] U. Nekanti, S. Dastidar, P. Venugopal, S. Totey, and M. Ta, “Increased proliferation and analysis of differential gene expression in human Wharton’s jelly-derived mesenchymal stromal cells under hypoxia,” *International Journal of Biological Sciences*, vol. 6, no. 5, pp. 499–512, 2010.
- [34] E. Russo, J. Y. Lee, H. Nguyen et al., “Energy metabolism analysis of three different mesenchymal stem cell populations of umbilical cord under normal and pathologic conditions,” *Stem Cell Reviews and Reports*, vol. 16, no. 3, pp. 585–595, 2020.
- [35] Y. Kaneko, J. Y. Lee, N. Tajiri et al., “Translating intracarotid artery transplantation of bone marrow-derived NCS-01 cells for ischemic stroke: behavioral and histological readouts and mechanistic insights into stem cell therapy,” *Stem Cells Translational Medicine*, vol. 9, no. 2, pp. 203–220, 2020.
- [36] E. G. Neal, M. G. Liska, T. Lippert et al., “An update on intracerebral stem cell grafts,” *Expert Review of Neurotherapeutics*, vol. 18, no. 7, pp. 557–572, 2018.
- [37] B. Cozene, E. Russo, R. Anzalone, G. La Rocca, and C. Borlongan, “Mitochondrial activity of human umbilical cord mesenchymal stem cells,” *Brain Circulation*, vol. 7, no. 1, pp. 33–36, 2021.
- [38] E. Russo, T. Lippert, J. P. Tuazon, and C. V. Borlongan, “Advancing stem cells: new therapeutic strategies for treating central nervous system disorders,” *Brain Circulation*, vol. 4, no. 3, pp. 81–83, 2018.
- [39] K. Sobolewski, A. Małkowski, E. Bańkowski, and S. Jaworski, “Wharton’s jelly as a reservoir of peptide growth factors,” *Placenta*, vol. 26, no. 10, pp. 747–752, 2005.
- [40] L. Qin and F. Beier, “EGFR Signaling: friend or foe for cartilage?,” *JBMR Plus*, vol. 3, no. 2, article e10177, 2019.
- [41] D. L. Long, V. Ulici, S. Chubinskaya, and R. F. Loeser, “Heparin-binding epidermal growth factor-like growth factor (HB-EGF) is increased in osteoarthritis and regulates chondrocyte catabolic and anabolic activities,” *Osteoarthritis and Cartilage*, vol. 23, no. 9, pp. 1523–1531, 2015.
- [42] X. Zhang, S. Liu, Z. Wang et al., “Implanted 3D gelatin microcryogel enables low-dose cell therapy for osteoarthritis by preserving the viability and function of umbilical cord MSCs,” *Chemical Engineering Journal*, vol. 416, article 129140, 2021.
- [43] H. Tonomura, M. Nagae, R. Takatori, H. Ishibashi, T. Itsuji, and K. Takahashi, “The potential role of hepatocyte growth factor in degenerative disorders of the synovial joint and spine,” *International Journal of Molecular Sciences*, vol. 21, no. 22, p. 8717, 2020.
- [44] Y. Wang, M. Yuan, Q. Guo, S. Lu, and J. Peng, “Mesenchymal stem cells for treating articular cartilage defects and osteoarthritis,” *Cell Transplantation*, vol. 24, no. 9, pp. 1661–1678, 2015.
- [45] Y. Petrenko, I. Vackova, K. Kekulova et al., “A comparative analysis of multipotent mesenchymal stromal cells derived from different sources, with a focus on neuroregenerative potential,” *Scientific Reports*, vol. 10, no. 1, p. 4290, 2020.
- [46] E. Sulpice, S. Ding, B. Muscatelli-Groux et al., “Cross-talk between the VEGF-A and HGF signalling pathways in endothelial cells,” *Biology of the Cell*, vol. 101, no. 9, pp. 525–539, 2009.
- [47] B. E. Bobick, F. H. Chen, A. M. Le, and R. S. Tuan, “Regulation of the chondrogenic phenotype in culture,” *Birth Defects Research Part C: Embryo Today: Reviews*, vol. 87, no. 4, pp. 351–371, 2009.
- [48] Y. Tao, X. Zhou, C. Liang et al., “TGF- β 3 and IGF-1 synergy ameliorates nucleus pulposus mesenchymal stem cell differentiation towards the nucleus pulposus cell type through MAPK/ERK signaling,” *Growth Factors*, vol. 33, no. 5-6, pp. 326–336, 2015.
- [49] J. Palka, E. Bańkowski, and S. Jaworski, “An accumulation of IGF-I and IGF-binding proteins in human umbilical cord,” *Molecular and Cellular Biochemistry*, vol. 206, no. 1/2, pp. 133–139, 2000.
- [50] G. La Rocca, M. Lo Iacono, T. Corsello, S. Corrao, F. Farina, and R. Anzalone, “Human Wharton’s jelly mesenchymal stem cells maintain the expression of key immunomodulatory molecules when subjected to osteogenic, adipogenic and chondrogenic differentiation in vitro: new perspectives for cellular therapy,” *Current Stem Cell Research & Therapy*, vol. 8, no. 1, pp. 100–113, 2013.
- [51] W. Wang, D. Rigueur, and K. M. Lyons, “TGF β signaling in cartilage development and maintenance,” *Birth Defects Research Part C: Embryo Today: Reviews*, vol. 102, no. 1, pp. 37–51, 2014.
- [52] A. S. Patil, R. B. Sable, and R. M. Kothari, “An update on transforming growth factor- β (TGF- β): sources, types, functions and clinical applicability for cartilage/bone healing,” *Journal of Cellular Physiology*, vol. 226, no. 12, pp. 3094–3103, 2011.
- [53] G. Y. Liu, Y. Xu, Y. Li, L. H. Wang, Y. J. Liu, and D. Zhu, “Secreted galectin-3 as a possible biomarker for the immunomodulatory potential of human umbilical cord mesenchymal stromal cells,” *Cytotherapy*, vol. 15, no. 10, pp. 1208–1217, 2013.
- [54] R. Donders, J. F. Bogie, S. Ravanidis et al., “Human Wharton’s jelly-derived stem cells display a distinct immunomodulatory and proregenerative transcriptional signature compared to bone marrow-derived stem cells,” *Stem Cells and Development*, vol. 27, no. 2, pp. 65–84, 2018.
- [55] I. B. Copland, S. L. Adamson, M. Post, S. J. Lye, and I. Caniggia, “TGF- β 3 Expression During Umbilical Cord Development and its Alteration in Pre-eclampsia,” *Placenta*, vol. 23, no. 4, pp. 311–321, 2002.
- [56] Z. H. Deng, Y. S. Li, X. Gao, G. H. Lei, and J. Huard, “Bone morphogenetic proteins for articular cartilage regeneration,” *Osteoarthritis and Cartilage*, vol. 26, no. 9, pp. 1153–1161, 2018.
- [57] S. Scarfi, “Use of bone morphogenetic proteins in mesenchymal stem cell stimulation of cartilage and bone repair,” *World Journal of Stem Cells*, vol. 8, no. 1, pp. 1–12, 2016.
- [58] M. Kosinski, A. Figiel-Dabrowska, W. Lech et al., “Bone defect repair using a bone substitute supported by mesenchymal stem cells derived from the umbilical cord,” *Stem Cells International*, vol. 2020, Article ID 1321283, 15 pages, 2020.
- [59] J. Choi, T. Bae, N. Byambasuren et al., “CRISPR-Cpf1 Activation of Endogenous BMP4 Gene for Osteogenic

- Differentiation of Umbilical-Cord-Derived Mesenchymal Stem Cells," *Molecular Therapy - Methods & Clinical Development*, vol. 17, pp. 309–316, 2020.
- [60] D. B. Guo, X. Q. Zhu, Q. Q. Li et al., "Efficacy and mechanisms underlying the effects of allogeneic umbilical cord mesenchymal stem cell transplantation on acute radiation injury in tree shrews," *Cytotechnology*, vol. 70, no. 5, pp. 1447–1468, 2018.
- [61] J. Zeng, F. Wang, and M. Mao, "Co-culture of fibroblast-like synoviocytes with umbilical cord-mesenchymal stem cells inhibits expression of pro-inflammatory proteins, induces apoptosis and promotes chondrogenesis," *Molecular Medicine Reports*, vol. 14, no. 4, pp. 3887–3893, 2016.
- [62] Q. Wang, L. Xu, R. Willumeit-Römer, and B. J. Luthringer-Feyerabend, "Macrophage-derived oncostatin M/bone morphogenetic protein 6 in response to Mg-based materials influences pro-osteogenic activity of human umbilical cord perivascular cells," *Acta Biomaterialia*, vol. 133, pp. 268–279, 2020.
- [63] S. R. Frenkel, P. B. Saadeh, B. J. Mehrara et al., "Transforming growth factor beta superfamily members: role in cartilage modeling," *Plastic and Reconstructive Surgery*, vol. 105, no. 3, pp. 980–990, 2000.
- [64] R. S. Tuan, A. F. Chen, and B. A. Klatt, "Cartilage regeneration," *The Journal of the American Academy of Orthopaedic Surgeons*, vol. 21, no. 5, pp. 303–311, 2013.
- [65] P. Kangari, T. Talaei-Khozani, I. Razeghian-Jahromi, and M. Razmkhah, "Mesenchymal stem cells: amazing remedies for bone and cartilage defects," *Stem Cell Research & Therapy*, vol. 11, no. 1, p. 492, 2020.
- [66] A. Mauro, M. Buscemi, and A. Gerbino, "Immunohistochemical and transcriptional expression of matrix metalloproteinases in full-term human umbilical cord and human umbilical vein endothelial cells," *Journal of Molecular Histology*, vol. 41, no. 6, pp. 367–377, 2010.
- [67] M. Lo Iacono, E. Russo, R. Anzalone et al., "Wharton's jelly mesenchymal stromal cells support the expansion of cord blood-derived CD34+ Cells mimicking a hematopoietic niche in a direct cell-cell contact culture system," *Cell Transplantation*, vol. 27, no. 1, pp. 117–129, 2018.
- [68] A. Gupta, S. F. el-Amin III, H. J. Levy, R. Sze-Tu, S. E. Ibim, and N. Maffulli, "Umbilical cord-derived Wharton's jelly for regenerative medicine applications," *Journal of Orthopaedic Surgery and Research*, vol. 15, no. 1, p. 49, 2020.
- [69] M. Trapani, G. La Rocca, and O. Parolini, "Chapter 6. The immunomodulatory features of mesenchymal stromal cells derived from Wharton's jelly, amniotic membrane, and chorionic villi: in vitro and in vivo data," in *Placenta: The Tree of Life*, pp. 91–128, CRC Press, Boca Raton, FL, USA, 2016.
- [70] G. la Rocca, R. Anzalone, S. Corrao et al., "Isolation and characterization of Oct-4+/HLA-G+ mesenchymal stem cells from human umbilical cord matrix: differentiation potential and detection of new markers," *Histochemistry and Cell Biology*, vol. 131, no. 2, pp. 267–282, 2009.
- [71] G. La Rocca, S. Corrao, M. Lo Iacono, T. Corsello, F. Farina, and R. Anzalone, "Novel immunomodulatory markers expressed by human WJ-MSc: an updated review in regenerative and reparative medicine," *The Open Tissue Engineering and Regenerative Medicine Journal*, vol. 5, no. 1, pp. 50–58, 2012.
- [72] R. Anzalone, M. Lo Iacono, T. Loria et al., "Wharton's jelly mesenchymal stem cells as candidates for beta cells regeneration: extending the differentiative and immunomodulatory benefits of adult mesenchymal stem cells for the treatment of type 1 diabetes," *Stem Cell Reviews and Reports*, vol. 7, no. 2, pp. 342–363, 2011.
- [73] T. Corsello, G. Amico, S. Corrao et al., "Wharton's jelly mesenchymal stromal cells from human umbilical cord: a close-up on immunomodulatory molecules featured in situ and in vitro," *Stem Cell Reviews and Reports*, vol. 15, no. 6, pp. 900–918, 2019.
- [74] Q. Wang, Q. Yang, Z. Wang et al., "Comparative analysis of human mesenchymal stem cells from fetal-bone marrow, adipose tissue, and Wharton's jelly as sources of cell immunomodulatory therapy," *Human Vaccines & Immunotherapeutics*, vol. 12, no. 1, pp. 85–96, 2016.
- [75] M. Najar, G. Raicevic, H. I. Boufker et al., "Mesenchymal stromal cells use PGE2 to modulate activation and proliferation of lymphocyte subsets: combined comparison of adipose tissue, Wharton's Jelly and bone marrow sources," *Cellular Immunology*, vol. 264, no. 2, pp. 171–179, 2010.
- [76] R. Anzalone, M. L. Iacono, S. Corrao et al., "New emerging potentials for human Wharton's jelly mesenchymal stem cells: immunological features and hepatocyte-like differentiative capacity," *Stem Cells and Development*, vol. 19, no. 4, pp. 423–438, 2010.
- [77] M. di Nicola, C. Carlo-Stella, M. Magni et al., "Human bone marrow stromal cells suppress T-lymphocyte proliferation induced by cellular or nonspecific mitogenic stimuli," *Blood*, vol. 99, no. 10, pp. 3838–3843, 2002.
- [78] L. Ma, Z. Zhou, D. Zhang et al., "Immunosuppressive function of mesenchymal stem cells from human umbilical cord matrix in immune thrombocytopenia patients," *Thrombosis and Haemostasis*, vol. 107, no. 5, pp. 937–950, 2012.
- [79] W. Li, Q. Zhang, M. Wang et al., "Macrophages are involved in the protective role of human umbilical cord-derived stromal cells in renal ischemia-reperfusion injury," *Stem Cell Research*, vol. 10, no. 3, p. 405, 2013.
- [80] X. Zhao, Y. Zhao, X. Sun, Y. Xing, X. Wang, and Q. Yang, "Immunomodulation of MSCs and MSC-derived extracellular vesicles in osteoarthritis," *Frontiers in Bioengineering and Biotechnology*, vol. 8, article 575057, 2020.
- [81] W. Tong, X. Zhang, Q. Zhang et al., "Multiple umbilical cord-derived MSCs administrations attenuate rat osteoarthritis progression via preserving articular cartilage superficial layer cells and inhibiting synovitis," *Journal of Orthopaedic Translation*, vol. 23, pp. 21–28, 2020.
- [82] Q. Zhang, E. Xiang, W. Rao et al., "Intra-articular injection of human umbilical cord mesenchymal stem cells ameliorates monosodium iodoacetate-induced osteoarthritis in rats by inhibiting cartilage degradation and inflammation," *Bone & Joint Research*, vol. 10, no. 3, pp. 226–236, 2021.
- [83] H. Kim, G. Yang, J. Park, J. Choi, E. Kang, and B. K. Lee, "Therapeutic effect of mesenchymal stem cells derived from human umbilical cord in rabbit temporomandibular joint model of osteoarthritis," *Scientific Reports*, vol. 9, no. 1, article 13854, 2019.
- [84] C. Voisin, G. Cauchois, L. Reppel et al., "Are the immune properties of mesenchymal stem cells from Wharton's jelly maintained during chondrogenic differentiation?," *Journal of Clinical Medicine*, vol. 9, no. 2, p. 423, 2020.
- [85] D. Giannini, M. Antonucci, F. Petrelli, S. Bilia, A. Alunno, and I. Puxeddu, "One year in review 2020: pathogenesis of

- rheumatoid arthritis," *Clinical and Experimental Rheumatology*, vol. 38, no. 3, pp. 387–397, 2020.
- [86] C. Zhao, L. Zhang, W. Kong et al., "Umbilical cord-derived mesenchymal stem cells inhibit cadherin-11 expression by fibroblast-like synoviocytes in rheumatoid arthritis," *Journal of Immunology Research*, vol. 2015, Article ID 137695, 10 pages, 2015.
- [87] F. Hildner, S. Wolbank, H. Redl, M. van Griensven, and A. Peterbauer, "How chondrogenic are human umbilical cord matrix cells? A comparison to adipose-derived stem cells," *Journal of Tissue Engineering and Regenerative Medicine*, vol. 4, no. 3, pp. 242–245, 2010.
- [88] D. Ruan, Y. Zhang, D. Wang et al., "Differentiation of human Wharton's jelly cells toward nucleus pulposus-like cells after coculture with nucleus pulposus CellsIn vitro," *Tissue Engineering. Part A*, vol. 18, no. 1-2, pp. 167–175, 2012.
- [89] B. H. Chon, E. J. Lee, L. Jing, L. A. Setton, and J. Chen, "Human umbilical cord mesenchymal stromal cells exhibit immature nucleus pulposus cell phenotype in a laminin-rich pseudo-three-dimensional culture system," *Stem Cell Research & Therapy*, vol. 4, no. 5, p. 120, 2013.
- [90] M. Caballero, M. D. Skancke, A. E. Halevi et al., "Effects of connective tissue growth factor on the regulation of elastogenesis in human umbilical cord-derived mesenchymal stem cells," *Annals of Plastic Surgery*, vol. 70, no. 5, pp. 568–573, 2013.
- [91] A. Marmotti, S. Mattia, M. Bruzzone et al., "Minced umbilical cord fragments as a source of cells for orthopaedic tissue engineering: an in vitro study," *Stem Cells International*, vol. 2012, Article ID 326813, 13 pages, 2012.
- [92] L. Danišovič, M. Boháč, R. Zamborský et al., "Comparative analysis of mesenchymal stromal cells from different tissue sources in respect to articular cartilage tissue engineering," *General Physiology and Biophysics*, vol. 35, no. 2, pp. 207–214, 2016.
- [93] H. Wu, X. Zeng, J. Yu et al., "Comparison of nucleus pulposus stem/progenitor cells isolated from degenerated intervertebral discs with umbilical cord derived mesenchymal stem cells," *Experimental Cell Research*, vol. 361, no. 2, pp. 324–332, 2017.
- [94] M. M. Bailey, L. Wang, C. J. Bode, K. E. Mitchell, and M. S. Detamore, "A comparison of human umbilical cord matrix stem cells and temporomandibular joint condylar chondrocytes for tissue engineering temporomandibular joint condylar cartilage," *Tissue Engineering*, vol. 13, no. 8, pp. 2003–2010, 2007.
- [95] A. Islam, I. Urbarova, J. A. Bruun, and I. Martinez-Zubiaurre, "Large-scale secretome analyses unveil the superior immunosuppressive phenotype of umbilical cord stromal cells as compared to other adult mesenchymal stromal cells," *European Cells & Materials*, vol. 37, pp. 153–174, 2019.
- [96] Y. Zhang, S. Liu, W. Guo et al., "Coculture of hWJMSCs and pACs in oriented scaffold enhances hyaline cartilage regeneration in vitro," *Stem Cells International*, vol. 2019, Article ID 5130152, 11 pages, 2019.
- [97] X. Li, Y. Liang, X. Xu et al., "Cell-to-cell culture inhibits dedifferentiation of chondrocytes and induces differentiation of human umbilical cord-derived mesenchymal stem cells," *BioMed Research International*, vol. 2019, Article ID 5871698, 11 pages, 2019.
- [98] Z. Han, Y. Zhang, L. Gao, S. Jiang, and D. Ruan, "Human Wharton's jelly cells activate degenerative nucleus pulposus cells in vitro," *Tissue Engineering. Part A*, vol. 24, no. 13-14, pp. 1035–1043, 2018.
- [99] W. S. Toh, E. H. Lee, and T. Cao, "Potential of human embryonic stem cells in cartilage tissue engineering and regenerative medicine," *Stem Cell Reviews and Reports*, vol. 7, no. 3, pp. 544–559, 2011.
- [100] R. Castro-Viñuelas, C. Sanjurjo-Rodríguez, M. Piñeiro-Ramil et al., "Induced pluripotent stem cells for cartilage repair: current status and future perspectives," *European Cells & Materials*, vol. 36, pp. 96–109, 2018.
- [101] J. J. Hwang, Y. A. Rim, Y. Nam, and J. H. Ju, "Recent developments in clinical applications of mesenchymal stem cells in the treatment of rheumatoid arthritis and osteoarthritis," *Frontiers in Immunology*, vol. 12, article 631291, 2021.
- [102] S. Jyothi Prasanna and V. Sowmya Jahnavi, "Wharton's jelly mesenchymal stem cells as off-the-shelf cellular therapeutics: a closer look into their regenerative and immunomodulatory properties," *The Open Tissue Engineering and Regenerative Medicine Journal*, vol. 4, no. SPEC. ISSUE 1, pp. 28–38, 2011.
- [103] W. S. Khan, S. R. Tew, A. B. Adesida, and T. E. Hardingham, "Human infrapatellar fat pad-derived stem cells express the pericyte marker 3G5 and show enhanced chondrogenesis after expansion in fibroblast growth factor-2," *Arthritis Research & Therapy*, vol. 10, no. 4, p. R74, 2008.
- [104] A. Hatakeyama, S. Uchida, H. Utsunomiya et al., "Isolation and characterization of synovial mesenchymal stem cell derived from hip joints: a comparative analysis with a matched control knee group," *Stem Cells International*, vol. 2017, Article ID 9312329, 13 pages, 2017.
- [105] P. R. Amable, M. V. Teixeira, R. B. Carias, J. M. Granjeiro, and R. Borojevic, "Protein synthesis and secretion in human mesenchymal cells derived from bone marrow, adipose tissue and Wharton's jelly," *Stem Cell Research & Therapy*, vol. 5, no. 2, p. 53, 2014.
- [106] G. Raicevic, M. Najar, B. Stamatopoulos et al., "The source of human mesenchymal stromal cells influences their TLR profile as well as their functional properties," *Cellular Immunology*, vol. 270, no. 2, pp. 207–216, 2011.
- [107] S. Balasubramanian, P. Venugopal, S. Sundarraj, Z. Zakaria, A. S. Majumdar, and M. Ta, "Comparison of chemokine and receptor gene expression between Wharton's jelly and bone marrow-derived mesenchymal stromal cells," *Cytotherapy*, vol. 14, no. 1, pp. 26–33, 2012.
- [108] F. Mckinnirey, B. Herbert, G. Vesey, and S. McCracken, "Immune modulation via adipose derived mesenchymal stem cells is driven by donor sex in vitro," *Scientific Reports*, vol. 11, no. 1, p. 12454, 2021.
- [109] S. Mohamed-Ahmed, I. Fristad, S. A. Lie et al., "Adipose-derived and bone marrow mesenchymal stem cells: a donor-matched comparison," *Stem Cell Research & Therapy*, vol. 9, no. 1, p. 168, 2018.
- [110] B. Mead, A. Logan, M. Berry, W. Leadbeater, and B. A. Scheven, "Paracrine-mediated neuroprotection and neurogenesis of axotomised retinal ganglion cells by human dental pulp stem cells: comparison with human bone marrow and adipose-derived mesenchymal stem cells," *PLoS One*, vol. 9, no. 10, article e109305, 2014.
- [111] A. K. Batsali, C. Pontikoglou, D. Koutroulakis et al., "Differential expression of cell cycle and WNT pathway-related genes accounts for differences in the growth and differentiation potential of Wharton's jelly and bone marrow-derived

- mesenchymal stem cells,” *Stem Cell Research & Therapy*, vol. 8, no. 1, p. 102, 2017.
- [112] C. Y. Li, X. Y. Wu, J. B. Tong et al., “Comparative analysis of human mesenchymal stem cells from bone marrow and adipose tissue under xeno-free conditions for cell therapy,” *Stem Cell Research & Therapy*, vol. 6, no. 1, p. 55, 2015.
- [113] S. Shin, J. Lee, Y. Kwon et al., “Comparative proteomic analysis of the mesenchymal stem cells secretome from adipose, bone marrow, placenta and Wharton's jelly,” *International Journal of Molecular Sciences*, vol. 22, no. 2, p. 845, 2021.
- [114] A. Heirani-Tabasi, S. Toosi, M. Mirahmadi et al., “Chemokine receptors expression in MSCs: comparative analysis in different sources and passages,” *Tissue engineering and regenerative medicine*, vol. 14, no. 5, pp. 605–615, 2017.
- [115] M. Najar, G. Raicevic, F. Jebbawi et al., “Characterization and functionality of the CD200-CD200R system during mesenchymal stromal cell interactions with T-lymphocytes,” *Immunology Letters*, vol. 146, no. 1-2, pp. 50–56, 2012.
- [116] E. Karaöz, P. C. Demircan, G. Erman, E. Güngörürler, and A. E. Sarıboyacı, “Comparative analyses of immunosuppressive characteristics of bone-marrow, Wharton's jelly, and adipose tissue-derived human mesenchymal stem cells,” *Turkish Journal of Haematology*, vol. 34, no. 3, pp. 213–225, 2017.
- [117] B. Purandare, T. Teklemariam, L. Zhao, and B. M. Hantash, “Temporal HLA profiling and immunomodulatory effects of human adult bone marrow- and adipose-derived mesenchymal stem cells,” *Regenerative Medicine*, vol. 9, no. 1, pp. 67–79, 2014.
- [118] C. Mennan, J. Garcia, S. Roberts, C. Hulme, and K. Wright, “A comprehensive characterisation of large-scale expanded human bone marrow and umbilical cord mesenchymal stem cells,” *Stem Cell Research & Therapy*, vol. 10, no. 1, p. 99, 2019.
- [119] E. T. Camilleri, M. P. Gustafson, A. Dudakovic et al., “Identification and validation of multiple cell surface markers of clinical-grade adipose-derived mesenchymal stromal cells as novel release criteria for good manufacturing practice-compliant production,” *Stem Cell Research & Therapy*, vol. 7, no. 1, p. 107, 2016.
- [120] A. K. Pappa, M. Caballero, R. G. Dennis et al., “Biochemical properties of tissue-engineered cartilage,” *The Journal of Craniofacial Surgery*, vol. 25, no. 1, pp. 111–115, 2014.
- [121] A. T. Cashion, M. Caballero, A. Halevi, A. Pappa, R. G. Dennis, and J. A. van Aalst, “Programmable mechanobioreactor for exploration of the effects of periodic vibratory stimulus on mesenchymal stem cell differentiation,” *BioResearch Open Access*, vol. 3, no. 1, pp. 19–28, 2014.
- [122] N. S. Remya and P. D. Nair, “Mechanoresponsiveness of human umbilical cord mesenchymal stem cells in in vitro chondrogenesis—a comparative study with growth factor induction,” *Journal of Biomedical Materials Research. Part A*, vol. 104, no. 10, pp. 2554–2566, 2016.
- [123] L. Zhao and M. S. Detamore, “Chondrogenic differentiation of stem cells in human umbilical cord stroma with PGA and PLLA scaffolds,” *Journal of Biomedical Science and Engineering*, vol. 3, no. 11, pp. 1041–1049, 2010.
- [124] C. Y. Fong, A. Subramanian, K. Gauthaman et al., “Human umbilical cord Wharton's jelly stem cells undergo enhanced chondrogenic differentiation when grown on nanofibrous scaffolds and in a sequential two-stage culture medium environment,” *Stem Cell Reviews and Reports*, vol. 8, no. 1, pp. 195–209, 2012.
- [125] X. Chen, F. Zhang, X. He et al., “Chondrogenic differentiation of umbilical cord-derived mesenchymal stem cells in type I collagen-hydrogel for cartilage engineering,” *Injury*, vol. 44, no. 4, pp. 540–549, 2013.
- [126] R. S. Nirmal and P. D. Nair, “Significance of soluble growth factors in the chondrogenic response of human umbilical cord matrix stem cells in a porous three dimensional scaffold,” *European Cells & Materials*, vol. 26, pp. 234–251, 2013.
- [127] B. Sridharan, S. M. Lin, A. T. Hwu, A. D. Laflin, and M. S. Detamore, “Stem cells in aggregate form to enhance chondrogenesis in hydrogels,” *PLoS One*, vol. 10, no. 12, article e0141479, 2015.
- [128] J. Jaipaew, P. Wangkulangkul, J. Meesane, P. Raungrut, and P. Puttawibul, “Mimicked cartilage scaffolds of silk fibroin/hyaluronic acid with stem cells for osteoarthritis surgery: morphological, mechanical, and physical clues,” *Materials Science & Engineering. C, Materials for Biological Applications*, vol. 64, pp. 173–182, 2016.
- [129] J. Wang, B. Sun, L. Tian et al., “Evaluation of the potential of rhTGF- β 3 encapsulated P(LLA-CL)/collagen nanofibers for tracheal cartilage regeneration using mesenchymal stem cells derived from Wharton's jelly of human umbilical cord,” *Materials Science & Engineering. C, Materials for Biological Applications*, vol. 70, Part 1, pp. 637–645, 2017.
- [130] E. Aleksander-Konert, P. Paduszyński, A. Zajdel, Z. Dzierżewicz, and A. Wilczok, “In vitro chondrogenesis of Wharton's jelly mesenchymal stem cells in hyaluronic acid-based hydrogels,” *Cellular & Molecular Biology Letters*, vol. 21, p. 11, 2016.
- [131] W. Zhang, J. Yang, Y. Zhu et al., “Extracellular matrix derived by human umbilical cord-deposited mesenchymal stem cells accelerates chondrocyte proliferation and differentiation potential in vitro,” *Cell and Tissue Banking*, vol. 20, no. 3, pp. 351–365, 2019.
- [132] L. Wang, I. Tran, K. Seshareddy, M. L. Weiss, and M. S. Detamore, “A comparison of human bone marrow-derived mesenchymal stem cells and human umbilical cord-derived mesenchymal stromal cells for cartilage tissue engineering,” *Tissue Engineering. Part A*, vol. 15, no. 8, pp. 2259–2266, 2009.
- [133] L. Wang, K. Seshareddy, M. L. Weiss, and M. S. Detamore, “Effect of initial seeding density on human umbilical cord mesenchymal stromal cells for fibrocartilage tissue engineering,” *Tissue Engineering. Part A*, vol. 15, no. 5, pp. 1009–1017, 2009.
- [134] L. Wang, L. Zhao, and M. S. Detamore, “Human umbilical cord mesenchymal stromal cells in a sandwich approach for osteochondral tissue engineering,” *Journal of Tissue Engineering and Regenerative Medicine*, vol. 5, no. 9, pp. 712–721, 2011.
- [135] L. Qi, R. Wang, Q. Shi, M. Yuan, M. Jin, and D. Li, “Umbilical cord mesenchymal stem cell conditioned medium restored the expression of collagen II and aggrecan in nucleus pulposus mesenchymal stem cells exposed to high glucose,” *Journal of Bone and Mineral Metabolism*, vol. 37, no. 3, pp. 455–466, 2019.
- [136] L. Penolazzi, M. Pozzobon, L. S. Bergamin et al., “Extracellular matrix from decellularized Wharton's jelly improves the behavior of cells from degenerated intervertebral disc,” *Frontiers in Bioengineering and Biotechnology*, vol. 8, p. 262, 2020.
- [137] S. K. Leckie, G. A. Sowa, B. P. Bechara et al., “Injection of human umbilical tissue-derived cells into the nucleus

- pulposus alters the course of intervertebral disc degeneration in vivo," *The Spine Journal*, vol. 13, no. 3, pp. 263–272, 2013.
- [138] N. Beeravolu, J. Brougham, I. Khan, C. McKee, M. Perez-Cruet, and G. R. Chaudhry, "Human umbilical cord derivatives regenerate intervertebral disc," *Journal of Tissue Engineering and Regenerative Medicine*, vol. 12, no. 1, pp. e579–e591, 2018.
- [139] M. Perez-Cruet, N. Beeravolu, C. McKee et al., "Potential of human nucleus pulposus-like cells derived from umbilical cord to treat degenerative disc disease," *Neurosurgery*, vol. 84, no. 1, pp. 272–283, 2019.
- [140] S. Ekram, S. Khalid, I. Bashir, A. Salim, and I. Khan, "Human umbilical cord-derived mesenchymal stem cells and their chondroprogenitor derivatives reduced pain and inflammation signaling and promote regeneration in a rat intervertebral disc degeneration model," *Molecular and Cellular Biochemistry*, vol. 476, no. 8, pp. 3191–3205, 2021.
- [141] N. Saulnier, E. Viguier, E. Perrier-Groult et al., "Intra-articular administration of xenogeneic neonatal mesenchymal stromal cells early after meniscal injury down-regulates metalloproteinase gene expression in synovium and prevents cartilage degradation in a rabbit model of osteoarthritis," *Osteoarthritis and Cartilage*, vol. 23, no. 1, pp. 122–133, 2015.
- [142] A. L. Raines, M. Shih, L. Chua, C. Su, S. C. Tseng, and J. O'Connell, "Efficacy of particulate amniotic membrane and umbilical cord tissues in attenuating cartilage destruction in an osteoarthritis model," *Tissue Engineering. Part A*, vol. 23, no. 1-2, pp. 12–19, 2017.
- [143] H. S. Chang, K. C. Wu, H. W. Liu, T. Y. Chu, and D. C. Ding, "Human umbilical cord-derived mesenchymal stem cells reduce monosodium iodoacetate-induced apoptosis in cartilage," *Ci Ji Yi Xue Za Zhi*, vol. 30, no. 2, pp. 71–80, 2018.
- [144] B. Y. Zhang, B. Y. Wang, S. C. Li et al., "Evaluation of the curative effect of umbilical cord mesenchymal stem cell therapy for knee arthritis in dogs using imaging technology," *Stem Cells International*, vol. 2018, Article ID 1983025, 12 pages, 2018.
- [145] S. E. Kim, A. Pozzi, J. C. Yeh et al., "Intra-articular umbilical cord derived mesenchymal stem cell therapy for chronic elbow osteoarthritis in dogs: a Double-Blinded, Placebo-Controlled Clinical Trial," *Frontiers in veterinary science*, vol. 6, p. 474, 2019.
- [146] Y. Geng, J. Chen, M. Alahdal et al., "Intra-articular injection of hUC-MSCs expressing miR-140-5p induces cartilage self-repairing in the rat osteoarthritis," *Journal of Bone and Mineral Metabolism*, vol. 38, no. 3, pp. 277–288, 2020.
- [147] K. C. Wu, Y. H. Chang, H. W. Liu, and D. C. Ding, "Transplanting human umbilical cord mesenchymal stem cells and hyaluronate hydrogel repairs cartilage of osteoarthritis in the minipig model," *Ci Ji Yi Xue Za Zhi*, vol. 31, no. 1, pp. 11–19, 2019.
- [148] C. Magri, M. Schramme, M. Febre et al., "Comparison of efficacy and safety of single versus repeated intra-articular injection of allogeneic neonatal mesenchymal stem cells for treatment of osteoarthritis of the metacarpophalangeal/metatarsophalangeal joint in horses: a clinical pilot study," *PLoS One*, vol. 14, no. 8, article e0221317, 2019.
- [149] J. Perry, H. S. McCarthy, G. Bou-Gharios et al., "Injected human umbilical cord-derived mesenchymal stromal cells do not appear to elicit an inflammatory response in a murine model of osteoarthritis," *Osteoarthritis and cartilage open*, vol. 2, no. 2, article 100044, 2020.
- [150] D. Xing, J. Wu, B. Wang et al., "Intra-articular delivery of umbilical cord-derived mesenchymal stem cells temporarily retard the progression of osteoarthritis in a rat model," *International Journal of Rheumatic Diseases*, vol. 23, no. 6, pp. 778–787, 2020.
- [151] X. D. Wang, X. C. Wan, A. F. Liu, R. Li, and Q. Wei, "Effects of umbilical cord mesenchymal stem cells loaded with graphene oxide granular lubrication on cytokine levels in animal models of knee osteoarthritis," *International Orthopaedics*, vol. 45, no. 2, pp. 381–390, 2021.
- [152] Y. Liu, R. Mu, S. Wang et al., "Therapeutic potential of human umbilical cord mesenchymal stem cells in the treatment of rheumatoid arthritis," *Arthritis Research & Therapy*, vol. 12, no. 6, p. R210, 2010.
- [153] C. C. Wu, T. C. Wu, F. L. Liu, H. K. Sytwu, and D. M. Chang, "TNF- α inhibitor reverse the effects of human umbilical cord-derived stem cells on experimental arthritis by increasing immunosuppression," *Cellular Immunology*, vol. 273, no. 1, pp. 30–40, 2012.
- [154] J. Gu, W. Gu, C. Lin et al., "Human umbilical cord mesenchymal stem cells improve the immune-associated inflammatory and prothrombotic state in collagen type-II-induced arthritic rats," *Molecular Medicine Reports*, vol. 12, no. 5, pp. 7463–7470, 2015.
- [155] Q. Zhang, Q. Li, J. Zhu et al., "Comparison of therapeutic effects of different mesenchymal stem cells on rheumatoid arthritis in mice," *PeerJ*, vol. 7, p. e7023, 2019.
- [156] D. Ma, K. Xu, G. Zhang et al., "Immunomodulatory effect of human umbilical cord mesenchymal stem cells on T lymphocytes in rheumatoid arthritis," *International Immunopharmacology*, vol. 74, article 105687, 2019.
- [157] M. Vohra, A. Sharma, R. Bagga, and S. K. Arora, "Human umbilical cord-derived mesenchymal stem cells induce tissue repair and regeneration in collagen-induced arthritis in rats," *Journal of Clinical and Translational Research*, vol. 6, no. 6, pp. 203–216, 2020.
- [158] K. Xu, D. Ma, G. Zhang et al., "Human umbilical cord mesenchymal stem cell-derived small extracellular vesicles ameliorate collagen-induced arthritis via immunomodulatory T lymphocytes," *Molecular Immunology*, vol. 135, pp. 36–44, 2021.
- [159] P. Zhao, S. Liu, Y. Bai et al., "hWJECM-derived oriented scaffolds with autologous chondrocytes for rabbit cartilage defect repairing," *Tissue Engineering. Part A*, vol. 24, no. 11-12, pp. 905–914, 2018.
- [160] Y. Zhang, S. Liu, W. Guo et al., "Human umbilical cord Wharton's jelly mesenchymal stem cells combined with an acellular cartilage extracellular matrix scaffold improve cartilage repair compared with microfracture in a caprine model," *Osteoarthritis and Cartilage*, vol. 26, no. 7, pp. 954–965, 2018.
- [161] Y. Zhang, C. Hao, W. Guo et al., "Co-culture of hWJMSCs and pACs in double biomimetic ACECM oriented scaffold enhances mechanical properties and accelerates articular cartilage regeneration in a caprine model," *Stem Cell Research & Therapy*, vol. 11, no. 1, p. 180, 2020.
- [162] L. Yan and X. Wu, "Exosomes produced from 3D cultures of umbilical cord mesenchymal stem cells in a hollow-fiber bioreactor show improved osteochondral regeneration activity," *Cell Biology and Toxicology*, vol. 36, no. 2, pp. 165–178, 2020.
- [163] Z. Li, Y. Bi, Q. Wu et al., "A composite scaffold of Wharton's jelly and chondroitin sulphate loaded with human umbilical cord mesenchymal stem cells repairs articular cartilage

- defects in rat knee,” *Journal of Materials Science. Materials in Medicine*, vol. 32, no. 4, p. 36, 2021.
- [164] N. H. Dormer, M. Singh, L. Zhao, N. Mohan, C. J. Berkland, and M. S. Detamore, “Osteochondral interface regeneration of the rabbit knee with macroscopic gradients of bioactive signals,” *Journal of Biomedical Materials Research. Part A*, vol. 100, no. 1, pp. 162–170, 2012.
- [165] S. Liu, Y. Jia, M. Yuan et al., “Repair of Osteochondral Defects Using Human Umbilical Cord Wharton’s Jelly- Derived Mesenchymal Stem Cells in a Rabbit Model,” *BioMed Research International*, vol. 2017, Article ID 8760383, 12 pages, 2017.
- [166] S. Jiang, G. Tian, Z. Yang et al., “Enhancement of acellular cartilage matrix scaffold by Wharton’s jelly mesenchymal stem cell-derived exosomes to promote osteochondral regeneration,” *Bioactive Materials*, vol. 6, no. 9, pp. 2711–2728, 2021.
- [167] J. Matas, M. Orrego, D. Amenabar et al., “Umbilical cord-derived mesenchymal stromal cells (MSCs) for knee osteoarthritis: repeated MSC dosing is superior to a single MSC dose and to hyaluronic acid in a controlled randomized phase I/II trial,” *Stem Cells Translational Medicine*, vol. 8, no. 3, pp. 215–224, 2019.
- [168] I. H. Dilogu, A. F. Canintika, A. L. Hanitya, J. A. Pawitan, I. K. Liem, and J. Pandelaki, “Umbilical cord-derived mesenchymal stem cells for treating osteoarthritis of the knee: a single-arm, open-label study,” *European Journal of Orthopaedic Surgery and Traumatology*, vol. 30, no. 5, pp. 799–807, 2020.
- [169] O. G. Mead and L. P. Mead, “Intra-articular injection of amniotic membrane and umbilical cord particulate for the management of moderate to severe knee osteoarthritis,” *Orthopedic Research and Reviews*, vol. 12, pp. 161–170, 2020.
- [170] L. Wang, S. Huang, S. Li et al., “Efficacy and safety of umbilical cord mesenchymal stem cell therapy for rheumatoid arthritis patients: a prospective phase I/II study,” *Drug Design, Development and Therapy*, vol. Volume 13, pp. 4331–4340, 2019.
- [171] T. Qi, H. Gao, Y. Dang, S. Huang, and M. Peng, “Cervus and cucumis peptides combined umbilical cord mesenchymal stem cells therapy for rheumatoid arthritis,” *Medicine (Baltimore)*, vol. 99, no. 28, article e21222, 2020.
- [172] X. He, Y. Yang, M. Yao et al., “Combination of human umbilical cord mesenchymal stem (stromal) cell transplantation with IFN- γ treatment synergistically improves the clinical outcomes of patients with rheumatoid arthritis,” *Annals of the Rheumatic Diseases*, vol. 79, no. 10, pp. 1298–1304, 2020.

Research Article

Characterization and miRNA Profiling of Extracellular Vesicles from Human Osteoarthritic Subchondral Bone Multipotential Stromal Cells (MSCs)

Clara Sanjurjo-Rodríguez ^{1,2,3} Rachel E. Crossland ¹ Monica Reis ^{1,4}
Hemant Pandit ^{2,5} Xiao-nong Wang ¹ and Elena Jones ²

¹Translational and Clinical Research Institute, Newcastle University, Newcastle upon Tyne, NE2 4HH, UK

²Leeds Institute of Rheumatic and Musculoskeletal Medicine, University of Leeds, Leeds LS9 7TF, UK

³Cell Therapy and Regenerative Medicine Group, Physiotherapy, Medicine and Biomedical Sciences Department, Universidade da Coruña, A Coruña 15006, Spain

⁴Department of Pediatrics, Harvard Medical School, Boston, MA 02115, USA

⁵Leeds Teaching Hospitals NHS Trust, Leeds LS7 4SA, UK

Correspondence should be addressed to Xiao-nong Wang; x.n.wang@newcastle.ac.uk and Elena Jones; e.jones@leeds.ac.uk

Received 20 April 2021; Revised 26 July 2021; Accepted 19 August 2021; Published 9 October 2021

Academic Editor: Quanyi Guo

Copyright © 2021 Clara Sanjurjo-Rodríguez et al. This is an open access article distributed under the Creative Commons Attribution License, which permits unrestricted use, distribution, and reproduction in any medium, provided the original work is properly cited.

Osteoarthritis (OA) is a heterogeneous disease in which the cross-talk between the cells from different tissues within the joint is affected as the disease progresses. Extracellular vesicles (EVs) are known to have a crucial role in cell-cell communication by means of cargo transfer. Subchondral bone (SB) resident cells and its microenvironment are increasingly recognised to have a major role in OA pathogenesis. The aim of this study was to investigate the EV production from OA SB mesenchymal stromal cells (MSCs) and their possible influence on OA chondrocytes. Small EVs were isolated from OA-MSCs, characterized and cocultured with chondrocytes for viability and gene expression analysis, and compared to small EVs from MSCs of healthy donors (H-EVs). OA-EVs enhanced viability of chondrocytes and the expression of chondrogenesis-related genes, although the effect was marginally lower compared to that of the H-EVs. miRNA profiling followed by unsupervised hierarchical clustering analysis revealed distinct microRNA sets in OA-EVs as compared to their parental MSCs or H-EVs. Pathway analysis of OA-EV miRNAs showed the enrichment of miRNAs implicated in chondrogenesis, stem cells, or other pathways related to cartilage and OA. In conclusion, OA SB MSCs were capable of producing EVs that could support chondrocyte viability and chondrogenic gene expression and contained microRNAs implicated in chondrogenesis support. These EVs could therefore mediate the cross-talk between the SB and cartilage in OA potentially modulating chondrocyte viability and endogenous cartilage regeneration.

1. Introduction

Osteoarthritis (OA) is a heterogeneous disease that affects synovial joints, which starts from injury or as a molecular alteration and results in structural changes, such as loss of cartilage, bone sclerosis or osteophyte formation, pain, and other clinical symptoms [1]. OA is one of the most prevalent joint diseases and frequently causes disability, with high incidence worldwide due to population aging [2–4].

Early OA changes in articular cartilage include regional proteoglycan loss, chondrocyte clustering, collagen disorganization, and tissue fibrillation [5]. While the catabolic/anabolic imbalance in bone is associated to overloading microdamages, in cartilage it seems to be associated with persistent, low-grade inflammation [6]. It begins in the synovial tissue where it is characterized by cytokine release and immune cell infiltration and is commonly associated with pain in OA [7, 8]. With OA progression, subchondral

bone (SB) gains more influence on OA chondrocytes as osteochondral junction becomes more porous [5, 6, 9–13]. Bone-targeting treatments have a positive effect on OA chondrocytes [6] while cocultures of OA subchondral bone osteoblasts [10] or osteoclasts [14] with OA chondrocytes have a negative effect on chondrocytes' viability or anabolic activity. The bone-cartilage crosstalk is therefore emerging as a novel therapeutic target for OA [13, 15].

In OA, different types of SB cells enter normally the non-vascular calcified cartilage through the cracks and fissures or along the newly formed vessels, all contributing to cartilage destruction “from below” [12, 16–18]. These SB cells include osteo/chondroclasts that dissolve the calcified cartilage matrix [18, 19], neurons that exacerbate joint pain [13, 20, 21], and multipotential stromal cells (MSCs) that may be involved in both, cartilage formation and cartilage degradation [12, 18]. Besides the cells themselves, SB-cartilage communication in OA may be mediated via soluble proteins [22], for example, VEGF or IL6, which are increased in damaged SB areas in OA [23], and or via extracellular vesicles (EVs); the influence of which on OA chondrocyte homeostasis remains poorly understood [24].

EVs are nonreplicative bilipid-layered particles that are released naturally from most of the cells, carrying peptides, miRNAs, lipids, and other molecules in their cargo, which can be transmitted to other cells. They can be broadly subcategorized based on their biogenesis, size, and markers into exosomes, microvesicles, and apoptotic bodies [25–27]. EVs have a crucial role in cell-to-cell communication, allowing the cargo transfer through endocytic internalization or direct fusion to provoke a biological response [28–31]. Recently, studies of EVs in joint diseases and their therapeutic use started to rise [24, 32–35], but these studies are primarily focused on EVs derived from osteoarthritic synovial fluid rather than SB [36, 37].

The aim of this study was to investigate EV production from SB MSCs, the cells previously shown to contribute to disease pathogenesis in OA [18, 38, 39]. We hypothesised that SB MSC-EVs may have an influence on OA chondrocytes' viability and their anabolic gene expression and that they contain specific sets of miRNAs that are different from their parental MSCs.

2. Materials and Methods

2.1. Patients and Cells. Ethical approval for cartilage and MSC osteoarthritic sample collection was obtained from the NRES Committees Yorkshire & The Humber—South Yorkshire (14/YH/0087) and NRES Committees North East—Newcastle & North Tyneside 1 (14/NE/1212). From this collection, 11 cartilage samples (6 females and 5 males with median age 74 years, range 55–83) and 5 subchondral bone samples (3 females and 2 males with median age 73 years, range 64–83) were collected from total knee arthroplasty.

Healthy MSC collection was obtained from surplus material remaining in 10 bone marrow-processing bags used for hematopoietic stem cell transplantation (NRES Committee North East—Newcastle & North Tyneside 2, 14/NE/1136).

Patients were 7 males and 3 females with the median age of 14 years (range 4–44).

2.2. Isolation and Culture of OA Chondrocytes. Articular cartilage was harvested from tibiofemoral surfaces, and chondrocytes were isolated as previously described [18]. Briefly, the cartilage was harvested and minced using a scalpel and digested with collagenase overnight. Chondrocytes were expanded in a high-glucose Dulbecco's Modified Eagle Medium (DMEM; MilliporeSigma, USA) supplemented with glutamine, 10% fetal bovine serum (FBS; ThermoFisher Scientific, USA), and 1% penicillin/streptomycin (P/S; MilliporeSigma, USA). Media were changed twice a week, and subculture was performed when chondrocytes reached 80% confluence, and passaged to passage 2 (p2).

2.3. Isolation and Culture of MSCs. Osteoarthritic MSCs were obtained from the subchondral bone of medial femoral condyles after removal of cartilage, as previously described [18]. Medial condyles were chosen as they commonly display a more prominent OA phenotype compared to lateral condyles [18, 40]. Bone was weighted and mechanically minced into small fragments with a rongeur and digested with collagenase, as previously described [18]. MSC cultures were established in StemMACs™ MSC expansion media (Miltenyi Biotec, Germany) then transferred to DMEM supplemented with 5% human platelet lysate (PL; PLTMax, MilliporeSigma), 100 IU/ml penicillin, 100ug/ml streptomycin, 2,500 IU/ml heparin and 2 mM L-glutamine (all from MilliporeSigma) (5%PL/DMEM).

Healthy control MSCs were cultured from surplus cells (wash-outs) of hematopoietic stem cell transplantation bags, as previously described [41]. Briefly, bone marrow mononuclear cells (MNCs) were isolated by density gradient centrifugation and cultured in 5%PL/DMEM.

Both types of MSCs were previously characterized [18, 41] (Supplementary Figures 1 and 2) according to the criteria set by the International Society of Cellular Therapy (ISCT) [42] and expanded in 5%PL/DMEM to passage 3 before changing the media to EV-depleted 5%PL/DMEM, for EV isolation. EV-depleted MSC media were prepared by 18-hour ultracentrifugation of 10%PL/DMEM at $100,000 \times g$ followed by 1:1 dilution in DMEM.

2.4. EV Isolation from OA and Control MSCs. EVs were isolated from both osteoarthritic (OA-EVs) and control healthy (H-EVs) p3 MSCs, as previously described [41]. In brief, when the cells reached 50% confluence, they were washed twice with phosphate buffered saline (PBS, MilliporeSigma) and cultured in a 5%PL/DMEM-EV-depleted medium, for a further duration of 48 hours prior to harvesting the conditioned media and MSC-EV isolation. In addition to collecting the conditioned medium, the number of MSCs in the flask was counted and an aliquot of cells was frozen as pellets in a QIAzol lysis reagent (Qiagen, Germany) for RNA isolation. To obtain MSC-EVs, the conditioned medium was centrifuged at $400 \times g$ for 5 min, $2,000 \times g$ for 20 min at 4°C, then transferred to ultracentrifuge tubes (Beckman Coulter, USA) and centrifuged again sequentially at $10,000 \times g$ for

45 min and at $100,000 \times g$ for 90 min at 4°C , using a 45Ti rotor (Beckman Coulter) in a Optima XE-90 ultracentrifuge (Beckman Coulter). The MSC-EVs pellet was washed in PBS then resuspended in approximately 200–300 μl sterile PBS and stored at -80°C .

2.5. MSC-EV Characterization. MSC-EV characterization was performed by electron microscopy (TEM), flow cytometry, and nanoparticle tracking analysis (NTA) [41].

For TEM, 5 μl of MSC-EVs was adsorbed for 30 s onto a carbon-coated, glow-discharged grid. Excess liquid was removed and samples were stained with 1% uranyl acetate (Agar Scientific, UK). Excess uranyl acetate solution was removed, and the MSC-EV-loaded grids were dried then examined using a Hitachi HT7800 transmission electron microscope. Digital images were collected using an Emsis Xarosa camera with Radius software.

EV surface markers CD63, CD9, and CD81 were analyzed by flow cytometry following coating of 4 μm aldehyde/sulfate latex beads (ThermoFisher Scientific) with 10 μl of MSC-EVs suspension. The reaction was stopped by incubation with 1 M glycine (MilliporeSigma), and the MSC-EV-bead complex was washed twice with PBS then incubated with mouse anti-human PE CD63 (clone H5C6), PerCPCy5.5 CD9 (clone M-L13), and APC CD81 (clone JS-81) antibodies or corresponding isotype controls (all from BD Biosciences, USA). Following further washes, cells were resuspended in particle-free PBS (ThermoFisher Scientific) and data was acquired using a BD FACS Canto II cytometer (BD Biosciences) and analyzed with FlowJo 10.0 software (Tree Star Inc., USA).

For NTA, MSC-EV pellets were diluted with sterile particle-free PBS and analyzed using Nanosight LM10 (Malvern Panalytical Ltd, UK), as described by the manufacturer's protocol. Three 60 s measurements of the particle size and concentration were measured for each sample. The acquired data was processed using NTA 2.3 software (Malvern Panalytical Ltd).

2.6. ATP-Based Viability Assessment of Chondrocytes following Coculture with MSC-EVs. The CellTiter-Glo 2.0 Luminescent Cell Viability Assay (Promega, UK) measures total ATP levels produced by metabolically active cells. For this assay, EV-depleted chondrocyte media was first prepared by 18-hour ultracentrifugation of DMEM/Nutrient Mixture F-12 (DMEM:F12, ThermoFisher Scientific) containing 10% FBS (DMEM:F12/10%FBS) at $100,000 \times g$ and optimal conditions (5×10^3 chondrocytes/well, 24-hour treatment duration) established by seeding different cell concentrations and determining the ATP levels.

To determine the effect of MSC-EVs (both OA- and H-EVs) on chondrocytes' ATP levels, EVs from 6×10^4 MSCs were added into 300 μl of EV-depleted DMEM:F12/10%FBS containing 1.5×10^4 chondrocytes (MSC to chondrocyte ratio of 4:1 [43]), and 100 μl of the mix (containing 5×10^3 chondrocytes) was seeded in triplicate wells of the same 96-well Nunclon delta plates. As a control, 5×10^3 chondrocytes without MSC-EVs were plated in triplicate wells containing 100 μl of the same EV-depleted DMEM:F12/10%FBS media.

A second dose of EVs from 6×10^4 MSCs was added on day 3, and luminescence measurements were performed on day 5. For this, 100 μl of equilibrated CellTiter-Glo 2.0 reagent was added to the wells and luminescence was measured 10 min afterwards, using the Spark multimode microplate reader (Tecan, Switzerland) and the Sparkcontrol method editor software (Tecan). In these experiments, OA-EVs and H-EVs were from 3 and 6 MSC donors, respectively.

2.7. Three-Dimensional (3D) Pellet Coculture of MSC-EVs and OA Chondrocytes. To characterize whether MSC-EVs (both OA- and H-EVs) have an effect on chondrocytes' expression of genes implicated in the extracellular matrix (ECM) metabolism, EVs from 6×10^6 OA or control MSCs were added to 6×10^5 chondrocytes resuspended in EV-depleted DMEM:F12/10%FBS media (MSC-EVs to chondrocytes ratio 10:1). Afterwards, chondrocytes were separated into 3 different tubes and centrifuged at $450 \times g$ for 10 min to create 3D pellets, for each treatment. In addition, 2×10^5 chondrocytes were pelleted in EV-depleted DMEM:F12/10%FBS media without MSC EVs and used as negative controls (No EVs). After 2 and 7 days, EV-depleted media was half-changed and cell pellets were taken for RNA isolation. In these experiments, OA-EVs and H-EVs were from 2 different donors each, and the chondrocyte cultures ($n = 3$) were not donor-matched to OA-MSCs.

Longer-term effect of OA and healthy MSC-EVs on chondrocyte gene expression in the pellet culture was tested using a single-donor chondrocyte culture and MSC to chondrocyte ratio of 4:1, with half-change medium every 3–4 days.

2.8. RNA Isolation from OA and Healthy MSC-EVs, Parental MSCs, and MSC-EV-Treated Chondrocytes. For isolation of RNA from EVs (60 μl of the EVs suspension in PBS), total Exosome RNA and Protein Isolation kit (ThermoFisher Scientific) were used following the manufacturer's instructions. The RNA concentration from EVs was assessed using the Bioanalyzer 2100 and the RNA 6000 pico kit (Agilent Technologies, USA).

RNA from parental MSCs (from which EVs were produced from) and from chondrocyte pellets was obtained using the miRNeasy Mini kit (Qiagen) following the manufacturer's instructions. The RNA was quantified using the Nanodrop spectrophotometer (ThermoFisher Scientific).

2.9. miRNA Profiling from OA and Healthy MSC-EVs. miRNA profiling was carried out using the nCounter® Human v3.0 miRNA Expression Assay Kit (NanoString Technologies), based on miRBase v21, from total RNA obtained from OA-EVs and H-EVs as well as parental MSCs (the MSCs from which the respective EVs were obtained from). The code set incorporated 799 mature microRNAs and included 6 positive controls, 8 negative controls, 6 ligation controls, 5 mRNA housekeeping controls (*ACTB*, *B2M*, *GAPDH*, *RPL19* and *RPLP0*) and 5 spike-in controls. miRtag ligation, miRNA CodeSet Hybridization and post-hybridization were performed following the manufacturer's instructions. The resulting miRNA expression profiles were

TABLE 1: Taqman assays used for qPCR on MSC-EV (both OA- and H-EVs) treated chondrocytes.

Gene name	Gene symbol	Probe/assay ID
SRY (sex determining region Y)-box 9	SOX9	Hs00165814_m1
Collagen type II alpha 1 chain	COL2A1	Hs00264051_m1
Aggrecan	ACAN	Hs04982230_s1
Collagen type I alpha 2 chain	COL1	Hs01028969_m1
Matrix metalloproteinase 13	MMP13	Hs00942586_m1
A disintegrin and metalloproteinase with thrombospondin motifs 4	ADAMTS4	Hs00192708_m1
A disintegrin and metalloproteinase with thrombospondin motifs 5	ADAMTS5	Hs01095518_m1
Glyceraldehyde 3-phosphate dehydrogenase	GAPDH	Hs02758991_g1

analyzed using the nSolver software V4 (NanoString Technologies). Samples were normalized to the geometric mean of the Top100 miRNAs taking into account background thresholding and positive control normalization (geometric mean). Fold change (FC) expression differences between groups were calculated using nSolver v2.5 (NanoString Technologies) ratio data, based on normalized count data. Further analysis was performed using a pipeline designed by Newcastle University, Haematological Sciences Department. This integrated a number of R (R project) statistical packages in the R programming language; p values between two groups were generated using a two-tailed t -test. Analysis on miRNA targets was performed using mirWalk [44], mirPath from DIANA Tools [45], Reactome [46] and miRDIP [47], utilizing default parameters for Human or *Homo sapiens*.

2.10. Quantitative Real Time PCR. Gene expression was assessed in 2, 7, and 21 day-cultured OA and healthy MSC-EV-treated pellets and control chondrocyte pellets. Total RNA was isolated and reverse transcribed with the High-Capacity cDNA Reverse Transcription kit (Applied Biosystems). qRT-PCR was performed using the Taqman assays (ThermoFisher Scientific; Table 1) and Fast Advanced Master Mix (Applied Biosystems, ThermoFisher Scientific) in a QuantStudio 3 Real-Time PCR system (Applied Biosystems). Genes for the analysis were selected based on the literature evidence of their involvement in the chondrogenesis and chondrocyte catabolic and anabolic activity [12, 48] and are shown in Table 1.

3. Results

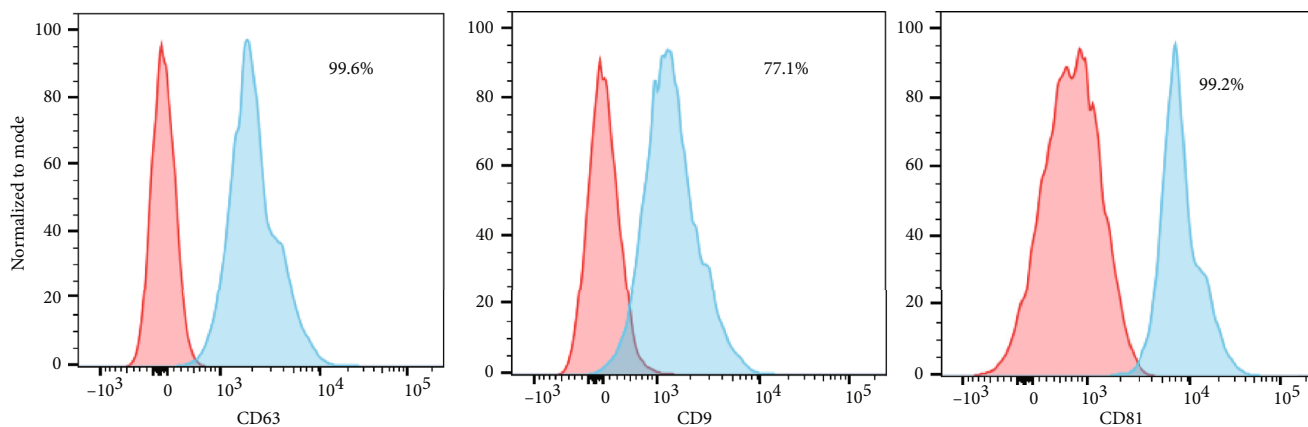
3.1. EV Characterization. EVs isolated from OA-MSCs ($n = 5$) showed similar basic characteristics (Figure 1) than previously shown for control healthy MSCs [41]. Expression of different markers of small EVs [25] in OA-EV preparations was first tested using flow cytometry (Figure 1(a)). CD63 (95.9% \pm 7.4%) and CD81 (90.1% \pm 13.0%) were the highest expressed markers followed by CD9 (66.1% \pm 23.8%) indicating presence of small EVs (Figure 1(a)). The morphology of OA-EVs observed using TEM was a typical cup-shape (Figure 1(b)). The concentration of particles and the size of the EVs was measured using NTA (Figure 1(c), Table 2). The mode of the OA-EV size ranged between 107.9-

169.8 nm (Table 2) not significantly different to H-EVs (81.3-132.9), and consistent with the modal size previously reported for control H-EVs [41]. The mean concentration of particles per ml in OA-EV preparations was $1.38 \times 10^{11} \pm 2.07 \times 10^{10}$ and is similar to that of the H-EVs ($1.12 \times 10^{11} \pm 8.50 \times 10^9$) (Table 2). As cell number was counted after OA and healthy MSC-EV media collection, no differences ($p > 0.05$) were found in the mean number of particles obtained per cell from either OA or control MSCs: 634 ± 176 and 709 ± 447 , respectively. Neither difference was observed when comparing mean EV size between healthy and OA-MSC-EVs ($p > 0.05$): 112.7 ± 23.50 nm and 138.2 ± 25.68 nm, respectively, but OA-EVs seemed less variable than H-EVs (Figure 1(c)). These data indicated that OA-MSCs had a similar capacity to produce EVs with a comparable modal size and particle concentration as control healthy MSCs.

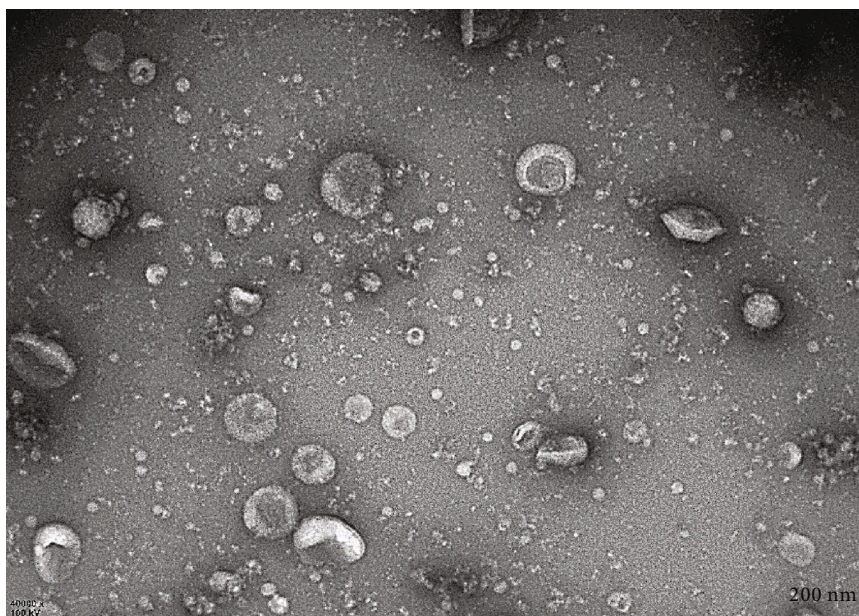
3.2. The Effects of OA and Healthy MSC-EVs on Chondrocyte Viability. An ATP-based viability assessment was performed following coculture of OA chondrocytes with OA- or H-EVs. When comparing untreated chondrocytes with those treated with control H-EVs, an average 6.27% increase in chondrocyte viability was found (p value = 0.020) (Figure 2(a)). OA-EV treated chondrocytes also showed increased viability compared to untreated chondrocytes (average 5.92%, p value = 0.042) (Figure 2(b)). However, the difference in the percentage increase of viability between OA and H-EVs failed to reach statistical significance (p value = 0.768) (Figure 2(c)).

3.3. The Effects of OA and Healthy MSC-EVs on Chondrocyte Gene Expression. In these experiments, pellet culture of chondrocytes and EVs was used to facilitate EV uptake by chondrocytes, as reported previously [49]. The media used in these experiments did not contain any chondrogenic inducers because the latter could ‘mask’ potentially smaller effects by EVs. To confirm that pellet culture environment was sufficient to induce chondrogenic gene up-regulation in chondrocytes, and to investigate how it affected the expression of the selected catabolic and anabolic genes, a time-course experiment in untreated pelleted chondrocytes from 4 donors was performed (Figure 3(a)).

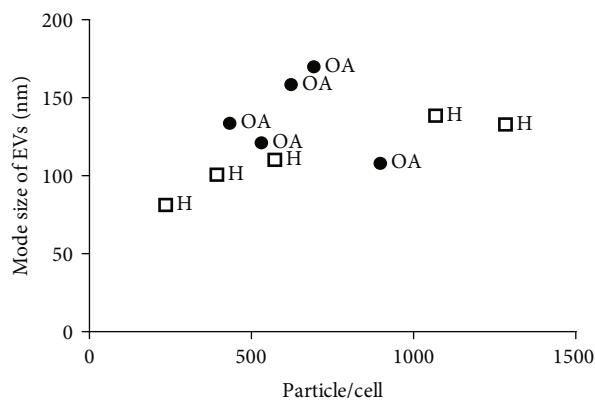
As expected, gradual increases in chondrogenesis markers SOX9, COL2 and ACAN, as well as COL1, were seen from day 2 onwards confirming that pellet culture in the



(a)



(b)



(c)

FIGURE 1: OA-MSC-EV characterization. (a) Flow cytometry of CD63, CD9, and CD81 surface markers (representative OA-EV sample). Red and blue histograms illustrate isotype controls and stained samples, respectively. (b) Transmission Electron Microscopy showing the cup-shape morphology of EVs (representative OA-EV sample, scale bar 200 nm). (c) Scatter plot showing size and number of particles/cell analysis of OA and control H-EVs, assessed by nanoparticle tracking analysis.

TABLE 2: Summary of EV characteristics isolated from OA and healthy MSCs: particle size, concentration of particles, and the number of cells from which EVs were obtained.

Sample	Mean (nm)	Particle size		Concentration of particles		Particles/cell*
		SD (nm)	Mode (nm)	Particles/ml*	Particles/frame*	
OA-EV1	161.6	69.3	169.8	$1.19 \times 10^{11} \pm 1.64 \times 10^{10}$	12.1 ± 1.7	692 ± 95
OA-EV2	172.2	75.0	121.1	$1.30 \times 10^{11} \pm 1.69 \times 10^{10}$	13.2 ± 1.7	531 ± 69
OA-EV3	177.2	87.4	158.4	$1.15 \times 10^{11} \pm 1.07 \times 10^{10}$	11.7 ± 1.1	622 ± 58
OA-EV4	160.0	71.6	133.7	$1.35 \times 10^{11} \pm 3.20 \times 10^{10}$	13.7 ± 3.2	433 ± 103
OA-EV5	172.0	71.1	107.9	$1.92 \times 10^{11} \pm 2.75 \times 10^{10}$	29.2 ± 4.2	897 ± 128
H-EV1	184.1	89.4	132.9	$2.36 \times 10^{11} \pm 2.53 \times 10^{10}$	77.4 ± 8.1	3670 ± 393
H-EV2	152.3	67.4	110.2	$7.43 \times 10^{10} \pm 4.76 \times 10^9$	61.7 ± 4.0	1265 ± 81
H-EV3	125.2	52.9	100.7	$5.58 \times 10^{10} \pm 2.9 \times 10^9$	27.2 ± 1.5	1240 ± 64
H-EV4	154.8	63.6	107.9	$9.41 \times 10^{10} \pm 1.11 \times 10^{10}$	46.7 ± 5.7	752 ± 88
H-EV5	129.6	55.3	81.3	$5.76 \times 10^{10} \pm 3.32 \times 10^9$	21.6 ± 1.4	694 ± 40
H-EV6	152.1	79.7	98.4	$1.53 \times 10^{11} \pm 3.59 \times 10^9$	77.7 ± 2.2	3035 ± 71

*Data shows mean \pm SD from measurements of 3 different frames within the Nanosight.

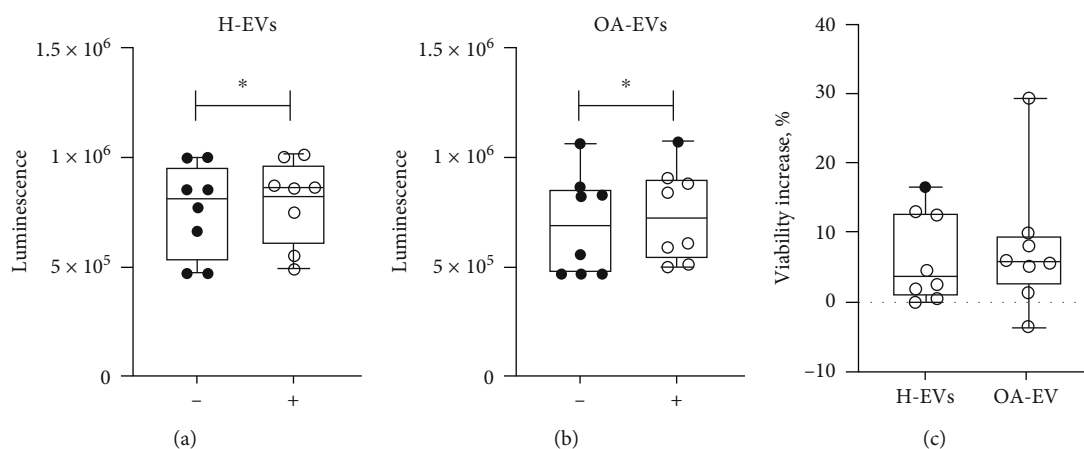


FIGURE 2: The effect of EVs on chondrocyte viability in CellTiter-Glo assay. (a) Viability of chondrocytes measured in luminescence units when treated with H-EVs (+), compared with untreated OA chondrocytes (-). (b) Viability of chondrocytes when treated with EVs from OA-MSCs (+), compared with untreated chondrocytes (-). (c) Percentage increase in viability above the untreated controls between H-EVs and OA-EVs. Horizontal bars show medians, and whiskers represent min to max. * p value < 0.05 . Paired t -test analysis.

absence of chondrogenic inducers was sufficient to monitor the effect of EVs on chondrogenic gene up-regulation. The up-regulation of other transcripts (*MMP13*, *ADAMTS4* and *ADAMTS5*) did not similarly continue beyond day 7 (Figure 3(a)).

An average 18% up-regulation of *SOX9* transcript compared to untreated chondrocytes was observed in coculture with H-EVs and the effect was smaller (average 4% increase) in coculture with OA-EVs however the differences failed to reach statistical significance (Figure 3(b)). A trend for lower-level upregulation of *SOX9* by OA-EVs compared to H-EVs, as well as of transcripts for mature cartilage ECM proteins *COL2* and *ACAN* was evident following longer-term culture (Figure 3(c)). Higher *COL2/COL1* ratio indicating chondrogenic lineage commitment displayed the same trend, unlike the expression of cartilage catabolic molecules

where no specific trends were found (both short- and long-term) (Figure 3(c)).

3.4. miRNA Profiling. Albeit not being statistically significant, average of 1.5-fold differences in chondrocytes' chondrogenesis gene expression (*SOX9*, *COL2* and *ACAN* expression at 21 days), indicated potential differences in microRNA cargo between H-EVs and OA-EVs. microRNA expression profiling was next performed on H-EVs and OA-EVs ($n = 4$ cultures each) using NanoString technology ($n = 799$ microRNA). Expression of 590 mature microRNAs was detected across all samples after correcting for background (Supplementary Data 1). Healthy and OA-EVs showed distinct microRNA expression profiles, as demonstrated using unsupervised hierarchical clustering analysis (Figure 4). There were 75 miRNAs that were significantly

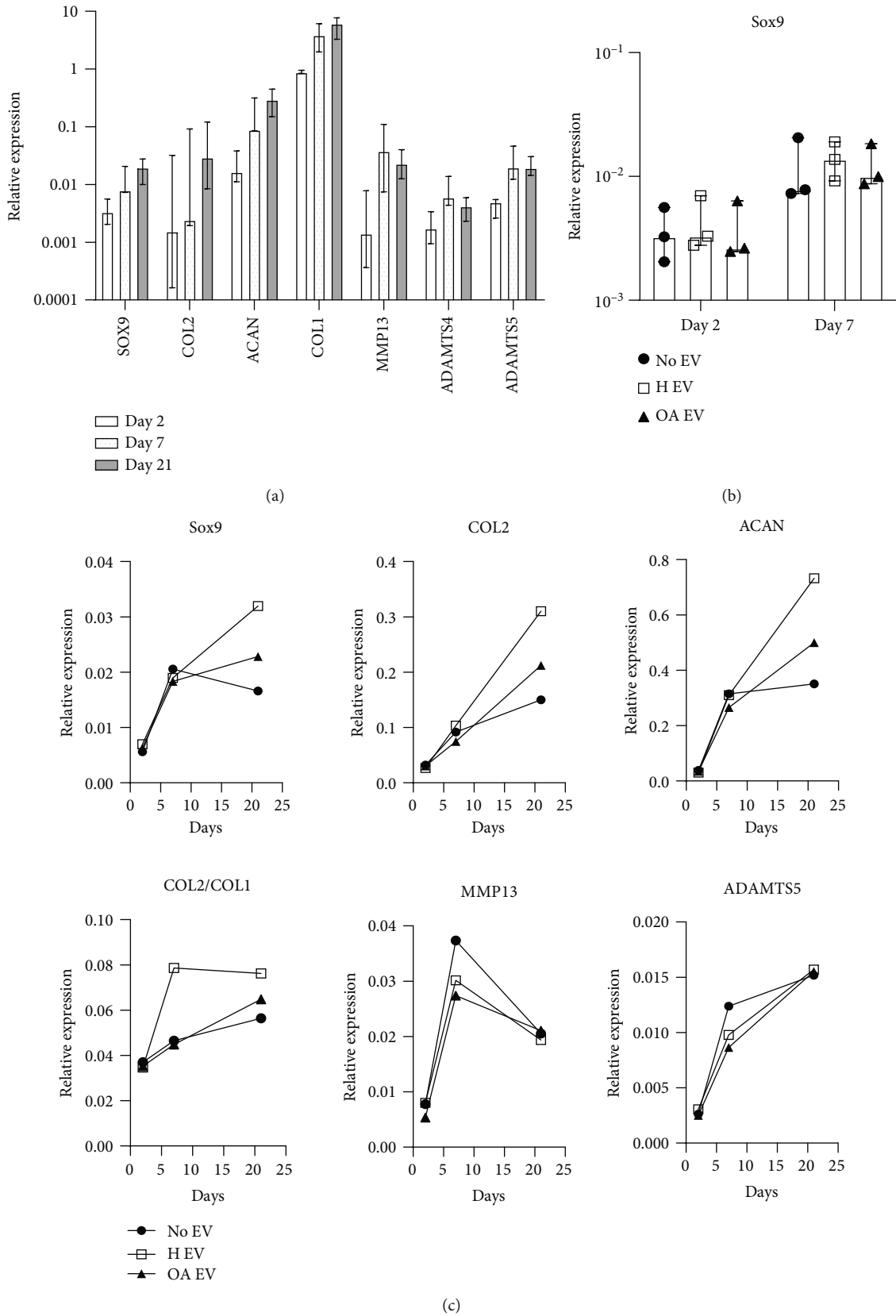


FIGURE 3: Gene expression of characteristic cartilage catabolic and anabolic genes measured in (a) untreated chondrocytes (no EVs) cultured for 2, 7, and 21 days. Horizontal bars show medians, and whiskers represent interquartile range. (b) *SOX9* expression in untreated and H-EV or OA-EV treated chondrocytes after 2 and 7 days. Symbols represent individual donor-derived chondrocyte cultures. (c) Chondrogenic gene expression in untreated (no EVs) and treated (H-EVs and OA-EVs) chondrocytes after 2, 7, and 21 days.

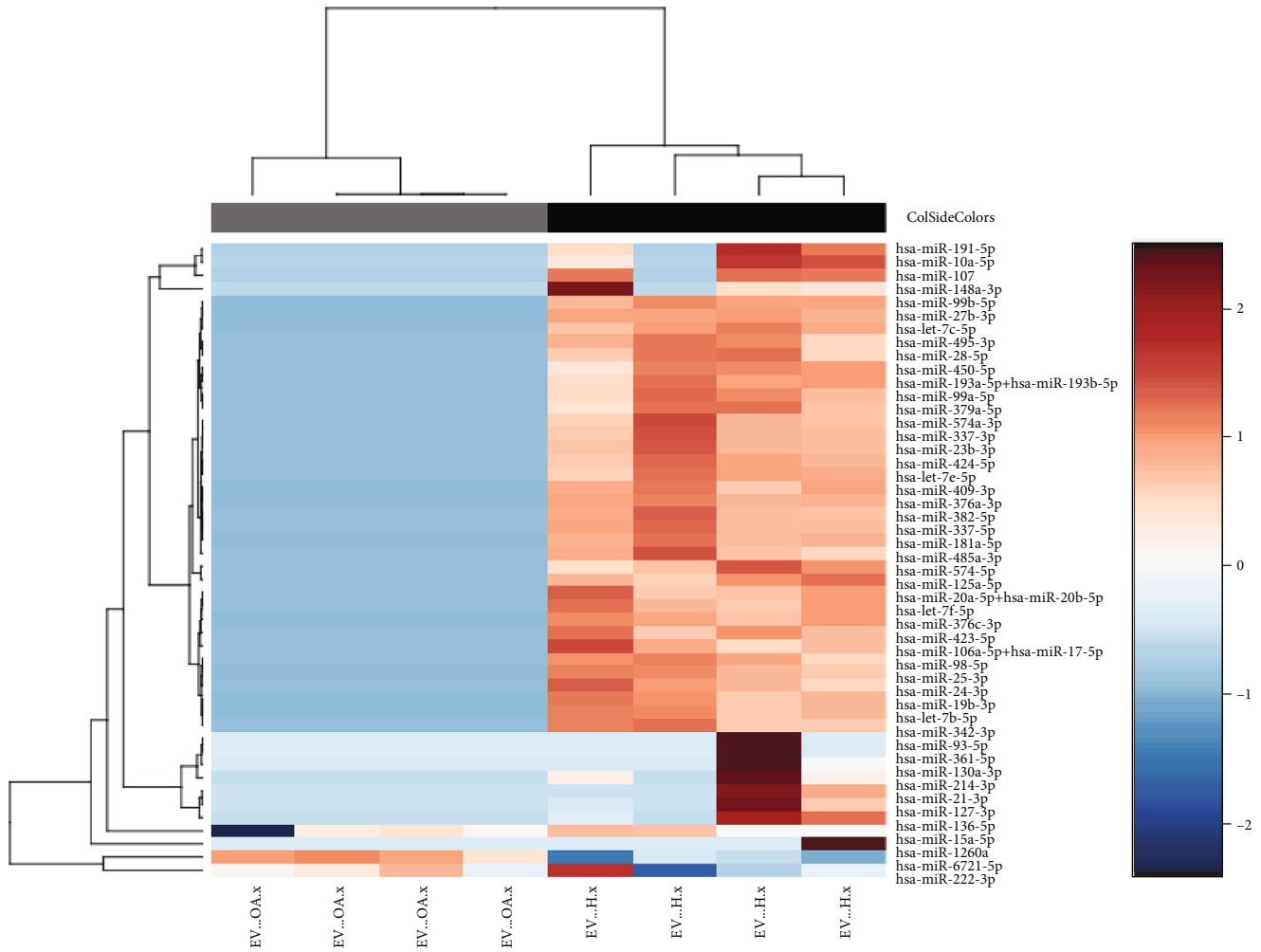


FIGURE 4: OA-EV and H-EV miRNA expression profiling using NanoString technology. Heatmap showing unsupervised hierarchical clustering of significantly differentially expressed microRNAs ($p < 0.05$, $n = 48$), based on normalized digital expression counts in OA-EVs vs. H-EVs. Each column represents an individual sample. Relative expression changes are indicated by the colour key (red: high; blue: low). OA-EVs are depicted by grey shading, while H-EVs are depicted by black shading.

differentially expressed between H-EVs and OA-EVs, of which 48 retained significance after FDR correction. A total of 47 were upregulated in healthy EVs and 1 in OA-EVs (fold change (FC) range = $-12.3 - 26.67$, p value range = $0.002-0.037$) (Figure 4).

The 48 DE-expressed microRNAs were predicted to target KEGG pathways [50] using mirPath [45], with key implications in chondrogenesis or stem cells, including extracellular matrix interaction (56 genes, 36 microRNAs, $p < 0.001$), N-glycan biosynthesis (30 genes, 29 microRNA, $p < 0.001$), focal adhesion (133 genes, 43 microRNAs, $p < 0.001$) and signalling pathways regulating pluripotency of stem cells (94 genes, 45 microRNAs, $p < 0.001$). Predicted gene targets identified with ‘very high’ score class (top 1%) via the microRNA Data Integration Portal (mirDIP) were filtered for duplicates, resulting in 10,755 unique gene targets. Reactome pathways implicated by the target genes included cell-cell communication (95/133 genes), transcriptional regulation of pluripotent stem cells (38/45 genes), extracellular matrix organisation (207/329 genes), transport of small molecules (483/967 genes), and vesicle-mediated

transport (510/824 genes). miRWalk also predicted target map to signalling pathways “regulating pluripotency of stem cells” pathway.

In addition to microRNAs that were significantly differentially expressed between OA-EVs and H-EVs, we also assessed the top 20 most highly expressed microRNAs in each population, as well as those that were commonly highly expressed in both OA and H-EVs. 17 microRNA were expressed at a high level in both populations, while miR-6721-5p, miR-579-3p and miR-199a-5p were uniquely highly expressed in OA-MSC-EVs, and miR-145-5p, miR-126-3p and miR-15b-5p were uniquely highly expressed in control healthy MSC-EVs (Table 3).

The top 5 most highly expressed microRNAs in each population comprised over 50% of all microRNA reads (OA – EVs = 50.2%, H – EVs = 62.0%) (Figure 5), of which miR-4454/-7975, miR-125b-5p, and miR-21-5p were commonly highly expressed.

When we compared miRNAs in OA-EVs with their parental MSCs (Supplementary Data 2), we found that they clustered separately (Figure 6). There were 130 miRNAs that

TABLE 3: microRNAs highly expressed in OA-EVs and control H-EVs.

Names	Total	microRNAs
Shared OA-EVs & H-EVs	17	hsa-miR-142-3p
		hsa-miR-199a-3p + hsa-miR-199b-3p
		hsa-miR-4286
		hsa-let-7a-5p
		hsa-miR-16-5p
		hsa-miR-21-5p
		hsa-miR-29a-3p
		hsa-miR-29b-3p
		hsa-let-7i-5p
		hsa-miR-4454+ hsa-miR-7975
		hsa-miR-630
		hsa-let-7b-5p
		hsa-miR-221-3p
		hsa-miR-23a-3p
		hsa-miR-100-5p
		hsa-miR-125b-5p
		hsa-miR-223-3p
OA-EVs	3	hsa-miR-6721-5p
		hsa-miR-579-3p
		hsa-miR-199a-5p
H-EVs	3	hsa-miR-145-5p
		hsa-miR-126-3p
		hsa-miR-15b-5p

were significantly differentially expressed between OA-EVs and parental OA-MSCs, of which 124 retained significance after FDR correction (Figure 6). A total of 120 were upregulated in healthy EVs and 4 in OA-EVs (fold change (FC) range = -75.95 – 68.62, p value range \leq 0.001-0.049) (Figure 4).

For KEGG pathway analysis [50], 100 miRNA with higher FC out of the 124 DE expressed microRNAs were analyzed using mirPath [45]. The same key implications in chondrogenesis or stem cells were found as above, with the exception of pathways regulating pluripotency of stem cells: extracellular matrix receptor interaction (71 genes, 77 microRNAs, $p < 0.001$), N-glycan biosynthesis (44 genes, 58 microRNA, $p < 0.001$) and focal adhesion (177 genes, 82 microRNAs, $p < 0.001$). Other pathways observed were proteoglycans in cancer (180 genes, 80 microRNAs, $p < 0.001$), fatty acid metabolism (42 genes, 66 microRNAs, $p < 0.001$) or cell cycle (111 genes, 77 microRNAs, $p < 0.001$). Predicted gene targets with ‘very high’ score class (top 1%) via the microRNA Data Integration Portal (mirDIP) were identified, resulting in 100,714 unique gene targets. Reactome pathways implicated by the target genes included MECP2 regulated neuronal receptors and channels (32/32), transcription factor forkhead box O (FOXO)-mediated transcription (85/110 genes), TP53 regulated transcription of genes involved in G1 cell cycle arrest (20/20), transcriptional regulation by RUNX family transcription

factor 3 (RUNX3) (87/118 genes), extracellular matrix organization (249/329 genes), programmed cell death (170/238 genes), and vesicle-mediated transport (552/824 genes). miRWalk predicted target map to signalling pathways related to cartilage and osteoarthritis as “glycolysis gluconeogenesis”, “fatty acid metabolism”, “glycosaminoglycan biosynthesis”, “autophagy”, “FOXO signaling pathway”, “calcium signaling pathway”, “osteoclast differentiation”, and other pathways like “endocytosis” or “cell cycle”.

Assessing the top 20 most highly expressed microRNAs, 14 microRNAs were expressed at a high level in both parental OA-MSCs and their EVs, while 6 miRNAs were uniquely highly expressed in OA-MSC-EVs and other 6 were uniquely highly expressed in parental MSCs (Table 4).

4. Discussion

Previous studies on EVs in OA have almost exclusively focused on the synovial fluid (SF) EVs, which mediate the cross-talk between the damaged cartilage and the inflamed synovium [51, 52] and have shown their considerable influence on chondrocyte catabolism, senescence, and death [53–57]. In contrast, the cross-talk between subchondral bone (SB) cells and chondrocytes in OA is comparatively less explored, despite the fact that SB pathology is implicated in all stages of OA progression [13, 58, 59]. Furthermore, in previous studies of SF-resident EVs, their tissues of origin, as well as the cells of origin, remained unknown. In contrast, our study is uniquely focused on the cross-talk between cartilage and SB in OA and investigated EV production from a specific type of SB cells, SB MSCs, which are directly implicated in SB OA pathology and cartilage destruction “from below” [60–62]. Although SB MSCs from healthy amputees would be a better control than the MSCs from bone marrow used in this work, these samples are difficult to access while MSCs from amputated knees from diabetics could carry underlying negative effects such as described previously [63–65].

In this work, when comparing EV size and yields (particle/cell) released from OA and control healthy MSCs, no differences were found, similar to results previously described for healthy and OA-EVs from SF [55, 57]. Previous works on SF-EVs have presented slightly lower EV sizes [53–55], which could be explained by different methods used for EV isolation in these studies: using ultracentrifugation combined with precipitation [54, 55] or using immunoaffinity [53]. EVs obtained from ultracentrifugation alone, as was in our study, are known to be less purified due to the overlap in sizes between EVs and microvesicles [25], however ultracentrifugation is less harmful for EVs [66].

One of the principal aims of this study was to identify specific sets of miRNAs in the OA-EVs derived from SB-MSCs. Depending on the cell of origin, EVs (including exosomes) can contain many constituents of a cell including DNA, RNA, lipids, metabolites, and cytosolic and cell-surface proteins [67]. We have identified several miRNAs that in our experimental conditions were packaged into their EVs and may be characteristic of OA-EVs from these cells.

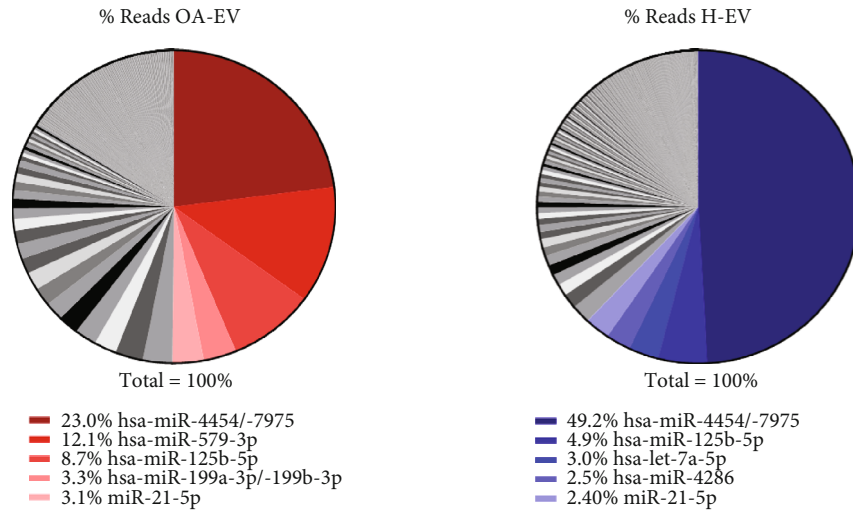


FIGURE 5: OA-EV and H-EV miRNA profiling analysis. Diagrams showing the percentages of reads from the top 5 most highly expressed miRNAs. H-EVs: EVs from control healthy MSCs; OA-EVs: EVs from OA-MSCs.

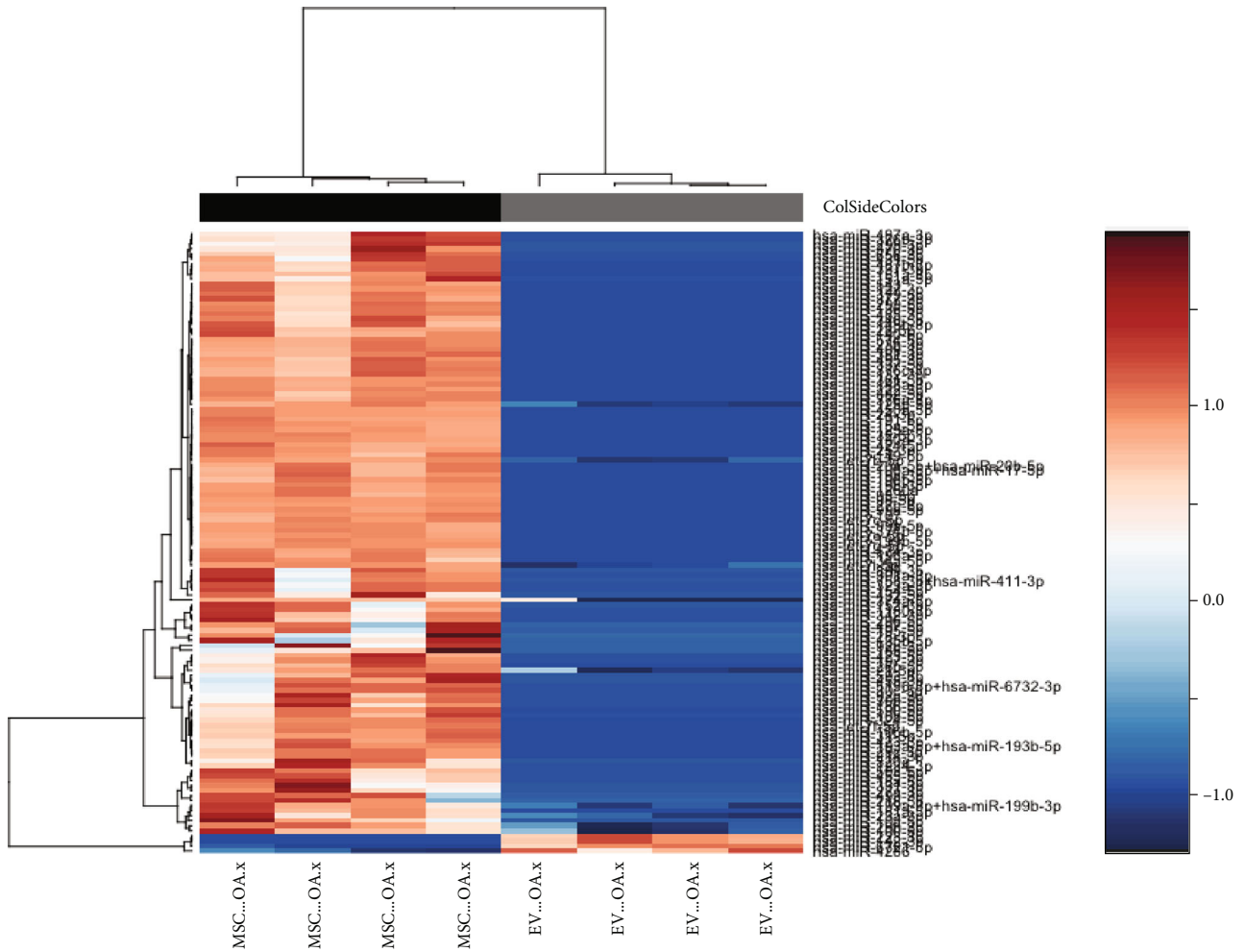


FIGURE 6: miRNA profiling of OA-EVs and their parental MSCs using NanoString technology. Heatmap showing unsupervised hierarchical clustering of significantly differentially expressed microRNAs ($p < 0.05$, $n = 124$), based on normalized digital expression counts in OA-MSC-EVs vs. OA-MSCs. Each column represents an individual sample. Relative expression changes are indicated by the colour key (red: high; blue: low). OA-MSC-EVs are depicted by grey shading, while MSC are depicted by black shading.

TABLE 4: microRNAs highly expressed in OA-MSCs and OA-EVs.

Names	Total	microRNAs
Shared OA-EVs & OA-MSCs	14	hsa-miR-199a-3p+ hsa-miR-199b-3p
		hsa-let-7a-5p
		hsa-miR-16-5p
		hsa-miR-21-5p
		hsa-miR-29a-3p
		hsa-miR-29b-3p
		hsa-let-7i-5p
		hsa-miR-4454+ hsa-miR-7975
		hsa-let-7b-5p
		hsa-miR-221-3p
		hsa-miR-199a-5p
		hsa-miR-23a-3p
		hsa-miR-100-5p
		hsa-miR-125b-5p
OA-EVs	6	hsa-miR-142-3p
		hsa-miR-4286
		hsa-miR-6721-5p
		hsa-miR-630
		hsa-miR-579-3p
		hsa-miR-223-3p
OA-MSCs	6	hsa-miR-199b-5p
		hsa-miR-15a-5p
		hsa-let-7c-5p
		hsa-miR-99a-5p
		hsa-miR-15b-5p
		hsa-let7g-5p

Many previous studies compared miRNA expression in MSC-EVs and their parental MSCs [68–72], but these studies were all focused on healthy MSCs. Our study has identified 14 miRNAs that were highly expressed in both OA-MSC-EVs and their parental SB MSCs. These included miR-125b, which has been previously shown to regulate the expression of matrix-degrading enzymes in human chondrocytes [73–75] as well as regulate MSC osteogenesis [76], and miR-199a involved in repression of chondrogenesis [77], regulation of chondrocyte ageing and cartilage metabolism [78], and highly expressed in OA SF EVs [57]. Previous studies including ours [18, 61, 79] have described gene expression profiles of OA SB MSCs as predisposed towards bone formation and cartilage extracellular matrix regulation. The current study complements these findings by showing that highly expressed miRNA in these MSCs, including those packaged in their EVs, may be regulating cartilage homeostasis in OA. Although further functional analysis would be necessary to confirm that these miRNAs contained in the EVs may produce this chondrogenic effect.

Furthermore, the present study has identified four miRNAs that are higher-expressed in OA-MSC-EVs compared to parental MSCs and may be involved in regulating the viability and the metabolic status of OA chondrocytes. Of a

particular interest are miR-142-3p previously shown to be selectively packaged into EVs [80] and miR-223-3p that have been both shown to inhibit cell apoptosis and inflammation in OA chondrocytes [81, 82], as well as miR-630 that has been earlier documented to regulate chondrogenic lineage commitment [83]. In our previous work we have used qPCR and validated the enrichment of miR-142-3p and miR-223-3p in H-EVs coming from MSCs [41]. The role of miR-630 and other miRNAs has not yet been explored in OA and is awaiting further validation.

Pathway analysis has indicated that OA-EVs and/or OA-MSCs expresses miRNAs implicated in chondrogenesis, stem cells, or other pathways related to cartilage and OA. Interestingly, “fatty acid metabolism” points out to the already known role of fatty acids in OA [84]. Also, FOXO transcription factors have been described as chondroprotectors and regulating autophagy and inflammation [85]. Altogether, these data suggest that despite their altered gene expression and predisposition to osteogenesis in OA, SB MSCs produce miRNAs and release EVs that contain miRNAs involved in positive regulation of chondrocyte viability and differentiation.

MSC-EVs from various human tissues including bone marrow (BM) and adipose tissue are beginning to be used as a therapy for OA [52, 86]. In this context, it was interesting to compare the miRNA cargo of OA-EVs with H-EVs obtained from BM aspirates from healthy individuals. Amongst top highly expressed miRNAs, 17 were shared in both types of EVs (Table 3), 13 of which were also abundant in OA-MSCs (Table 4). Common abundant miRNAs included miR-16-5p previously used as an endogenous reference gene for the normalization of urinary exosomal miRNA expression [87], and some let family members previously described amongst the top 10 most abundant miRNAs in humans’ samples [88, 89]. Common miRNAs between OA-EVs and H-EVs that were not present in OA-MSCs included previously noted miR-142-3p and miR-630 [86] that have been described as “cartilage-protective.” Also miR-29a-3p was described as protective for cartilage [86]. Healthy EVs higher-expressed miR-145-5p (uniquely highly expressed in H-EVs compared to OA-EVs) described as having a dual role in OA [90], while OA-EVs higher-expressed hsa-miR-199a-5p involved in chondrogenesis regulation and bone formation [91], as well as highly expressed in OA SF EVs [57] and in plasma of early OA patients [92]. Our *in vitro* data have revealed that both H-EVs and OA-EVs marginally but significantly improved the viability of OA chondrocytes, with no difference to each other, which could be a result of consorted activity of multiple miRNAs.

Recent *in vitro* studies on MSC-EVs in OA have used inflammatory stimulation of chondrocytes before coculturing with H-EVs [93–96], and they obtained a reduction in the expression of chondrocyte inflammatory markers. It could be possible that this stimulation made the EV-effect on chondrocytes stronger than observed in our study. In our study, we aimed to reflect more closely the *in vivo* conditions of chondrocytes based on our previous findings that OA chondrocytes grown in the same

conditions already present the signs of inflammation, evident by high-level expression of matrix-degrading enzymes and pro-inflammatory cytokines [18].

Even though our data on MSC-EV (both OA- and H-EVs) effects on chondrocyte gene expression are limited, they point towards a worse induction of chondrogenic gene expression by OA-EVs compared to H-EVs. The lack of statistical significance could be explained by donor-to-donor variation in both chondrocytes and EVs preparations that we have used. To minimise donor effects and generate larger EV batches for use in multiple experiments, future studies could utilise EVs [54] or chondrocytes [49] which are pooled from several donors.

Smaller than expected effects of EVs on chondrocyte gene expression could be also explained by the 3D assay conditions we used. Mortati and colleagues [49] added MSC-EVs to 4-week cultured-chondrocyte pellets and showed that EVs could diffuse into the matrix. Differently from their study, we mixed the EVs with the chondrocytes before the 3D pellet formation as investigated their effect at different time points of chondrogenesis. Also, no chondrogenic inducers such as TGF β 1 [49] were added to the media in our study because these strong inducers could “mask” or conflict with potentially smaller effects from MSC-EVs. In support of our assay design, previous studies have documented the presence of TGF β 1 in MSC-EVs [97], which could explain long-term, enhanced chondrogenic gene expression with the addition of H-EVs in our experiments. While some studies report on MSC-EV enhancement of chondrocyte collagen II expression in 2D formats [94], 3D pellets [48], cells encapsulated in cartilage-mimicking hydrogels [49] are likely to provide conditions more representative to EV traffic *in vivo*. Specific to OA osteochondral pathology, such constructs should take into the account intercellular distances between SB MSCs and chondrocytes, which can be established from histological studies [6, 18], as well as a known heterogeneity of chondrocyte subpopulations in OA [98, 99], which is difficult to re-capitulate in *in vitro* systems.

In summary, OA-EVs were capable to enhance the viability of OA chondrocytes; also, the expression of chondrogenic genes was enhanced in the chondrocytes by the EVs from OA-MSCs. However, both effects were less evident than the ones shown for H-EVs. This variation could be partially explained by the differential expression of miRNAs found in the cargo of H-EVs and OA-EVs.

5. Conclusions

The present study reports on the production, characterization and miRNA profile of EVs from SB MSCs in OA. For the first time, it shows that SB MSCs in OA are capable of producing EVs that support chondrocyte viability and chondrogenic gene expression, although future studies would be needed to confirm it using functional assays for chondrogenesis. This supports the notion that modulation of SB MSCs represents a valid strategy for endogenous cartilage regeneration in OA. This may be achieved via enhancement of their trophic activity and EV production in addition to triggering

their chondrogenic differentiation, thus representing a new potential tool for cartilage regeneration.

Data Availability

miRNA profiling data are attached as supplementary files.

Disclosure

The views expressed in this article are those of the authors and not necessarily those of the BRC, NIHR, or the Department of Health and Social Care.

Conflicts of Interest

The authors declare that there is no conflict of interest regarding the publication of this paper.

Authors' Contributions

Xiao-nong Wang and Elena Jones are equal last authors.

Acknowledgments

We acknowledge Tracey Davey from the Newcastle University EM Research Services for the assistance with the generation of images using the Hitachi TEM (BBSRC grant reference BB/R013942/1); Anastasia Resteu from Human Dendritic Cell Lab (Institute of Cellular Medicine, Newcastle) for the assistance with Nanostring protocol; Adam Davison and Liz Straszynski for research support services at the Leeds Institute of Rheumatic and Musculoskeletal Medicine (LIRMM); surgeons, patients, and staff of Chapel Allerton Orthopaedic Centre; and Thomas Baboolal, Dragos Ilas, and Payal Ganguly from LIRMM for laboratory support. CSR was a beneficiary of a fellowship from Xunta de Galicia. RC and XW would like to acknowledge the support from Versus Arthritis through the Tissue Engineering and Regenerative Therapies Centre Versus Arthritis (Award 21156). Professor Pandit is a National Institute for Health Research (NIHR) Senior Investigator.

Supplementary Materials

Supplementary 1. Supplementary Figure 1: characterization of MSCs from subchondral bone (SB) of OA patients (OA-MSCs). (A) Trilineage differentiation of OA-MSCs following induction and staining with Oil Red O (day 21), Alkaline phosphatase (day 14) and Toluidine Blue (day 21), for adipogenesis, osteogenesis and chondrogenesis, respectively. (B) Phenotypic profile of OA-MSCs showing the % expression of CD73, CD90, CD105, hematopoietic-lineage markers (CD45, CD34, CD19, CD14) and HLA-DR measured by flow cytometry. Original magnification x200 for adipogenesis and osteogenesis and x40 for chondrogenesis.

Supplementary 2. Supplementary Figure 2: characterization of MSCs from healthy controls (H-MSCs). (A) Trilineage differentiation of H-MSCs following induction and staining with Oil Red O (day 21), Alkaline phosphatase/Von Kossa (day 14) and Alcian Blue (day 21) for adipogenesis,

osteogenesis and chondrogenesis, respectively. (B) Phenotypic profile of H-MSCs showing the % expression of CD73, CD90, CD105, hematopoietic-lineage markers (CD45, CD34, CD19, CD14) and HLA-DR measured by flow cytometry. Scale bar 200 μm for adipo- and osteo- genesis and 500 μm for chondrogenesis.

Supplementary 3. Supplementary Data 1: analysis of miRNAs in OA-EVs compared with H-EVs, showing the differential expression, with and without FDR correction, fold change (FC) and p value.

Supplementary 4. Supplementary Data 2: analysis of miRNAs in OA-EVs compared with their parental MSCs, showing the differential expression, with and without FDR correction, fold change (FC) and p value.

References

- [1] V. B. Kraus, F. J. Blanco, M. Englund, M. A. Karsdal, and L. S. Lohmander, "Call for standardized definitions of osteoarthritis and risk stratification for clinical trials and clinical use," *Osteoarthritis and Cartilage*, vol. 23, no. 8, pp. 1233–1241, 2015.
- [2] A. Mobasheri, G. Kalamegam, G. Musumeci, and M. E. Batt, "Chondrocyte and mesenchymal stem cell-based therapies for cartilage repair in osteoarthritis and related orthopaedic conditions," *Maturitas*, vol. 78, no. 3, pp. 188–198, 2014.
- [3] L. Kock, C. C. van Donkelaar, and K. Ito, "Tissue engineering of functional articular cartilage: the current status," *Cell and Tissue Research*, vol. 347, no. 3, pp. 613–627, 2012.
- [4] S. Safiri, A. A. Kolahi, E. Smith et al., "Global, regional and national burden of osteoarthritis 1990–2017: a systematic analysis of the global burden of disease study 2017," *Annals of the Rheumatic Diseases*, vol. 79, no. 6, pp. 819–828, 2020.
- [5] H. Fang, L. Huang, I. Welch et al., "Early changes of articular cartilage and Subchondral bone in the DMM mouse model of osteoarthritis," *Scientific Reports*, vol. 8, no. 1, p. 2855, 2018.
- [6] D. M. Findlay and G. J. Atkins, "Osteoblast-chondrocyte interactions in osteoarthritis," *Current Osteoporosis Reports*, vol. 12, no. 1, pp. 127–134, 2014.
- [7] B. J. E. de Lange-Brokaar, A. Ioan-Facsinay, G. J. V. M. van Osch et al., "Synovial inflammation, immune cells and their cytokines in osteoarthritis: a review," *Osteoarthritis and Cartilage*, vol. 20, no. 12, pp. 1484–1499, 2012.
- [8] C. R. Scanzello and S. R. Goldring, "The role of synovitis in osteoarthritis pathogenesis," *Bone*, vol. 51, no. 2, pp. 249–257, 2012.
- [9] C. Sanchez, M. A. Deberg, N. Piccardi, P. Msika, J. Y. L. Reginster, and Y. E. Henrotin, "Osteoblasts from the sclerotic subchondral bone downregulate aggrecan but upregulate metalloproteinases expression by chondrocytes. This effect is mimicked by interleukin-6, -1 β and oncostatin M pre-treated non-sclerotic osteoblasts," *Osteoarthritis and Cartilage*, vol. 13, no. 11, pp. 979–987, 2005.
- [10] C. Sanchez, M. A. Deberg, N. Piccardi, P. Msika, J. Y. L. Reginster, and Y. E. Henrotin, "Subchondral bone osteoblasts induce phenotypic changes in human osteoarthritic chondrocytes," *Osteoarthritis and Cartilage*, vol. 13, no. 11, pp. 988–997, 2005.
- [11] M. Stock, S. Menges, N. Eitzinger et al., "A Dual Role of Upper Zone of Growth Plate and Cartilage Matrix-Associated Protein in Human and Mouse Osteoarthritic Cartilage: Inhibition of Aggrecanases and Promotion of Bone Turnover," *Arthritis & Rheumatology*, vol. 69, no. 6, pp. 1233–1245, 2017.
- [12] A. R. Sharma, S. Jagga, S. S. Lee, and J. S. Nam, "Interplay between cartilage and subchondral bone contributing to pathogenesis of osteoarthritis," *International Journal of Molecular Sciences*, vol. 14, no. 10, pp. 19805–19830, 2013.
- [13] Y. Hu, X. Chen, S. Wang, Y. Jing, and J. Su, "Subchondral bone microenvironment in osteoarthritis and pain," *Bone Res*, vol. 9, no. 1, p. 20, 2021.
- [14] R. K. Zhang, G. W. Li, C. Zeng et al., "Mechanical stress contributes to osteoarthritis development through the activation of transforming growth factor beta 1 (TGF- β 1)," *Bone Joint Res*, vol. 7, no. 11, pp. 587–594, 2018.
- [15] D. M. Findlay and J. S. Kuliwaba, "Bone-cartilage crosstalk: a conversation for understanding osteoarthritis," *Bone Research*, vol. 4, no. 1, p. 16028, 2016.
- [16] D. B. Burr and E. L. Radin, "Microfractures and microcracks in subchondral bone: are they relevant to osteoarthritis?," *Rheumatic Diseases Clinics of North America*, vol. 29, no. 4, pp. 675–685, 2003.
- [17] W. Hu, Y. Chen, C. Dou, and S. Dong, "Microenvironment in subchondral bone: predominant regulator for the treatment of osteoarthritis," *Annals of the Rheumatic Diseases*, vol. 80, no. 4, pp. 413–422, 2020.
- [18] C. Sanjurjo-Rodriguez, T. G. Baboolal, A. N. Burska et al., "Gene expression and functional comparison between multipotential stromal cells from lateral and medial condyles of knee osteoarthritis patients," *Scientific Reports*, vol. 9, no. 1, p. 9321, 2019.
- [19] H. J. Knowles, L. Moskovsky, M. S. Thompson et al., "Chondroclasts are mature osteoclasts which are capable of cartilage matrix resorption," *Virchows Archiv*, vol. 461, no. 2, pp. 205–210, 2012.
- [20] R. E. Miller, P. B. Tran, A. M. Obeidat et al., "The role of peripheral nociceptive neurons in the pathophysiology of osteoarthritis pain," *Current Osteoporosis Reports*, vol. 13, no. 5, pp. 318–326, 2015.
- [21] A. Eitner, G. O. Hofmann, and H. G. Schaible, "Mechanisms of Osteoarthritic Pain. Studies in Humans and Experimental Models," *Frontiers in Molecular Neuroscience*, vol. 10, p. 349, 2017.
- [22] C. Sanchez, G. Mazzucchelli, C. Lambert, F. Comblain, E. DePauw, and Y. Henrotin, "Comparison of secretome from osteoblasts derived from sclerotic versus non-sclerotic subchondral bone in OA: a pilot study," *PLoS One*, vol. 13, no. 3, article e0194591, 2018.
- [23] M. Shabestari, Y. R. Shabestari, M. A. Landin et al., "Altered protein levels in bone marrow lesions of hip osteoarthritis: analysis by proteomics and multiplex immunoassays," *International Journal of Rheumatic Diseases*, vol. 23, no. 6, pp. 788–799, 2020.
- [24] S. Miyaki and M. K. Lotz, "Extracellular vesicles in cartilage homeostasis and osteoarthritis," *Current Opinion in Rheumatology*, vol. 30, no. 1, pp. 129–135, 2018.
- [25] C. Théry, K. W. Witwer, E. Aikawa et al., "Minimal information for studies of extracellular vesicles 2018 (MISEV 2018): a position statement of the International Society for Extracellular Vesicles and update of the MISEV2014 guidelines," *Journal of Extracellular Vesicles*, vol. 7, no. 1, p. 1535750, 2018.
- [26] J. Lötvall, A. F. Hill, F. Hochberg et al., "Minimal experimental requirements for definition of extracellular vesicles and their

- functions: a position statement from the International Society for Extracellular Vesicles,” *Journal of Extracellular Vesicles*, vol. 3, no. 1, p. 26913, 2014.
- [27] L. M. Doyle and M. Wang, “Overview of extracellular vesicles, their origin, composition, purpose, and methods for exosome isolation and analysis,” *Cell*, vol. 8, no. 7, p. 727, 2019.
- [28] R. C. Lai, R. W. Y. Yeo, and S. K. Lim, “Mesenchymal stem cell exosomes,” *Seminars in Cell & Developmental Biology*, vol. 40, pp. 82–88, 2015.
- [29] X. Liang, Y. Ding, Y. Zhang, H. F. Tse, and Q. Lian, “Paracrine mechanisms of mesenchymal stem cell-based therapy: current status and perspectives,” *Cell Transplantation*, vol. 23, no. 9, pp. 1045–1059, 2014.
- [30] M. P. Mycko and S. E. Baranzini, “microRNA and exosome profiling in multiple sclerosis,” *Multiple Sclerosis*, vol. 26, no. 5, pp. 599–604, 2020.
- [31] N. Dilsiz, “Role of exosomes and exosomal micro RNAs in cancer,” *Future Science OA*, vol. 6, article FSO465, 2020.
- [32] Z. Li, Y. Wang, K. Xiao, S. Xiang, Z. Li, and X. Weng, “Emerging role of Exosomes in the joint diseases,” *Cellular Physiology and Biochemistry*, vol. 47, no. 5, pp. 2008–2017, 2018.
- [33] S. Cosenza, M. Ruiz, M. Maumus, C. Jorgensen, and D. Noël, “Pathogenic or Therapeutic Extracellular Vesicles in Rheumatic Diseases: Role of Mesenchymal Stem Cell-Derived Vesicles,” *International Journal of Molecular Sciences*, vol. 18, no. 4, p. 889, 2017.
- [34] S. Asghar, G. J. Litherland, J. C. Lockhart, C. S. Goodyear, and A. Crilly, “Exosomes in intercellular communication and implications for osteoarthritis,” *Rheumatology (Oxford)*, vol. 59, no. 1, pp. 57–68, 2020.
- [35] A. Esa, K. D. Connolly, R. Williams, and C. W. Archer, “Extracellular vesicles in the synovial joint: is there a role in the pathophysiology of osteoarthritis?,” *Malaysian Orthopaedic Journal*, vol. 13, no. 1, pp. 1–7, 2019.
- [36] J. Withrow, C. Murphy, Y. Liu, M. Hunter, S. Fulzele, and M. W. Hamrick, “Extracellular vesicles in the pathogenesis of rheumatoid arthritis and osteoarthritis,” *Arthritis Research & Therapy*, vol. 18, no. 1, p. 286, 2016.
- [37] Z. Ni, S. Zhou, S. Li et al., “Exosomes: roles and therapeutic potential in osteoarthritis,” *Bone Research*, vol. 8, no. 1, p. 25, 2020.
- [38] C. Lin, L. Liu, C. Zeng et al., “Activation of mTORC1 in subchondral bone preosteoblasts promotes osteoarthritis by stimulating bone sclerosis and secretion of CXCL12,” *Bone Research*, vol. 7, no. 1, p. 5, 2019.
- [39] M. Cucchiari, L. de Girolamo, G. Filardo et al., “Basic science of osteoarthritis,” *J Exp Orthop*, vol. 3, no. 1, p. 22, 2016.
- [40] B. L. Wise, J. Niu, M. Yang et al., “Patterns of compartment involvement in tibiofemoral osteoarthritis in men and women and in whites and African Americans,” *Arthritis Care & Research*, vol. 64, no. 6, pp. 847–852, 2012.
- [41] M. Reis, E. Mavin, L. Nicholson, K. Green, A. M. Dickinson, and X. N. Wang, “Mesenchymal stromal cell-derived extracellular vesicles attenuate dendritic cell maturation and function,” *Frontiers in Immunology*, vol. 9, p. 2538, 2018.
- [42] M. Dominici, K. le Blanc, I. Mueller et al., “Minimal criteria for defining multipotent mesenchymal stromal cells. The International Society for Cellular Therapy position statement,” *Cytotherapy*, vol. 8, no. 4, pp. 315–317, 2006.
- [43] C. Qing, C. Wei-ding, and F. Wei-min, “Co-culture of chondrocytes and bone marrow mesenchymal stem cells in vitro enhances the expression of cartilaginous extracellular matrix components,” *Brazilian Journal of Medical and Biological Research*, vol. 44, no. 4, pp. 303–310, 2011.
- [44] C. Sticht, C. de la Torre, A. Parveen, and N. Gretz, “miRWalk: An online resource for prediction of microRNA binding sites,” *PLoS One*, vol. 13, no. 10, article e0206239, 2018.
- [45] I. S. Vlachos, K. Zagganas, M. D. Paraskevopoulou et al., “DIANA-miRPath v3.0: deciphering microRNA function with experimental support,” *Nucleic Acids Research*, vol. 43, no. W1, pp. W460–W466, 2015.
- [46] B. Jassal, L. Matthews, G. Viteri et al., “The reactome pathway knowledgebase,” *Nucleic Acids Research*, vol. 48, no. D1, pp. D498–D503, 2020.
- [47] T. Tokar, C. Pastrello, A. E. M. Rossos et al., “mirDIP 4.1-integrative database of human microRNA target predictions,” *Nucleic Acids Research*, vol. 46, no. D1, pp. D360–D370, 2018.
- [48] H. Kim, D. Kang, Y. Cho, and J. H. Kim, “Epigenetic regulation of chondrocyte catabolism and anabolism in osteoarthritis,” *Molecules and Cells*, vol. 38, no. 8, pp. 677–684, 2015.
- [49] L. Mortati, L. de Girolamo, C. Perucca Orfei et al., “In Vitro Study of Extracellular Vesicles Migration in Cartilage-Derived Osteoarthritis Samples Using Real-Time Quantitative Multimodal Nonlinear Optics Imaging,” *Pharmaceutics*, vol. 12, no. 8, p. 734, 2020.
- [50] H. Ogata, S. Goto, K. Sato, W. Fujibuchi, H. Bono, and M. Kanehisa, “KEGG: Kyoto encyclopedia of genes and genomes,” *Nucleic Acids Research*, vol. 27, no. 1, pp. 29–34, 1999.
- [51] J. Malda, J. Boere, C. H. A. van de Lest, P. R. van Weeren, and M. H. M. Wauben, “Extracellular vesicles – new tool for joint repair and regeneration,” *Nature Reviews Rheumatology*, vol. 12, no. 4, pp. 243–249, 2016.
- [52] J. J. Li, E. Hosseini-Beheshti, G. Grau, H. Zreiqat, and C. Little, “Stem Cell-Derived Extracellular Vesicles for Treating Joint Injury and Osteoarthritis,” *Nanomaterials (Basel)*, vol. 9, no. 2, p. 261, 2019.
- [53] R. Domenis, R. Zanutel, F. Caponnetto et al., “Characterization of the Proinflammatory profile of synovial fluid-derived Exosomes of patients with osteoarthritis,” *Mediators of Inflammation*, vol. 2017, Article ID 4814987, 11 pages, 2017.
- [54] K. Gao, W. Zhu, H. Li et al., “Association between cytokines and exosomes in synovial fluid of individuals with knee osteoarthritis,” *Modern Rheumatology*, vol. 30, no. 4, pp. 758–764, 2020.
- [55] R. Kolhe, M. Hunter, S. Liu et al., “Gender-specific differential expression of exosomal miRNA in synovial fluid of patients with osteoarthritis,” *Scientific Reports*, vol. 7, no. 1, p. 2029, 2017.
- [56] R. Kolhe, V. Owens, A. Sharma et al., “Sex-specific differences in extracellular vesicle protein cargo in synovial fluid of patients with osteoarthritis,” *Life (Basel)*, vol. 10, no. 12, p. 337, 2020.
- [57] O. H. Jeon, D. R. Wilson, C. C. Clement et al., “Senescence cell-associated extracellular vesicles serve as osteoarthritis disease and therapeutic markers,” *JCI Insight*, vol. 4, no. 7, 2019.
- [58] H. L. Stewart and C. E. Kawcak, “The importance of Subchondral bone in the pathophysiology of osteoarthritis,” *Front Vet Sci*, vol. 5, p. 178, 2018.
- [59] T. Hügle and J. Geurts, “What drives osteoarthritis?—synovial versus subchondral bone pathology,” *Rheumatology (Oxford)*, vol. 56, no. 9, pp. 1461–1471, 2017.

- [60] T. R. Coughlin and O. D. Kennedy, "The role of subchondral bone damage in post-traumatic osteoarthritis," *Annals of the New York Academy of Sciences*, vol. 1383, no. 1, pp. 58–66, 2016.
- [61] T. M. Campbell, S. M. Churchman, A. Gomez et al., "Mesenchymal stem cell alterations in bone marrow lesions in patients with hip osteoarthritis," *Arthritis & Rheumatology*, vol. 68, no. 7, pp. 1648–1659, 2016.
- [62] M. A. Karsdal, A. C. Bay-Jensen, R. J. Lories et al., "The coupling of bone and cartilage turnover in osteoarthritis: opportunities for bone antiresorptives and anabolics as potential treatments?," *Annals of the Rheumatic Diseases*, vol. 73, no. 2, pp. 336–348, 2014.
- [63] J. J. el-Jawhari, P. Ganguly, E. Jones, and P. V. Giannoudis, "Bone marrow multipotent Mesenchymal stromal cells as autologous therapy for osteonecrosis: effects of age and underlying causes," *Bioengineering (Basel)*, vol. 8, no. 5, p. 69, 2021.
- [64] M. Mahmoud, N. Abu-Shahba, O. Azmy, and N. El-Badri, "Impact of diabetes mellitus on human Mesenchymal stromal cell biology and functionality: implications for autologous transplantation," *Stem Cell Reviews and Reports*, vol. 15, no. 2, pp. 194–217, 2019.
- [65] F. C. Cassidy, C. Shortiss, C. G. Murphy et al., "Impact of type 2 diabetes mellitus on human bone marrow stromal cell number and phenotypic characteristics," *International Journal of Molecular Sciences*, vol. 21, no. 7, p. 2476, 2020.
- [66] P. Li, M. Kaslan, S. H. Lee, J. Yao, and Z. Gao, "Progress in exosome isolation techniques," *Theranostics*, vol. 7, no. 3, pp. 789–804, 2017.
- [67] R. Kalluri and V. S. LeBleu, "The biology, function, and biomedical applications of exosomes," *Science*, vol. 367, no. 6478, p. eaau6977, 2020.
- [68] Y. Nakamura, S. Miyaki, H. Ishitobi et al., "Mesenchymal-stem-cell-derived exosomes accelerate skeletal muscle regeneration," *FEBS Letters*, vol. 589, no. 11, pp. 1257–1265, 2015.
- [69] D. G. Phinney, M. di Giuseppe, J. Njah et al., "Mesenchymal stem cells use extracellular vesicles to outsource mitophagy and shuttle microRNAs," *Nature Communications*, vol. 6, no. 1, p. 8472, 2015.
- [70] S. R. Baglio, K. Rooijers, D. Koppers-Lalic et al., "Human bone marrow- and adipose-mesenchymal stem cells secrete exosomes enriched in distinctive miRNA and tRNA species," *Stem Cell Research & Therapy*, vol. 6, no. 1, p. 127, 2015.
- [71] F. Collino, M. C. Deregibus, S. Bruno et al., "Microvesicles derived from adult human bone marrow and tissue specific mesenchymal stem cells shuttle selected pattern of miRNAs," *PLoS One*, vol. 5, no. 7, article e11803, 2010.
- [72] X. Y. Zou, Y. Yu, S. Lin et al., "Comprehensive miRNA analysis of human umbilical cord-derived Mesenchymal stromal cells and extracellular vesicles," *Kidney & Blood Pressure Research*, vol. 43, no. 1, pp. 152–161, 2018.
- [73] T. Matsukawa, T. Sakai, T. Yonezawa et al., "MicroRNA-125b regulates the expression of aggrecanase-1 (ADAMTS-4) in human osteoarthritic chondrocytes," *Arthritis Research & Therapy*, vol. 15, no. 1, p. R28, 2013.
- [74] N. Xu, L. Zhang, F. Meisgen et al., "MicroRNA-125b Down-regulates Matrix Metalloproteinase 13 and Inhibits Cutaneous Squamous Cell Carcinoma Cell Proliferation, Migration, and Invasion," *The Journal of Biological Chemistry*, vol. 287, no. 35, pp. 29899–29908, 2012.
- [75] Z. Rasheed, N. Rasheed, W. A. Abdulmonem, and M. I. Khan, "MicroRNA-125b-5p regulates IL-1 β induced inflammatory genes via targeting TRAF6-mediated MAPKs and NF- κ B signaling in human osteoarthritic chondrocytes," *Scientific Reports*, vol. 9, no. 1, p. 6882, 2019.
- [76] Y. Mizuno, K. Yagi, Y. Tokuzawa et al., "miR-125b inhibits osteoblastic differentiation by down-regulation of cell proliferation," *Biochemical and Biophysical Research Communications*, vol. 368, no. 2, pp. 267–272, 2008.
- [77] E. A. Lin, L. Kong, X. H. Bai, Y. Luan, and C. J. Liu, "miR-199a, a Bone Morphogenic Protein 2-responsive MicroRNA, Regulates Chondrogenesis via Direct Targeting to Smad1," *The Journal of Biological Chemistry*, vol. 284, no. 17, pp. 11326–11335, 2009.
- [78] T. Ukai, M. Sato, H. Akutsu, A. Umezawa, and J. Mochida, "MicroRNA-199a-3p, microRNA-193b, and microRNA-320c are correlated to aging and regulate human cartilage metabolism," *Journal of Orthopaedic Research*, vol. 30, no. 12, pp. 1915–1922, 2012.
- [79] D. C. Ilas, S. M. Churchman, T. Baboolal et al., "The simultaneous analysis of mesenchymal stem cells and early osteocytes accumulation in osteoarthritic femoral head sclerotic bone," *Rheumatology (Oxford)*, vol. 58, no. 10, pp. 1777–1783, 2019.
- [80] J. Guduric-Fuchs, A. O'Connor, B. Camp, C. L. O'Neill, R. J. Medina, and D. A. Simpson, "Selective extracellular vesicle-mediated export of an overlapping set of microRNAs from multiple cell types," *BMC Genomics*, vol. 13, no. 1, p. 357, 2012.
- [81] X. Wang, Y. Guo, C. Wang, H. Yu, X. Yu, and H. Yu, "MicroRNA-142-3p inhibits chondrocyte apoptosis and inflammation in osteoarthritis by targeting HMGB1," *Inflammation*, vol. 39, no. 5, pp. 1718–1728, 2016.
- [82] H. C. Dong, P. N. Li, C. J. Chen et al., "Sinomenine attenuates cartilage degeneration by regulating miR-223-3p/NLRP3 Inflammasome signaling," *Inflammation*, vol. 42, no. 4, pp. 1265–1275, 2019.
- [83] B. Bakhshandeh, M. Soleimani, S. H. Paylakhi, and N. Ghaemi, "A microRNA signature associated with chondrogenic lineage commitment," *Journal of Genetics*, vol. 91, no. 2, pp. 171–182, 2012.
- [84] M. Loef, J. W. Schoones, M. Kloppenburg, and A. Ioan-Facsinay, "Fatty acids and osteoarthritis: different types, different effects," *Joint, Bone, Spine*, vol. 86, no. 4, pp. 451–458, 2019.
- [85] T. Matsuzaki, O. Alvarez-Garcia, S. Mokuda et al., "FoxO transcription factors modulate autophagy and proteoglycan 4 in cartilage homeostasis and osteoarthritis," *Science Translational Medicine*, vol. 10, no. 428, p. eaan0746, 2018.
- [86] E. Ragni, C. Perucca Orfei, P. de Luca, A. Colombini, M. Viganò, and L. de Girolamo, "Secreted Factors and EV-miRNAs Orchestrate the Healing Capacity of Adipose Mesenchymal Stem Cells for the Treatment of Knee Osteoarthritis," *International Journal of Molecular Sciences*, vol. 21, no. 5, p. 1582, 2020.
- [87] T. Lange, S. Stracke, R. Rettig et al., "Identification of miR-16 as an endogenous reference gene for the normalization of urinary exosomal miRNA expression data from CKD patients," *PLoS One*, vol. 12, no. 8, article e0183435, 2017.
- [88] L. W. Lee, S. Zhang, A. Etheridge et al., "Complexity of the microRNA repertoire revealed by next-generation sequencing," *RNA*, vol. 16, no. 11, pp. 2170–2180, 2010.
- [89] M. Drewry, I. Helwa, R. R. Allingham, M. A. Hauser, and Y. Liu, "miRNA profile in three different Normal human

- ocular tissues by miRNA-Seq,” *Investigative Ophthalmology & Visual Science*, vol. 57, no. 8, pp. 3731–3739, 2016.
- [90] M. Nugent, “MicroRNAs: exploring new horizons in osteoarthritis,” *Osteoarthritis and Cartilage*, vol. 24, no. 4, pp. 573–580, 2016.
- [91] J. B. van Meurs, C. G. Boer, L. Lopez-Delgado, and J. A. Riancho, “Role of Epigenomics in bone and cartilage disease,” *Journal of Bone and Mineral Research*, vol. 34, no. 2, pp. 215–230, 2019.
- [92] S. A. Ali, R. Gandhi, P. Potla et al., “Sequencing identifies a distinct signature of circulating microRNAs in early radiographic knee osteoarthritis,” *Osteoarthritis and Cartilage*, vol. 28, no. 11, pp. 1471–1481, 2020.
- [93] C. Cavallo, G. Merli, R. M. Borzì et al., “Small extracellular vesicles from adipose derived stromal cells significantly attenuate in vitro the NF- κ B dependent inflammatory/catabolic environment of osteoarthritis,” *Scientific Reports*, vol. 11, no. 1, p. 1053, 2021.
- [94] S. Li, S. Stöckl, C. Lukas et al., “hBMSC-derived extracellular vesicles attenuate IL-1 β -induced catabolic effects on OA-chondrocytes by regulating pro-inflammatory signaling pathways,” *Frontiers in Bioengineering and Biotechnology*, vol. 8, p. 603598, 2020.
- [95] S. Zhang, K. Y. W. Teo, S. J. Chuah, R. C. Lai, S. K. Lim, and W. S. Toh, “MSC exosomes alleviate temporomandibular joint osteoarthritis by attenuating inflammation and restoring matrix homeostasis,” *Biomaterials*, vol. 200, pp. 35–47, 2019.
- [96] C. H. Woo, H. K. Kim, G. Y. Jung et al., “Small extracellular vesicles from human adipose-derived stem cells attenuate cartilage degeneration,” *Journal of Extracellular Vesicles*, vol. 9, no. 1, p. 1735249, 2020.
- [97] M. Ruiz, K. Toupet, M. Maumus, P. Rozier, C. Jorgensen, and D. Noël, “TGFBI secreted by mesenchymal stromal cells ameliorates osteoarthritis and is detected in extracellular vesicles,” *Biomaterials*, vol. 226, p. 119544, 2020.
- [98] Q. Ji, Y. Zheng, G. Zhang et al., “Single-cell RNA-seq analysis reveals the progression of human osteoarthritis,” *Annals of the Rheumatic Diseases*, vol. 78, no. 1, pp. 100–110, 2019.
- [99] C. H. Chou, V. Jain, J. Gibson et al., “Synovial cell cross-talk with cartilage plays a major role in the pathogenesis of osteoarthritis,” *Scientific Reports*, vol. 10, no. 1, p. 10868, 2020.

Research Article

Chondrogenic Potential of Human Dental Pulp Stem Cells Cultured as Microtissues

Rubén Salvador-Clavell ¹, José Javier Martín de Llano ^{1,2}, Lara Milián ^{1,2},
María Oliver ¹, Manuel Mata ^{1,2}, Carmen Carda ^{1,2,3} and María Sancho-Tello ^{1,2}

¹Department of Pathology, Faculty of Medicine and Dentistry, University of Valencia, Valencia, Spain

²INCLIVA Biomedical Research Institute, Valencia, Spain

³Biomedical Research Networking Center on Bioengineering, Biomaterials and Nanomedicine (CIBER-BBN), Spain

Correspondence should be addressed to José Javier Martín de Llano; j.javier.martin@uv.es

Received 18 May 2021; Revised 22 July 2021; Accepted 16 August 2021; Published 8 September 2021

Academic Editor: Weimin Guo

Copyright © 2021 Rubén Salvador-Clavell et al. This is an open access article distributed under the Creative Commons Attribution License, which permits unrestricted use, distribution, and reproduction in any medium, provided the original work is properly cited.

Several tissue engineering stem cell-based procedures improve hyaline cartilage repair. In this work, the chondrogenic potential of dental pulp stem cell (DPSC) organoids or microtissues was studied. After several weeks of culture in proliferation or chondrogenic differentiation media, synthesis of aggrecan and type II and I collagen was immunodetected, and SOX9, ACAN, COL2A1, and COL1A1 gene expression was analysed by real-time RT-PCR. Whereas microtissues cultured in proliferation medium showed the synthesis of aggrecan and type II and I collagen at the 6th week of culture, samples cultured in chondrogenic differentiation medium showed an earlier and important increase in the synthesis of these macromolecules after 4 weeks. Gene expression analysis showed a significant increase of COL2A1 after 3 days of culture in chondrogenic differentiation medium, while COL1A1 was highly expressed after 14 days. Cell-cell proximity promotes the chondrogenic differentiation of DPSCs and important synthesis of hyaline chondral macromolecules.

1. Introduction

Nowadays, the incidence of articular pathologies is dramatically rising. Factors such as advanced age of the population, illnesses, lifestyle, or trauma can lead to damage on the articular cartilaginous tissue [1]. Hyaline cartilage extracellular matrix (ECM) is a highly hydrated and gelatinous one, due to the glycosaminoglycan (GAG) component, mainly aggrecan, and the glycoproteins content [2, 3]. In this tissue, type II collagen is the most characteristic fibrous component of the ECM [4]. In addition, articular cartilage has a low regenerative capability due to its physiological characteristics, the absence of vascularization, perichondrium or MSC, and the limited proliferative capability of mature chondrocytes [5]. Thus, the response of joint cartilage to damage is usually the formation of a fibrous scar composed of type I collagen and fibroblast-type cells [6]. This low capability of autono-

mous regeneration has put cartilage in the spotlight of biomedical research, being currently one of the goals to be achieved [3, 7, 8]. In larger lesions, the mosaicplasty technique can be performed [9], but joint arthroscopic surgery is required for this procedure, since it is used in lesions larger than 2 cm². Furthermore, cartilage cylindrical grafts have to be harvested from a healthy cartilage from a non-weight bearing area. The results obtained are favourable in some cases, with optimal chondral regeneration [9]. However, although classic therapies or surgical treatments (such as mosaicplasty) have been developed with acceptable results in the short term, they have frequently shown fibrocartilage formation in the repaired damage in the long term, and for this reason, they are applied only in a limited number of patients [10, 11].

Tissue engineering (TE) focuses on developing substitutes that help to repair tissue injuries, attempting to achieve

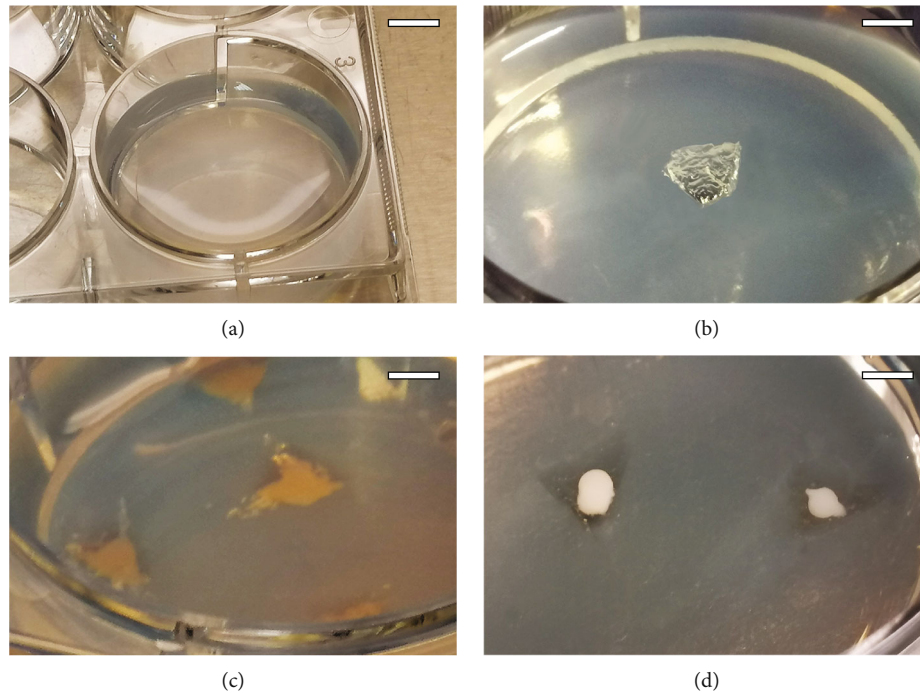


FIGURE 1: Process of the cell microtissues elaboration in 3% agarose wells. (a) 3% agarose hydrogel after 48 h at 4°C; (b) elaboration of wells in agarose hydrogel; (c) cellular seeding in agarose wells; and (d) completely formed microtissues after 72 h of cell culture. Scale bars—A: 12 mm; B-D: 3 mm.

optimal physiological and mechanical properties similar to the native tissue [1]. For articular cartilage lesions, this new interdisciplinary science is based on the use of cells, biomaterials, and stimulants such as growth factors [12–16]. Examples of the most popular techniques in which the use of cells is fundamental are Autologous Chondrocyte Implantation (ACI) and Matrix-induced Autologous Chondrocyte Implantation (MACI) techniques [17–20]. However, it has been shown that the use of chondrocytes entails problems associated with the isolation and proliferation procedures and the cellular dedifferentiation [21, 22].

The use of mesenchymal stem cells (MSCs), instead of chondrocytes, is an alternative for TE procedures [21, 23–25]. The plasticity and differentiation potential of these cells has been demonstrated using differentiation techniques [5, 26–31] and also their high proliferation capability when compared to chondrocytes [32–34]. Dental pulp stem cells (DPSCs) have become one of the most common stem cells used in several studies [25, 35], because of their easy accessibility, plasticity, high proliferative ability, and their multiple differentiation capability (chondrogenic, odontogenic, and neurogenic, among others) compared with other MSCs from bone marrow or adipose tissue origin [36–38]. The use of DPSCs in cartilage tissue repair has been reported by several authors (for a review, see [39]). Furthermore, DPSCs are good candidates for developing allogenic histocompatible cell biobanks for research and future clinical applications due to their aforementioned characteristics and immunomodulatory properties [40, 41]. In addition, the use of growth factors (such as IGF, FGF, or TGF β [42–45]) as well as physical and environmental conditions [46] can help to

improve cellular differentiation. In fact, TGF- β 1 has an important role in chondrogenic differentiation [29, 47]. Most researchers have chosen chondrogenic *in vitro* predifferentiation of MSCs, as DPSCs, with positive results [47–49]. Despite the extended use of biomaterials [29, 50–53], some researchers have demonstrated that pelleted cell cultures enhance chondrogenic differentiation of MSCs better than hydrogel cultures [54–56]. On the one hand, hydrogels are used to repair damaged cartilage [57–62] and can provide cell-matrix interactions and better mechanical support [52, 63]. However, the hydrogel matrix that encloses cells can affect the formation of cell-to-cell contacts, which in turn can influence cell differentiation [64, 65]. On the other hand, scaffold-free cellular organoids also show similar morphology to native cartilage [63]. The main inconvenience of pelleted cell cultures, or microtissues, is the need of a high cellular density per pellet but is tackled by using MSCs due to their high proliferation capacity [32–34]. For this reason, scaffold-free cell-based therapy could be a new treatment for cartilage repair and regeneration [64–66].

We hypothesize that a 3D arrangement of human DPSCs favours their chondrogenic differentiation. Thus, the aim of this work was to study the capability of human DPSCs cultured in microtissues or cellular organoids to develop a chondrogenic phenotype. To assess cellular differentiation, cell morphology and the expression of characteristic chondral macromolecules and genes were analysed in those cultures.

2. Material and Methods

2.1. Cell Culture. Human dental pulp stem cells (hDPSCs; Lonza, Switzerland) on passage 4 were seeded on culture

TABLE 1: Gene marker primers.

Gene	ID reference	Function
SOX9	Hs00165814_m1	Chondrogenic transcription factor
ACAN	Hs00153936_m1	Hyaline cartilage-related ECM component
COL2A1	Hs00264051_m1	Hyaline cartilage-related ECM component
COL1A1	Hs00164004_m1	Fibrous cartilage-related ECM component
GAPDH	Hs99999905_m1	Housekeeping gene

flasks with proliferation medium containing alpha minimum essential media (α MEM; Gibco, USA) supplemented with 10% foetal bovine serum (Gibco), 1% L-glutamine (Gibco), and 1% penicillin/streptomycin (Gibco) and cultured in a humidified atmosphere incubator at 37°C and 5% CO₂. Culture media were changed every 2-3 days. Cells were detached from the flask with a 0.25% (*w/v*) trypsin-0.91 mM EDTA solution (Gibco) and cultured at a density of 6×10^5 cells/sample as shown below. Culture media of half of the samples were changed for chondrogenic differentiation media (Lonza) supplemented with 5% FBS, 0.2% R³-insulin-like growth factor-1 (R³-IGF-1), 0.5% transforming growth factor beta 1 (TGF β 1), 0.2% transferrin, 0.2% insulin, 0.1% gentamicin/amphotericin-B (GA), and 70 mM ascorbic acid.

2.2. Agarose Hydrogel Preparation, Cytotoxicity Assay, and Microtissue Formation. Hydrogels of 3% type IX-A agarose were prepared as previously described [67], with minor modifications, and allowed to solidify for 48 h (Figure 1(a)). Cytotoxicity of the agarose hydrogel was tested using the MTS assay (CellTiter 96 Aqueous One Solution Cell Proliferation Assay, Promega, Spain). Cell culture medium was conditioned as follows: proliferation medium without phenol red was added to 3% agarose hydrogel at a 1:2 *v/v* ratio and incubated for 1, 3, and 7 days at 37°C and 5% CO₂. hDPSCs were seeded in 96-well plates at a density of 10^4 cells/well. After 24h of cell culture, the medium was removed and conditioned media were added. Latex-conditioned medium was used as a positive cytotoxic control, and nonconditioned medium was used as a negative control. After 24h of cell culture, the MTS assay was carried out following the manufacturer's indications.

Wells of 4 mm-diameter and 5 mm-deep were created in 3% agarose hydrogel blocks using a laboratory spoon (Figure 1(b)). Then, 6×10^5 cells were resuspended in 10 μ L proliferation culture medium and added to each well created in the agarose (Figure 1(c)); the agarose block was placed in the cell incubator, and the microtissues were allowed to form for 72 h (Figure 1(d)). This was considered the initial, control time ($t = 0$). Samples were cultured in proliferation or chondrogenic differentiation media for 3, 14, 28, and 42 days. The corresponding cell culture medium was changed every 2-3 days.

2.3. Histological Studies. Cell morphology and chondral components content were evaluated following standard histological procedures. Briefly, samples were rinsed twice with PBS and fixed with 4% buffered formaldehyde at 4°C for 20 min. Samples were rinsed twice again with PBS and

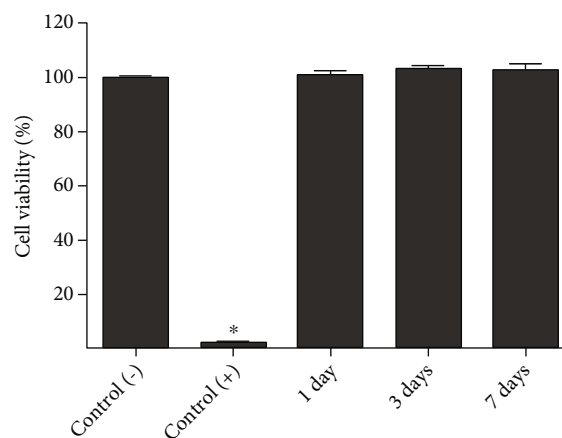


FIGURE 2: Cell viability assay results. hDPSCs were cultured with media conditioned for 1, 3, and 7 days with 3% agarose hydrogel. Nonconditioned medium and latex-conditioned medium were used as negative and positive cytotoxicity controls, respectively. MTS assay was carried out as described in Material and Methods, and bars show the mean \pm SD. * $p < 0.001$ compared to negative control.

embedded in paraffin (following standard protocols), and 3 μ m thick sections were obtained, which were stained with haematoxylin and eosin (H-E) solutions. Stained sections were analysed under an optical microscope (DM 4000B; Leica Biosystems, Germany) and photographed using the Leica DFC 420 camera. Cell density was analysed on stained samples by cellular counting of 10 randomized fields throughout the section, using Image-Pro Plus 6.0 software.

Aggrecan and type I and II collagen content were evaluated by immunofluorescence as previously described [25]. Microtissue sections were deparaffined and rehydrated through graded ethanol and rinsed with PBS, and immunofluorescence was carried out. Specific mouse IgG anti-human antibodies (sc-166951, aggrecan, Santa Cruz Biotechnology, dilution 1:200; C2456, type I collagen, Sigma, dilution 1:100; and CP18, type II collagen, Millipore, dilution 1:500) and secondary anti-mouse-IgG FITC-conjugated antibody (F2883, Sigma, dilution 1:200) were used. Some samples were incubated only with the secondary anti-mouse-IgG antibody as control. For nuclei and actin filament staining, samples were incubated with 300 nM DAPI (Sigma) and rhodamine-phalloidin (1:200 in PBS) (Invitrogen, USA), respectively, for 2 h at RT. Samples were analysed under a fluorescence microscope (DM 4000B; Leica Biosystems) and photographed using the Leica DFC 340FX camera.

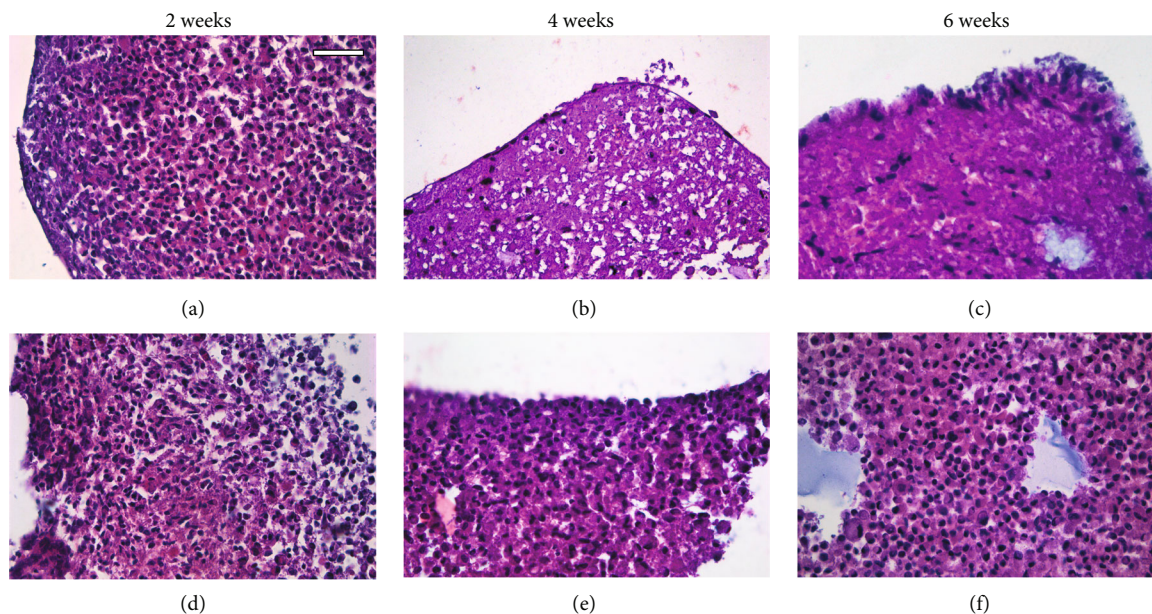


FIGURE 3: H-E staining images of hDPSC microtissue cultures after (a, d) 2 weeks, (b, e) 4 weeks, and (c, f) 6 weeks. Culture media used were (a–c) proliferation and (d–f) chondrogenic differentiation. Scale bar = 50 μm .

2.4. Gene Expression Analysis. Finally, the expression of chondrogenic-related genes in chondrogenic-induced hDPSCs microtissues was evaluated by real-time RT-PCR, as follows. On the one hand, SOX9, ACAN, and COL2A1 are characteristic genes associated with chondrogenesis; on the other hand, COL1A1 is related to fibrous tissues. After microtissue formation, culture medium was replaced by chondrogenic differentiation medium, and samples were cultured for different times: 1, 6, and 24 h and 3, 7, and 14 days. Culture medium was changed every 2–3 days. Then, RNA was isolated using Trizol LS reagent (Ambion, Life Technologies, USA), and RNA was converted to cDNA by reverse transcription PCR using High-Capability cDNA Reverse Transcription Kit (Applied Biosystems, USA). Finally, real-time PCR was performed using primers for the previously mentioned genes and GAPDH as housekeeping gene (Taqman, Applied Biosystems) as shown in Table 1. Relative gene expressions were normalized to GAPDH expression, and the fold change was presented using the $\Delta\Delta C_T$ method by comparing to control samples at initial time (without chondrogenic differentiation induction).

2.5. Data Presentation and Statistical Analysis. The results shown correspond to two independent experiments, and in each of them, experimental samples were replicated 3 times. The histological study was performed in a double-blinded manner, and the figures presented are representative images.

For statistical analysis, Tukey's test one-way ANOVA was performed to find differences between samples at different timepoints, with p value significance threshold of ≤ 0.05 .

3. Results

3.1. Agarose Hydrogel Cytotoxicity. Cell viability of hDPSCs cultured with media conditioned for 1, 3, or 7 days with

3% agarose hydrogels was maximum with no statistically significant differences from that of the negative control, whereas cell viability of hDPSCs cultured with latex-conditioned media (cytotoxicity-positive control) was significantly low, as expected (Figure 2).

3.2. H-E Staining. After 2-week culture, no morphological differences were observed between microtissues cultured with either proliferation or chondrogenic differentiation media (Figures 3(a) and 3(d)), showing cells tightly packed and homogeneously distributed throughout the cellular organoid without spaces between cells. At this time, cells showed a polygonal morphology with an eosinophilic cytoplasm and a round or elliptic basophilic nucleus with dense chromatin. Differences were observed at 4 and 6 weeks of cell culture, when samples cultured with proliferating medium showed the presence of a single layer of cells at the organoid periphery, whereas large areas of ECM and a lower density of cells were observed in the center of the organoid (Figures 3(b) and 3(c)). On the contrary, the samples cultured with chondrogenic differentiation medium for 4 and 6 weeks did not show differences from those cultured for 2 weeks with this same medium, and the cells were tightly packed and homogeneously distributed throughout the microtissue, with scarce ECM between them (Figures 3(e) and 3(f)).

3.3. Cell Density Quantification. Table 2 shows the cellular density of hDPSC microtissues. At the beginning of the cell culture ($t = 0$), samples showed a density of 9,400 cells/ mm^2 . After 3-day culture with proliferation and chondrogenic differentiation media, 12,800 and 12,200 cells/ mm^2 were counted, respectively, with no significant differences between both conditions. In 2-week microtissues cultured with proliferation medium, a slight increase to 13,000

TABLE 2: Cell density (cells/mm²) of hDPSC microtissues cultured with proliferation or chondrogenic differentiation media for 3 days and 2, 4, and 6 weeks. Samples at initial time ($t = 0$; cell density: $9,400 \pm 600$) were taken as control. Values shown (mean \pm SD) are $\times 10^3$. Statistical significance at $p \leq 0.05$ with respect to control (*) and to samples cultured with proliferation medium for the same period of time (#).

	3 days	2 weeks	4 weeks	6 weeks
Proliferation	$12.8 \pm 0.4^*$	$13.0 \pm 1.3^*$	$2.5 \pm 0.4^*$	$4.6 \pm 0.8^*$
Chondrogenic differentiation	$12.2 \pm 0.7^*$	$10.5 \pm 0.1^*$	$11.6 \pm 0.6^{*,\#}$	$12.1 \pm 1.3^{*,\#}$

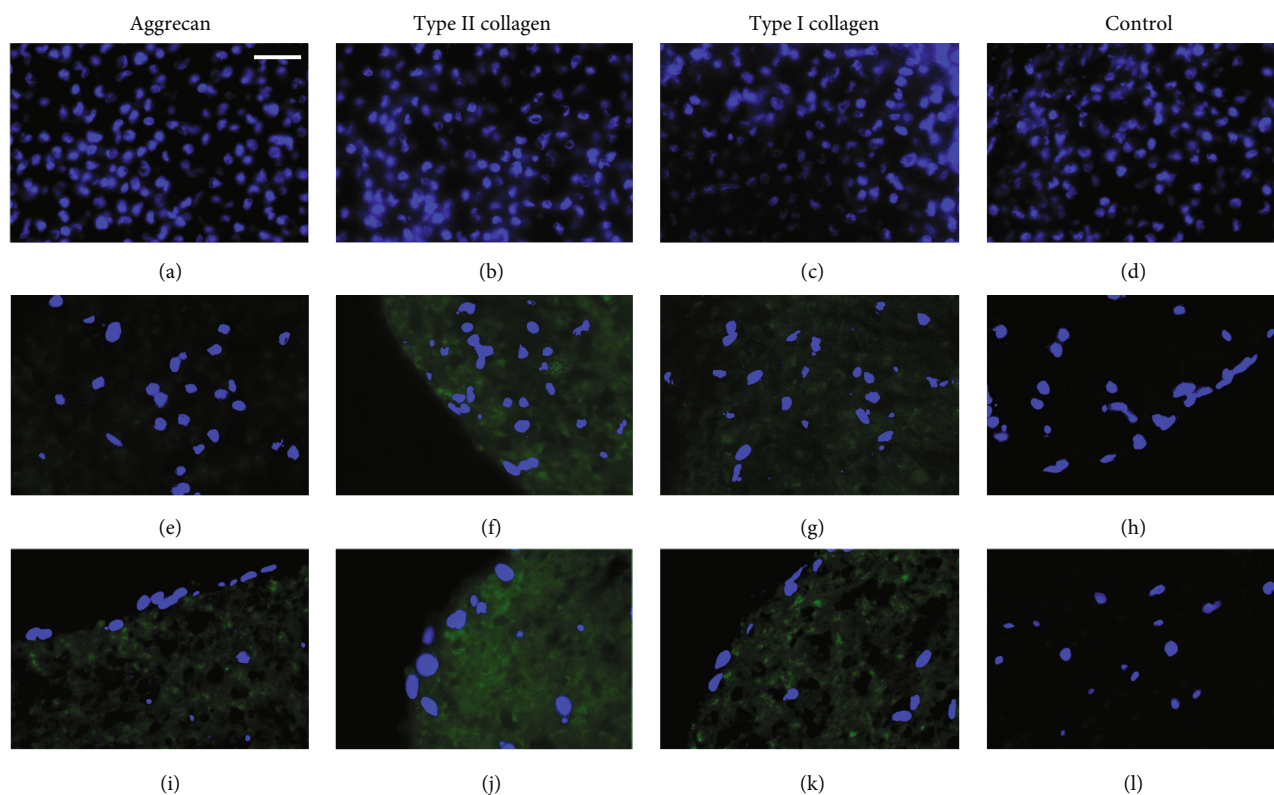


FIGURE 4: Immunofluorescence microphotographs of hDPSCs microtissue-cultures with proliferation medium for (a–d) 2 weeks, (e–h) 4 weeks, and (i–l) 6 weeks. Control samples were incubated only with the secondary antibody. Cellular nuclei are observed in blue, and the presence of the different specific macromolecules was analysed in green. To facilitate the visualization of the fluorescence signal, green channel parameters of some images were modified by PhotoShop: (e, g) saturation + 100% and luminosity + 50% and (f) saturation + 100% and luminosity + 25%. Scale bar = 25 μ m.

cells/mm² was observed, while in the samples with differentiation medium 10,500 cells/mm² were counted. No statistically significant differences were observed between both conditions. After 4-week culture, proliferation samples decreased to 2,500 cells/mm². On the contrary, chondrogenic differentiation microtissues reached values of 11,600 cells/mm², a cell density significantly different when compared to that of the proliferation samples. Finally, samples maintained for 6 weeks in proliferation culture medium showed cell density values of 4,600 cells/mm², while differentiation samples reached a cell density of 12,100 cells/mm². Significant differences were observed between both conditions. Microtissues cultured in chondrogenic differentiation media did not show significant differences in the number of cells throughout the time of culture.

3.4. Immunodetection. Initial time ($t = 0$) and 3-day samples showed a compact formation of the microtissues as previously described. In these cases, samples did not show aggrecan or type II and I collagens synthesis with either proliferation or chondrogenic differentiation culture media (data not shown).

Cells cultured with proliferation medium did not show the presence of aggrecan until the 4th week of culture, when small, scattered regions were labelled (Figures 4(a) and 4(e)). This labelling increased at the 6th week of culture, but interestingly, it showed different intensity at the different zones of the microtissue, since it was mainly located at the central zone of the organoid (Figure 4(i)). Synthesis of type II collagen was first observed at the 4th week in the external zone of microtissue, right under the layer of peripheral cells, and it

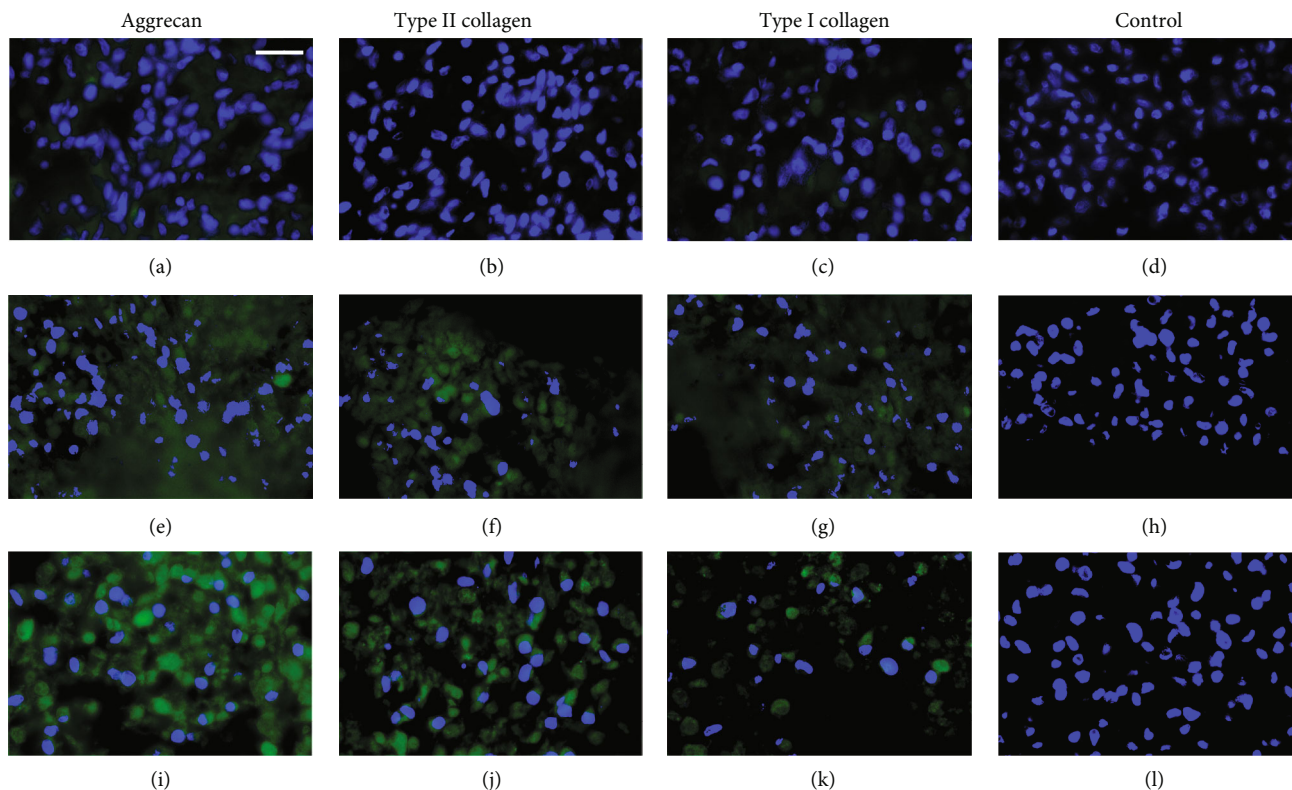


FIGURE 5: Immunofluorescence microphotographs of hDPSC microtissue cultures with chondrogenic differentiation medium for (a–d) 2 weeks, (e–h) 4 weeks, and (i–l) 6 weeks. Control samples were incubated only with the secondary antibody. Cellular nuclei are observed in blue, and the presence of the different specific macromolecules was analysed in green. To facilitate the visualization of the fluorescence signal, green channel parameters of some images were modified by PhotoShop: (a, c) saturation + 100% and luminosity + 50% and (e–g) saturation + 100% and luminosity + 25%. Scale bar = 25 μ m.

increased in the 6-week culture, when it was homogeneously distributed throughout the organoid (Figures 4(b), 4(f) and 4(j)). Finally, as regards to type I collagen, small areas adjacent to the cell nuclei were labelled at 4-week of culture, while at 6 weeks it was distributed throughout the microtissue (Figures 4(c), 4(g) and 4(k)).

In the case of chondrogenic differentiation cell cultures, in all microtissues, there was a homogeneous distribution of the cells throughout the organoids, as mentioned above. As expected, aggrecan synthesis was observed earlier than in those cells cultured in proliferation medium, since it was detected from the 2nd week, increased over time, and became abundant at 6 weeks (Figures 5(a), 5(e) and 5(i)). The presence of type II collagen was observed at 4-week cell culture, increasing throughout the 6 weeks of the microtissue culture (Figures 5(b), 5(f) and 5(j)). Finally, type I collagen labelling was also slightly observed at 2-week culture, especially around cell nuclei (suggesting intracellular location), and increased mildly its synthesis at 4 and 6 weeks (Figures 5(c), 5(g) and 5(k)).

3.5. Gene Expression Analysis. Histological results showed a lower cell density and a peripheral cell distribution in microtissues cultured in proliferation medium. Furthermore, as expected, chondral components were increased in microtissues cultured with differentiation rather than with proliferation media. Thus, the former microtissues were chosen for

further analysis of the gene expression. Since gene expression occurs earlier than protein synthesis, short periods of culture were included in this study. The analysis of the expression of gene markers was studied in microtissues cultured for short periods (1, 6, and 24 h) and longer periods (3, 7, and 14 days) with chondrogenic differentiation medium. Significant differences on COL2A1 and COL1A1 gene markers were observed. COL2A1 gene expression showed a 10-fold increase with respect to control on the third day of culture (Figure 6(c)). This increase was close to a 30-fold change after 7 days of culture and over a 70-fold change after 14 days. Besides, COL1A1 gene expression showed a 2-fold increase after 14 days of chondrogenic differentiation culture (Figure 6(d)). No significant differences were observed for SOX9 and ACAN gene expressions throughout the time of culture studied (Figures 6(a) and 6(b)).

4. Discussion

Since cartilage has a low regenerative capability [7, 8], a high number of therapies have emerged to solve chondral pathologies. These therapies have achieved acceptable results, but mainly result in the formation of fibrocartilage [10]. For this reason, tissue engineering approaches do not focus on repairing but on regenerating these injuries [1]. Different types of cells have been studied over the years, and researchers have demonstrated that MSCs [27, 28], such as

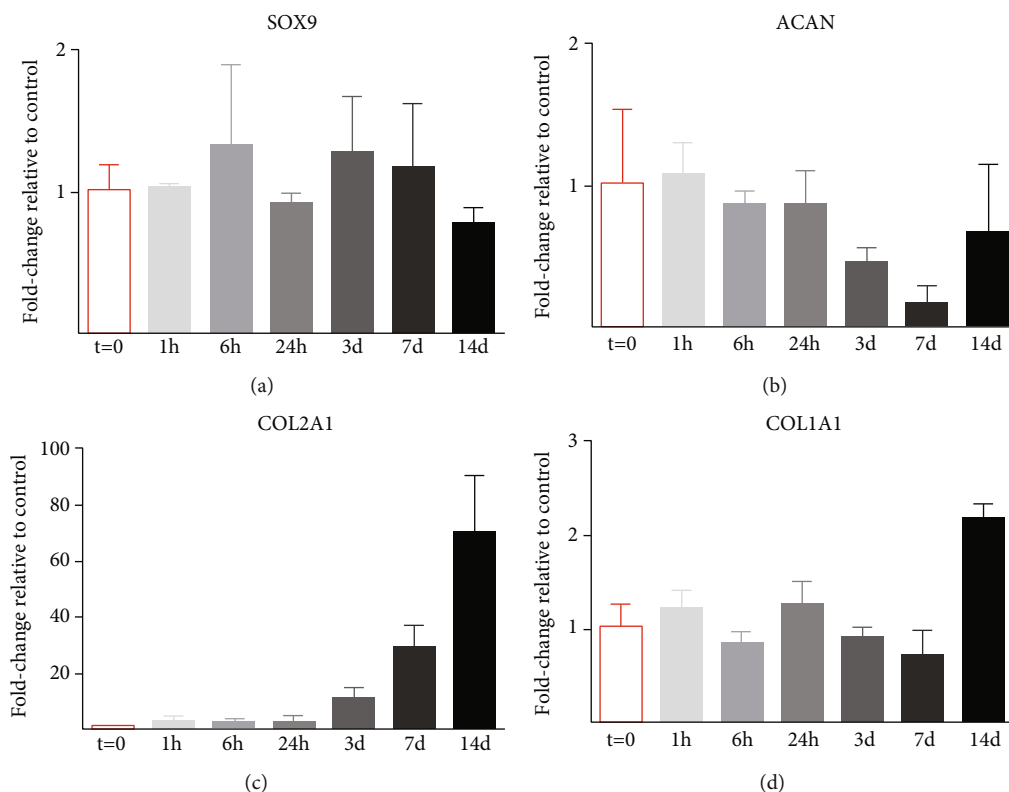


FIGURE 6: Relative expression of (a) SOX9, (b) ACAN, (c) COL2A1, and (d) COL1A1 genes after 1, 6, and 24 h and 3, 7, and 14 days of chondrogenic differentiation medium culture of hDPSC microtissues. Gene expression was normalized to GAPDH expression and compared to control samples ($t = 0$). Mean \pm SD are shown. Statistical significance at $*p \leq 0.05$ with respect to control.

DPSCs and ADSCs, among others, can differentiate to the chondrogenic lineage [36]. Moreover, 3D environments such as PLA scaffolds or hydrogels have been used to culture cells in them, improving cell differentiation and showing good results considering the synthesis of proteins characteristic of the chondral extracellular matrix [50, 51]. Finally, it is known that growth factors can promote an earlier chondrogenic differentiation of cells in culture [47].

In this work, hDPSC microtissues were generated and kept in 3% agarose wells. The results obtained using cell culture media conditioned with agarose hydrogel demonstrated that this hydrogel was not cytotoxic, as described by others [68, 69]. The microtissues formed were cultured for several weeks, with either proliferation or chondrogenic differentiation media. After that, the content of aggrecan and type II and I collagens was analysed, and the different culture conditions were compared to study the chondrogenic differentiation potential of this type of mesenchymal stem cell.

We observed that cells forming microtissues synthesized and secreted aggrecan and type II collagen and, to a lesser extent type I collagen, either in the presence of proliferation medium or chondrogenic differentiation medium, in the latter at shorter times of cell culture. These results agree with those of Mahboudi et al., where significant deposition of aggrecan and increased COL2A1 gene expression were detected in pelleted cultures of induced pluripotent stem cells (iPSCs) [70]. Therefore, cell-cell proximity, occurring

in these microtissues, induced the production of macromolecules of the extracellular chondral matrix, obtaining better results than in studies where cells were cultured in a hydrogel-scaffold matrix [52, 65, 66, 71].

HE staining and cell number quantification showed differences in both cell density and distribution when comparing microtissues cultured with proliferation or differentiation media for several weeks. In the former, microtissue cell density was lower and cell was distributed mainly on the surface, while in the latter cell distribution was homogenous across the microtissue volume. It is tentative to consider that the different ECM composition, as deduced from the HE staining and immunofluorescence results, interferes or makes the growth of the cells in the central zone of microtissues cultured with proliferation medium more difficult. Considering these results, we decided to study the expression of selected genes in microtissues cultured in differentiation medium. We observed that the expression of COL2A1 exhibited an early induction when hDPSC microtissues were exposed to chondrogenic differentiation medium, which agrees with the results of Zhang et al., which demonstrated the chondrogenic potential of MSC microtissues exposed to a chondrogenic inducing medium [54].

It has been demonstrated that a 3D cell niche is important to improve chondrogenic differentiation of MSCs, as DPSCs [72], and many research studies have focused on developing and optimising 3D architectures for that purpose.

Several polymers, such as PLA (polylactic acid), PCL (polycaprolactone), PEGMA (poly(ethylene glycol)methacrylate), and gelatine, among others, have been used to create suitable hydrogels or nanofiber-based scaffolds with adequate physical properties to promote chondrogenic differentiation [72–75]. However, also numerous studies are currently focused on the development of organoids, creating organomimetic tissues [67, 76–78], which mimic and improve the functions of the native tissues where they will be implanted. Our results agree with those of Torras et al., who reported that pluripotent cells, as DPSCs, have a high capability for intrinsic organization when cultured in an organoid or microtissue model, which is related to different cell functions, such as extracellular matrix synthesis, among others [76].

Thus, we have observed that the chondrogenic differentiation medium used promoted the early synthesis of these components, mainly aggrecan and type II collagen, while maintaining stable architecture of the microtissues. These results agree with the studies by Meyer-Wagner et al., where cell organoids exposed to electromagnetic fields (EMF) and cultured with chondrogenic differentiation medium showed a higher expression of gene characteristic of the chondral lineage than those cells exposed to EMF and cultured with cellular expansion medium [79].

Therefore, not only the cell culture medium but also the 3D environment is essential in chondrogenic differentiation to obtain good results considering the synthesis of components of the chondral matrix such as aggrecan and type II collagen. In this work, hDPSC microtissues cultured with chondrogenic differentiation medium promoted the onset of chondral components at shorter times than the same cells cultured with proliferation medium, which is an important point to improve the regeneration of articular chondral injuries.

5. Conclusions

The choice of the cell type, the culture environment, and the media are critical to obtain good results in biomedical studies. Firstly, we have shown that hDPSCs have a high chondrogenic potential. Secondly, a 3D environment, such as microtissues or organoids, favours the chondrogenic differentiation of cells. Finally, culture media with suitable growth factors, such as those present in the chondrogenic differentiation medium, can accelerate the synthesis of different macromolecules characteristics of the extracellular matrix of the hyaline articular cartilage, such as aggrecan and type II collagen.

We are establishing the experimental conditions for grafting hDPSCs microtissues in an animal model, to evaluate in the near future their in vivo chondrogenic differentiation potential. Furthermore, we are currently studying the effect of magnetic irradiation and mechanical stimuli on the chondrogenic differentiation of hDPSC microtissues formed as described herein.

Data Availability

The data used to support the findings of this study are included within the article.

Conflicts of Interest

The authors declare that there is no conflict of interest.

Acknowledgments

This work was supported by grants MAT2016-76039-C4-2-R and PID2019-106099RB-C42 from the Ministry of Economy and Competitiveness of the Spanish Government and by grant PROMETEO/2020/069 from Generalitat Valenciana (Spain). CIBER-BBN and CIBERER are funded by the VI National R&D&I Plan 2008-2011, Iniciativa Ingenio 2010, Consolider Program, CIBER Actions, and the Instituto de Salud Carlos III, with assistance from the European Regional Development Fund. We sincerely thank Teresa Sagrado Vives from the University of Valencia for her support with histological experiments.

References

- [1] R. Langer and J. Vacanti, "Tissue engineering," *Science*, vol. 260, no. 5110, pp. 920–926, 1993.
- [2] U. Welsch and T. Deller, *Histología de Sobotta*, Panamericana, Mexico, 3rd ed. edition, 2014.
- [3] M. Sancho-Tello, L. Milián, M. Mata Roig, J. J. Martín de Llano, and C. Carda, "Cartilage regeneration and tissue engineering," in *Advances in Biomechanics and Tissue Regeneration*, Elsevier, London, 2019.
- [4] D. Eyre, "Collagen of articular cartilage," *Arthritis Research*, vol. 4, no. 1, pp. 30–35, 2002.
- [5] A. Hamid, R. Idrus, A. Saim, S. Sathappan, and K. H. Chua, "Characterization of human adipose-derived stem cells and expression of chondrogenic genes during induction of cartilage differentiation," *Clinics*, vol. 67, no. 2, pp. 99–106, 2012.
- [6] K. D. Shelbourne, S. Jari, and T. Gray, "Outcome of untreated traumatic articular cartilage defects of the knee: a natural history study," *The Journal of Bone and Joint Surgery-American Volume*, vol. 85, pp. 8–16, 2003.
- [7] P. Guillén-García, E. Rodríguez-Iñigo, I. Guillén-Vicente et al., "Viability of pathologic cartilage fragments as a source for autologous chondrocyte cultures," *Cartilage*, vol. 7, no. 2, pp. 149–156, 2016.
- [8] M. K. Lotz and V. B. Kraus, "New developments in osteoarthritis: Posttraumatic osteoarthritis: pathogenesis and pharmacological treatment options," *Arthritis Research & Therapy*, vol. 12, no. 3, p. 211, 2010.
- [9] L. Hangody, G. Vásárhelyi, L. R. Hangody et al., "Autologous osteochondral grafting-technique and long-term results," *Injury*, vol. 39, pp. S32–S39, 2008.
- [10] L. Sharma, J. Song, D. T. Felson, S. Cahue, E. Shamiyeh, and D. D. Dunlop, "The role of knee alignment in disease progression and functional decline in knee osteoarthritis," *JAMA*, vol. 286, no. 2, pp. 188–195, 2001.
- [11] A. Dell'Isola, S. L. Smith, M. S. Andersen, and M. Steultjens, "Knee internal contact force in a varus malaligned phenotype in knee osteoarthritis (KOA)," *Osteoarthritis and Cartilage*, vol. 25, no. 12, pp. 2007–2013, 2017.
- [12] W. V. Giannobile, "Periodontal tissue engineering by growth factors," *Bone*, vol. 19, pp. 23–37, 1996.

- [13] K. H. Bouhadir and D. J. Mooney, "In vitro and in vivo models for the reconstruction of intercellular signaling," *Annals of the New York Academy of Sciences*, vol. 15, pp. 188–194, 1998.
- [14] A. H. Reddi, "Role of morphogenetic proteins in skeletal tissue engineering and regeneration," *Nature Biotechnology*, vol. 16, no. 3, pp. 247–252, 1998.
- [15] M. Nakashima and A. H. Reddi, "The application of bone morphogenetic proteins to dental tissue engineering," *Nature Biotechnology*, vol. 21, no. 9, pp. 1025–1032, 2003.
- [16] R. S. Prescott, R. Alsanea, M. I. Fayad et al., "In Vivo Generation of Dental Pulp-like Tissue by Using Dental Pulp Stem Cells, a Collagen Scaffold, and Dentin Matrix Protein 1 after Subcutaneous Transplantation in Mice," *Journal of Endodontia*, vol. 34, no. 4, pp. 421–426, 2008.
- [17] S. L. S. Vega, M. Y. Kwon, and J. A. Burdick, "Recent advances in hydrogels for cartilage tissue engineering," *European cells and materials journal*, vol. 33, pp. 59–75, 2017.
- [18] P. Guillén-García, E. Rodríguez-Iñigo, I. Guillén-Vicente et al., "Increasing the dose of autologous chondrocytes improves articular cartilage repair," *Cartilage*, vol. 5, no. 2, pp. 114–122, 2014.
- [19] J. M. Lopez-Alcorocho, L. Aboli, I. Guillen-Vicente et al., "Cartilage defect treatment using high-density autologous chondrocyte implantation: two-year follow-up," *Cartilage*, vol. 9, no. 4, pp. 363–369, 2018.
- [20] M. Sancho-Tello, F. Forriol, P. Gastaldi et al., "Time evolution of in vivo articular cartilage repair induced by bone marrow stimulation and scaffold implantation in rabbits," *The International Journal of Artificial Organs*, vol. 38, no. 4, pp. 210–223, 2015.
- [21] H. Yin, Y. Wang, X. Sun et al., "Functional tissue-engineered microtissue derived from cartilage extracellular matrix for articular cartilage regeneration," *Acta Biomaterialia*, vol. 77, pp. 127–141, 2018.
- [22] L. Zeng, X. Chen, Q. Zhang, F. Yu, Y. Li, and Y. Yao, "Redifferentiation of dedifferentiated chondrocytes in a novel three-dimensional microcavitary hydrogel," *Journal of Biomedical Materials Research Part A*, vol. 103, no. 5, pp. 1693–1702, 2015.
- [23] G. I. Im, "Clinical use of stem cells in orthopaedics," *European Cells and Materials*, vol. 33, pp. 183–196, 2017.
- [24] R. S. Clavell, J. J. M. de Llano, C. Carda, J. L. G. Ribelles, and A. Vallés-Lluch, "In vitro assessment of the biological response of Ti6Al4V implants coated with hydroxyapatite microdomains," *Journal of Biomedical Materials Research Part A*, vol. 104, no. 11, pp. 2723–2729, 2016.
- [25] M. Mata, L. Milian, M. Oliver et al., "In vivo articular cartilage regeneration using human dental pulp stem cells cultured in an alginate scaffold: a preliminary study," *Stem Cells International*, vol. 2017, Article ID 8309256, 9 pages, 2017.
- [26] B. Blum and N. Benvenisty, "The tumorigenicity of human embryonic stem cells," *Advances in Cancer Research*, vol. 100, pp. 133–158, 2008.
- [27] M. M. Kanafi, Y. B. Rajeshwari, S. Gupta et al., "Transplantation of islet-like cell clusters derived from human dental pulp stem cells restores normoglycemia in diabetic mice," *Cytotherapy*, vol. 15, no. 10, pp. 1228–1236, 2013.
- [28] M. Kanafi, D. Majumdar, R. Bhonde, P. Gupta, and I. Datta, "Midbrain cues dictate differentiation of human dental pulp stem cells towards functional dopaminergic neurons," *Journal of Cellular Physiology*, vol. 229, no. 10, pp. 1369–1377, 2014.
- [29] S. Ansari, I. M. Diniz, C. Chen et al., "Alginate/hyaluronic acid hydrogel delivery system characteristics regulate the differentiation of periodontal ligament stem cells toward chondrogenic lineage," *Journal of Materials Science. Materials in Medicine*, vol. 28, no. 10, p. ???, 2017.
- [30] I. Izal, P. Aranda, P. Sanz-Ramos et al., "Culture of human bone marrow-derived mesenchymal stem cells on poly(l-lactic acid) scaffolds: potential application for the tissue engineering of cartilage," *Knee Surgery, Sport Traumatol Arthrosc*, vol. 21, no. 8, pp. 1737–1750, 2013.
- [31] M. Esposito, A. Lucariello, C. Costanzo et al., "Differentiation of human umbilical cord-derived mesenchymal stem cells, WJ-MSCs, into chondrogenic cells in the presence of pulsed electromagnetic fields," *In Vivo*, vol. 27, no. 4, pp. 495–500, 2013.
- [32] F. H. Chen and R. S. Tuan, "Mesenchymal stem cells in arthritic diseases," *Arthritis Research & Therapy*, vol. 10, no. 5, p. 223, 2008.
- [33] M. R. Homicz, B. L. Schumacher, R. L. Sah, and D. Watson, "Effects of serial expansion of septal chondrocytes on tissue-engineered neocartilage composition," *Otolaryngol - Head Neck Surg*, vol. 127, no. 5, pp. 398–408, 2002.
- [34] T. C. MacKenzie and A. W. Flake, "Human mesenchymal stem cells: insights from a surrogate in vivo assay system," *Cells, Tissues, Organs*, vol. 171, no. 1, pp. 90–95, 2002.
- [35] J. J. Martín-de-Llano, M. Mata, S. Peydró, A. Peydró, and C. Carda, "Dentin tubule orientation determines odontoblastic differentiation in vitro: a morphological study," *PLoS One*, vol. 14, no. 5, article e0215780, 2019.
- [36] R. Karamzadeh, M. B. Eslaminejad, and R. Aflatoonian, "Isolation, characterization and comparative differentiation of human dental pulp stem cells derived from permanent teeth by using two different methods," *Journal of Visualized Experiments*, vol. 69, p. 4372, 2012.
- [37] X. Yang, L. Li, L. Xiao, and D. Zhang, "Recycle the dental fairy's package: overview of dental pulp stem cells," *Stem Cell Research & Therapy*, vol. 9, no. 1, 2018.
- [38] V. Mattei, S. Martellucci, F. Pulcini, F. Santilli, M. Sorice, and S. Delle Monache, "Regenerative potential of DPSCs and revascularization: direct, paracrine or autocrine effect?," *Stem Cell Reviews and Reports*, 2021.
- [39] T. L. Fernandes, J. P. Cortez de Sant'Anna, I. Frisene et al., "Systematic review of human dental pulp stem cells for cartilage regeneration," *Tissue Engineering. Part B, Reviews*, vol. 26, no. 1, pp. 1–12, 2020.
- [40] B. C. Kim, H. Bae, I. K. Kwon et al., "Osteoblastic/cementoblastic and neural differentiation of dental stem cells and their applications to tissue engineering and regenerative medicine," *Tissue Engineering. Part B, Reviews*, vol. 18, no. 3, pp. 235–244, 2012.
- [41] P. Y. Collart-Dutilleul, F. Chaubron, J. De Vos, and F. J. Cuisinier, "Allogenic banking of dental pulp stem cells for innovative therapeutics," *World Journal Stem Cells*, vol. 7, no. 7, pp. 1010–1021, 2015.
- [42] T. I. Morales, "The role and content of endogenous insulin-like growth factor-binding proteins in bovine articular cartilage," *Archives of Biochemistry and Biophysics*, vol. 343, no. 2, pp. 164–172, 1997.
- [43] S. B. Trippel, "Growth factor actions on articular cartilage," *The Journal of Rheumatology. Supplement*, vol. 43, pp. 129–132, 1995.

- [44] S. Chandrasekhar, A. K. Harvey, and S. T. Stack, "Degradative and repair responses of cartilage to cytokines and growth factors occur via distinct pathways," *Agents and Actions. Supplements*, vol. 39, pp. 121–125, 1993.
- [45] H. L. Glansbeek, P. M. van der Kraan, F. P. J. G. Lafeber, E. L. Vitters, and W. B. van den Berg, "Species-specific expression of type II TGF- β receptor isoforms by articular chondrocytes: effect of proteoglycan depletion and aging," *Cytokine*, vol. 9, no. 5, pp. 347–351, 1997.
- [46] R. Salvador-Clavell, J.-M. Rodríguez-Fortún, I. López et al., "Design and experimental validation of a magnetic device for stem cell culture," *The Review of Scientific Instruments*, vol. 91, no. 12, p. 124103, 2020.
- [47] A. T. Mehlhorn, H. Schmal, S. Kaiser et al., "Mesenchymal stem cells maintain TGF- β -mediated chondrogenic phenotype in alginate bead culture," *Tissue Engineering*, vol. 12, no. 6, pp. 1393–1403, 2006.
- [48] J. H. Spaas, S. Y. Broeckx, K. Chiers et al., "Chondrogenic priming at reduced Cell density enhances cartilage adhesion of equine allogeneic MSCs - a loading sensitive phenomenon in an organ culture study with 180 explants," *Cellular Physiology and Biochemistry*, vol. 37, no. 2, pp. 651–665, 2015.
- [49] K. Chen, C. Man, B. Zhang, J. Hu, and S. S. Zhu, "Effect of *in vitro* chondrogenic differentiation of autologous mesenchymal stem cells on cartilage and subchondral cancellous bone repair in osteoarthritis of temporomandibular joint," *International Journal of Oral and Maxillofacial Surgery*, vol. 42, no. 2, pp. 240–248, 2013.
- [50] T. C. Gamboa-Martínez, V. Luque-Guillén, C. González-García, J. L. Gómez Ribelles, and G. Gallego-Ferrer, "Crosslinked fibrin gels for tissue engineering: two approaches to improve their properties," *Journal of Biomedical Materials Research Part A*, vol. 103, no. 2, pp. 614–621, 2015.
- [51] E. G. Popa, R. L. Reis, and M. E. Gomes, "Seaweed polysaccharide-based hydrogels used for the regeneration of articular cartilage," *Critical Reviews in Biotechnology*, vol. 35, no. 3, pp. 410–424, 2015.
- [52] H. Park, D. Kim, and K. Y. Lee, "Interaction-tailored cell aggregates in alginate hydrogels for enhanced chondrogenic differentiation," *Journal of Biomedical Materials Research Part A*, vol. 105, no. 1, pp. 42–50, 2017.
- [53] F. Campos, A. B. Bonhome-Espinosa, J. Chato-Astrain et al., "Evaluation of fibrin-agarose tissue-like hydrogels biocompatibility for tissue engineering applications," *Frontiers in Bioengineering and Biotechnology*, vol. 8, p. 596, 2020.
- [54] L. Zhang, P. Su, C. Xu, J. Yang, W. Yu, and D. Huang, "Chondrogenic differentiation of human mesenchymal stem cells: a comparison between micromass and pellet culture systems," *Biotechnology Letters*, vol. 32, no. 9, pp. 1339–1346, 2010.
- [55] S. Varghese, N. S. Hwang, A. C. Canver, P. Theprungsirikul, D. W. Lin, and J. Elisseeff, "Chondroitin sulfate based niches for chondrogenic differentiation of mesenchymal stem cells," *Matrix Biology*, vol. 27, no. 1, pp. 12–21, 2008.
- [56] J. H. Lai, G. Kajiyama, R. L. Smith, W. Maloney, and F. Yang, "Stem cells catalyze cartilage formation by neonatal articular chondrocytes in 3D biomimetic hydrogels," *Scientific Reports*, vol. 3, no. 1, 2013.
- [57] A. H. Huang, M. J. Farrell, and R. L. Mauck, "Mechanics and mechanobiology of mesenchymal stem cell-based engineered cartilage," *Journal of Biomechanics*, vol. 43, no. 1, pp. 128–136, 2010.
- [58] I. L. Kim, R. L. Mauck, and J. A. Burdick, "Hydrogel design for cartilage tissue engineering: a case study with hyaluronic acid," *Biomaterials*, vol. 32, no. 34, pp. 8771–8782, 2011.
- [59] S. J. Bryant and K. S. Anseth, "Hydrogel properties influence ECM production by chondrocytes photoencapsulated in poly(ethylene glycol) hydrogels," *Journal of Biomedical Materials Research*, vol. 59, no. 1, pp. 63–72, 2002.
- [60] T. Wang, J. H. Lai, L. H. Han, X. Tong, and F. Yang, "Chondrogenic differentiation of adipose-derived stromal cells in combinatorial hydrogels containing cartilage matrix proteins with decoupled mechanical stiffness," *Tissue Engineering Part A*, vol. 20, no. 15–16, pp. 2131–2139, 2014.
- [61] M. W. Tibbitt and K. S. Anseth, "Hydrogels as extracellular matrix mimics for 3D cell culture," *Biotechnology and Bioengineering*, vol. 103, no. 4, pp. 655–663, 2009.
- [62] D. Bosnakovski, M. Mizuno, G. Kim, S. Takagi, M. Okumura, and T. Fujinaga, "Chondrogenic differentiation of bovine bone marrow mesenchymal stem cells (MSCs) in different hydrogels: influence of collagen type II extracellular matrix on MSC chondrogenesis," *Biotechnology and Bioengineering*, vol. 93, no. 6, pp. 1152–1163, 2006.
- [63] G. D. DuRaine, W. E. Brown, J. C. Hu, and K. A. Athanasiou, "Emergence of scaffold-free approaches for tissue engineering musculoskeletal cartilages," *Annals of Biomedical Engineering*, vol. 43, no. 3, pp. 543–554, 2015.
- [64] H. Rogan, F. Ilagan, and F. Yang, "Comparing single cell versus pellet encapsulation of mesenchymal stem cells in three-dimensional hydrogels for cartilage regeneration," *Tissue Engineering Part A*, vol. 25, no. 19–20, pp. 1404–1412, 2019.
- [65] R. S. Tare, D. Howard, J. C. Pound, H. I. Roach, and R. O. C. Oreffo, "Tissue engineering strategies for cartilage generation—Micromass and three dimensional cultures using human chondrocytes and a continuous cell line," *Biochemical and Biophysical Research Communications*, vol. 333, no. 2, pp. 609–621, 2005.
- [66] F. Taraballi, G. Bauza, P. McCulloch, J. Harris, and E. Tasciotti, "Concise review: biomimetic functionalization of biomaterials to stimulate the endogenous healing process of cartilage and bone tissue," *Stem Cells Translational Medicine*, vol. 6, no. 12, pp. 2186–2196, 2017.
- [67] D. Durand-Herrera, F. Campos, B. D. Jaimes-Parra et al., "Wharton's jelly-derived mesenchymal cells as a new source for the generation of microtissues for tissue engineering applications," *Histochemistry and Cell Biology*, vol. 150, no. 4, pp. 379–393, 2018.
- [68] R. T. Annamalai, D. R. Mertz, E. L. Daley, and J. P. Stegemann, "Collagen type II enhances chondrogenic differentiation in agarose-based modular microtissues," *Cytotherapy*, vol. 18, no. 2, pp. 263–277, 2016.
- [69] S. Tangtrongsup and J. D. Kisiday, "Modulating the oxidative environment during mesenchymal stem cells chondrogenesis with serum increases collagen accumulation in agarose culture," *Journal of Orthopaedic Research*, vol. 36, no. 1, pp. 506–514, 2018.
- [70] H. Mahboudi, M. Soleimani, S. E. Enderami et al., "Enhanced chondrogenesis differentiation of human induced pluripotent stem cells by MicroRNA-140 and transforming growth factor beta 3 (TGF β 3)," *Biologicals*, vol. 52, pp. 30–36, 2018.
- [71] S. Lee, K. Lee, S. H. Kim, and Y. Jung, "Enhanced cartilaginous tissue formation with a cell aggregate-fibrin-polymer scaffold complex," *Polymers*, vol. 9, no. 12, p. 348, 2017.

- [72] C. L. Nemeth, K. Janebodin, A. E. Yuan, J. E. Dennis, M. Reyes, and D. H. Kim, "Enhanced chondrogenic differentiation of dental pulp stem cells using nanopatterned PEG-GelMA-HA hydrogels," *Tissue Engineering. Part A*, vol. 20, no. 21-22, pp. 2817–2829, 2014.
- [73] H. Mahboudi, B. Kazemi, M. Soleimani et al., "Enhanced chondrogenesis of human bone marrow mesenchymal stem cell (BMSC) on nanofiber-based polyethersulfone (PES) scaffold," *Gene*, vol. 643, pp. 98–106, 2018.
- [74] T. Jiang, S. Heng, X. Huang et al., "Biomimetic poly(poly(ϵ -caprolactone)-polytetrahydrofuran urethane) based nanofibers enhanced chondrogenic differentiation and cartilage regeneration," *Journal of Biomedical Nanotechnology*, vol. 15, no. 5, pp. 1005–1017, 2019.
- [75] H. Mahboudi, F. Sadat Hosseini, M. Kehtari, H. Hassannia, S. E. Enderami, and S. Nojehdehi, "The effect of PLLA/PVA nanofibrous scaffold on the chondrogenesis of human induced pluripotent stem cells," *International Journal of Polymeric Materials and Polymeric Biomaterials*, vol. 69, no. 10, pp. 669–677, 2020.
- [76] N. Torras, M. García-Díaz, V. Fernández-Majada, and E. Martínez, "Mimicking epithelial tissues in three-dimensional cell culture models," *Frontiers in Bioengineering and Biotechnology*, vol. 6, 2018.
- [77] K. Schneeberger, B. Spee, P. Costa, N. Sachs, H. Clevers, and J. Malda, "Converging biofabrication and organoid technologies: the next frontier in hepatic and intestinal tissue engineering?," *Biofabrication*, vol. 9, no. 1, article 013001, 2017.
- [78] L. De Moor, E. Beyls, and H. Declercq, "Scaffold free microtissue formation for enhanced cartilage repair," *Annals of Biomedical Engineering*, vol. 48, no. 1, pp. 298–311, 2020.
- [79] S. Mayer-Wagner, A. Passberger, B. Sievers et al., "Effects of low frequency electromagnetic fields on the chondrogenic differentiation of human mesenchymal stem cells," *Bioelectromagnetics*, vol. 32, no. 4, pp. 283–290, 2011.

Research Article

Hydrostatic Pressure Modulates Intervertebral Disc Cell Survival and Extracellular Matrix Homeostasis via Regulating Hippo-YAP/TAZ Pathway

Yiyang Wang ^{1,2,3}, Baoshuai Bai,^{3,4,5} Yanzhu Hu ^{1,2}, Haoming Wang ^{2,6},
Ningyuan Liu ^{1,2}, Yibo Li ⁷, Pei Li ^{1,2}, Guangdong Zhou ^{3,4,5} and Qiang Zhou ^{1,2}

¹Department of Orthopedics, The Third Affiliated Hospital of Chongqing Medical University, Chongqing 401120, China

²Tissue Repairing and Biotechnology Research Center, The Third Affiliated Hospital of Chongqing Medical University, Chongqing 401120, China

³National Tissue Engineering Center of China, Shanghai 200241, China

⁴Department of Plastic and Reconstructive Surgery, Shanghai Ninth People's Hospital, Shanghai Jiaotong University School of Medicine, Shanghai Key Laboratory of Tissue Engineering, Shanghai 200011, China

⁵Research Institute of Plastic Surgery, Wei Fang Medical College, Wei Fang 261053, China

⁶Department of Orthopedics, Three Gorges Central Hospital of Chongqing University, Chongqing 404000, China

⁷Department of Orthopedics, General Hospital of Central Theater Command, Wuhan 430000, China

Correspondence should be addressed to Pei Li; lipei@hospital.cqmu.edu.cn, Guangdong Zhou; guangdongzhou@126.com, and Qiang Zhou; zhouqiang@hospital.cqmu.edu.cn

Received 19 April 2021; Accepted 5 June 2021; Published 16 June 2021

Academic Editor: Quanyi Guo

Copyright © 2021 Yiyang Wang et al. This is an open access article distributed under the Creative Commons Attribution License, which permits unrestricted use, distribution, and reproduction in any medium, provided the original work is properly cited.

Established studies proved that hydrostatic pressure had multiple effects on the biological behavior of the intervertebral disc (IVD). However, the conclusions of the previous studies were inconsistent, due to the difference in hydrostatic loading devices and observing methods used in these studies. The current study is aimed at investigating the role of dynamic hydrostatic pressure in regulating biological behavior of the notochordal nucleus pulposus (NP) and fibrocartilaginous inner annulus fibrosus (AF) and its possible mechanism using our novel self-developed hydrostatic pressure bioreactor. The differences in the biological behavior of the rabbit IVD tissues under different degree of hydrostatic pressure were evaluated via histological analysis. Results revealed that low-loading dynamic hydrostatic pressure was beneficial for cell survival and extracellular matrix (ECM) homeostasis in notochordal NP and fibrocartilaginous inner AF via upregulating N-cadherin (N-CDH) and integrin $\beta 1$. In comparison, high-magnitude dynamic hydrostatic pressure aggravated the breakdown of ECM homeostasis in NP and inner AF via enhancing the Hippo-YAP/TAZ pathway-mediated cell apoptosis. Moreover, inner AF exhibited greater tolerance to physiological medium-loading degree of hydrostatic pressure than notochordal NP. The potential mechanism was related to the differential expression of mechanosensing factors in notochordal NP and fibrocartilaginous inner AF, which affects the fate of the cells under hydrostatic pressure. Our findings may provide a better understanding of the regulatory role of hydrostatic pressure on the cellular fate commitment and matrix metabolism of the IVD and more substantial evidence for using hydrostatic pressure bioreactor in exploring the IVD degeneration mechanism as well as regeneration strategies.

1. Introduction

The intervertebral disc (IVD) consists of two compartments, nucleus pulposus (NP) and annulus fibrosus (AF) [1], which connects the adjacent bony vertebral bodies. NP tissue is a

type of gelatinous structure, containing collagen fibrils and proteoglycan molecules, primarily aggrecan [2]. NP is surrounded by AF, composed of type I and II collagen fibrils, arranged at alternating oblique angles to form concentric lamellae [3]. IVD tissue is formed by NP and AF, but they

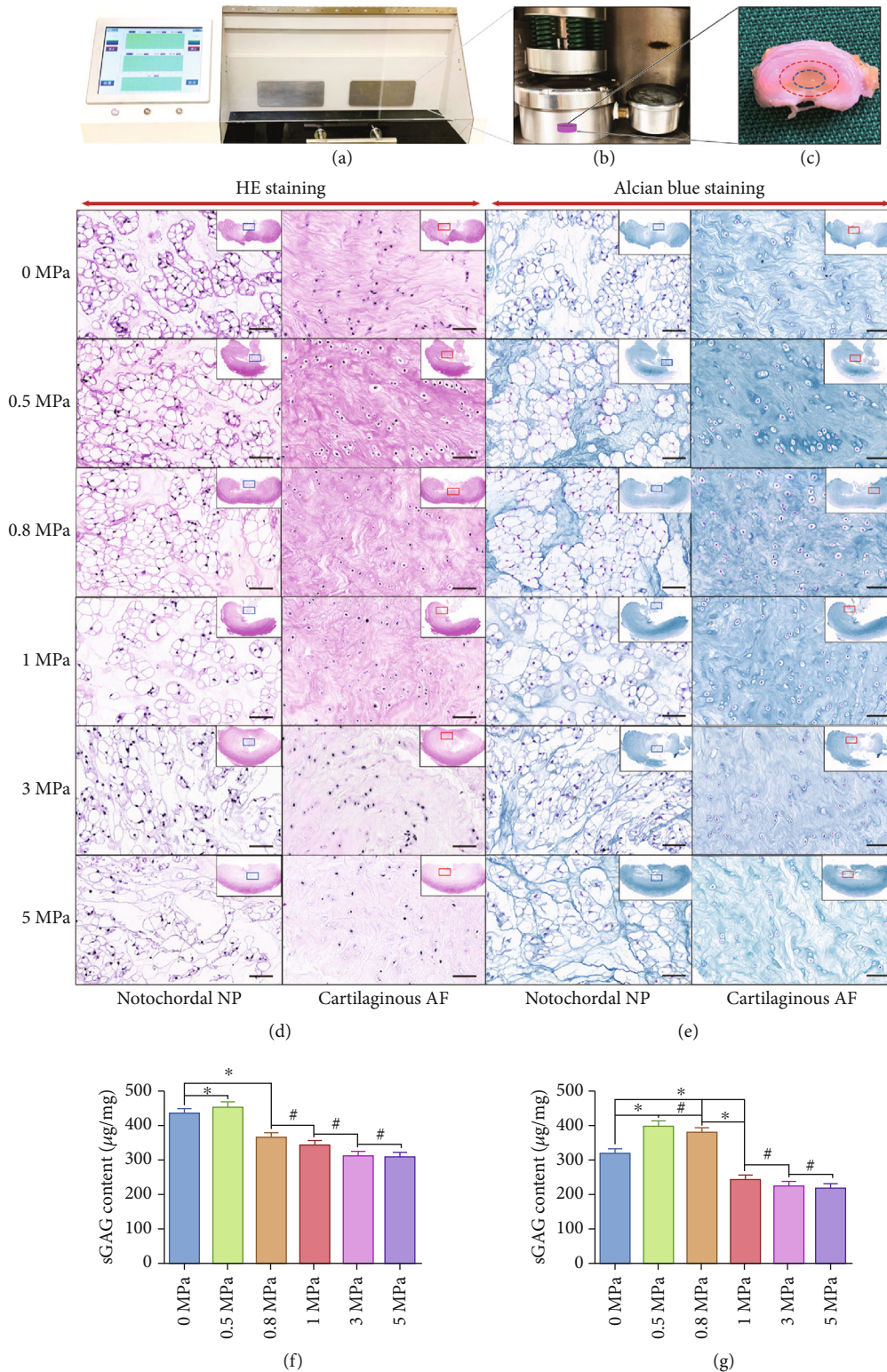


FIGURE 1: Effect of hydrostatic pressure on histomorphology and glycosaminoglycan synthesis of the rabbit notochordal NP and fibrocartilaginous inner AF: (a) appearance of the self-developed hydrostatic pressure bioreactor and touch-screen control system; (b) appearance of the tissue culture chamber of hydrostatic pressure bioreactor; (c) gross view of the endplate-removed rabbit IVD: the area in the blue circle indicates the notochordal NP, and the area between the red and blue circles indicates the fibrocartilaginous inner AF; (d) HE staining of the notochordal NP and fibrocartilaginous inner AF under graded hydrostatic pressure (200x); (e) alcian blue staining of the notochordal NP and fibrocartilaginous inner AF under graded hydrostatic pressure (200x); (f) quantification of the notochordal NP sGAG under graded hydrostatic pressure; (g) quantification of the fibrocartilaginous inner AF sGAG under graded hydrostatic pressure. * $P < 0.05$. # $P > 0.05$. Scale bar = 100 μm .

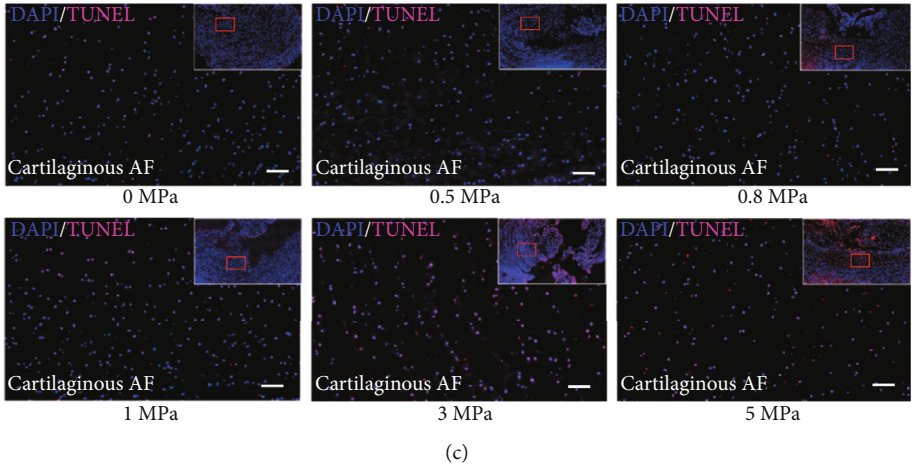
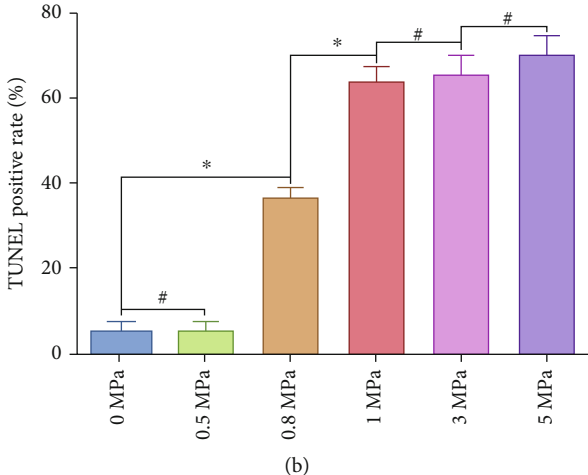
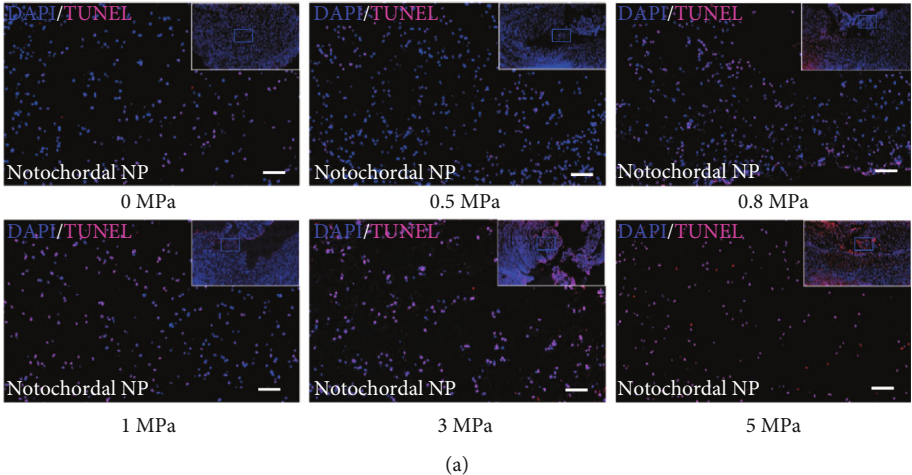


FIGURE 2: Continued.

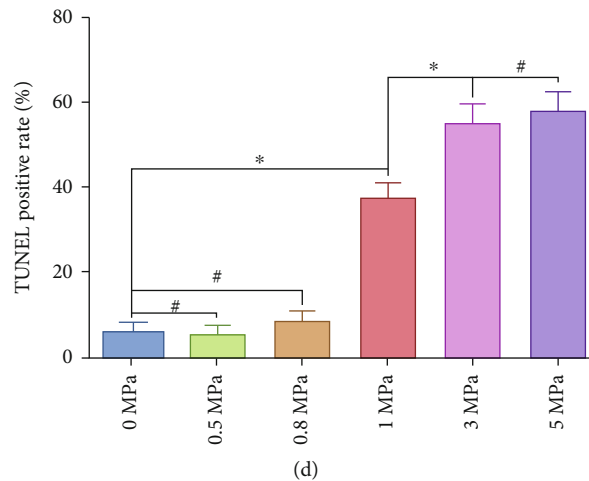


FIGURE 2: Effect of hydrostatic pressure on cellular survival of the rabbit notochordal NP and fibrocartilaginous inner AF: (a) fluorescent TUNEL staining of the notochordal NP under graded hydrostatic pressure (200x); (b) statistic analysis of TUNEL positive rate of the notochordal NP under graded hydrostatic pressure; (c) fluorescent TUNEL staining of the fibrocartilaginous inner AF under graded hydrostatic pressure (200x); (d) statistic analysis of TUNEL positive rate of the fibrocartilaginous inner AF under graded hydrostatic pressure. * $P < 0.05$. # $P > 0.05$. Scale bar = $100 \mu\text{m}$.

are derived from different embryonic structures. NP is derived from the notochord, while AF is derived from the somites [1, 4, 5]. In addition, proteoglycan molecules are more abundant in NP and inner AF than outer AF [3]. The high abundance of hydrated proteoglycan helps buffer the compressive loading of the spine and keep the collagen ultrastructure together within the tissues [6]. Thus, the cells in the NP and inner AF live in a unique microenvironment with hydrostatic pressure.

Some studies that reported the effects of hydrostatic pressure on IVD tissues or cells obtained from different species. However, the conclusions of the studies are not entirely consistent, due to the different quality of hydrostatic loading devices and observing methods used in the studies. It has been reported that the “physiological intensity (0.35–0.75 MPa)” of hydrostatic pressure acts as an anabolic factor for NP and AF cells, owing to the stimulation of proteoglycan synthesis [7–9]. In contrast, excessive pressure aggravates the catabolic metabolism of proteoglycan in NP and AF cells [7–9]. Another study reported that the proteoglycan synthesis is inhibited at 0.35 MPa compared to atmospheric pressure for both NP and AF cells harvested from the lumbar IVD tissue of dogs [10]. However, collagen synthesis is stimulated in NP cells but inhibited in AF cells [10]. The discrepancy of these experimental results may be caused by the reason that the cells used in the prior studies are cultured in dishes or alginate. The matrix stiffness, elastic modulus, and penetration of nutrients are quite different from the natural matrix of IVD [7, 8, 10]. Besides, NP tissue goes through a transition from a notochordal to a fibrocartilaginous one, which accompanies changes in cell type from notochordal to fibrochondrocyte-like cell. In humans, the transition usually is completed before twenty years old [11]. Whereas in some animals, such as rabbits or dogs, the notochordal NP is permanently preserved in some proportion [5, 12–14]. According to some studies, the response of mature nucleus

pulposus and notochordal cells to the hydrostatic pressure is quite different [15, 16]. In addition, it has been reported that hydrostatic pressure could induce the transition of notochordal NP to fibrocartilaginous NP [15–17].

Given the different cell phenotypes in IVD, the current study was conducted to demonstrate the response of notochordal NP and fibrocartilaginous inner AF to graded hydrostatic pressure. To that end, we set up a novel hydrostatic pressure tissue culturing model to investigate the different biological behavior of the two cohesive tissues in the same IVD sample. We cut off the cartilage endplates and exposed the NP and inner AF tissue of the rabbit lumbar IVD, which is a frequently used model for studying the IVD biological behavior and degeneration progress [12]. Next, the treated IVD were cultured in our newly developed hydrostatic pressure bioreactor for four weeks. Our previous study has demonstrated that the physiological degree of hydrostatic pressure could stimulate cell proliferation and ECM production of articular cartilage, which confirmed the feasibility and reliability of our hydrostatic pressure culturing system [18]. A previous study indicated that N-CDH and integrin-mediated adhesion modulated YAP-TAZ associated mechanosensing and fate commitment of cells [19]. Our previous study elucidated that N-cadherin (N-CDH) played as a protective role in NP cells against overloaded compression [20]. Additionally, some studies reported that fibronectin binding to integrin $\beta 1$ led to elevate the expression of apoptosis-related proteins [21, 22]. N-CDH and integrin-associated regulatory roles may involve histologic and biochemical alterations of disc cells induced by compression-loading stress. Hence, in the current study, we aim to figure out the differences and potential mechanism in the biological behavior of notochordal NP and fibrocartilaginous inner AF under different degree of hydrostatic pressure via investigating the histological feature, cellular survival, and ECM metabolism. The present study may

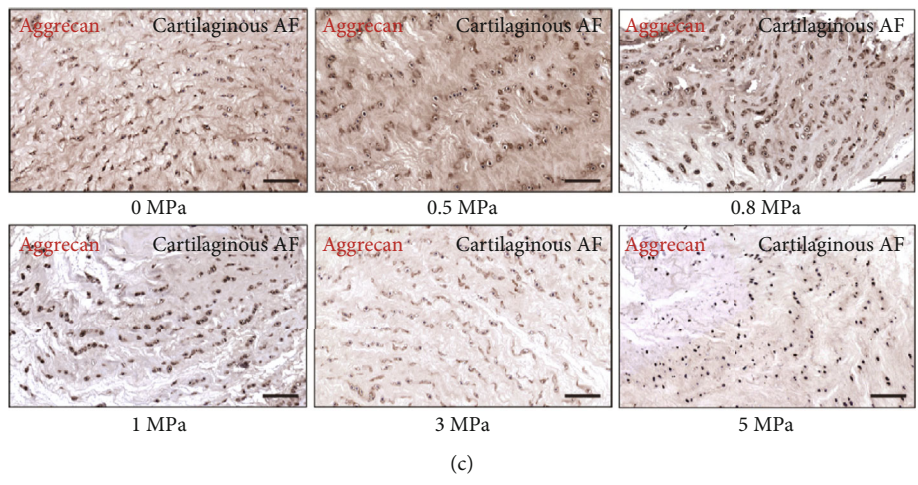
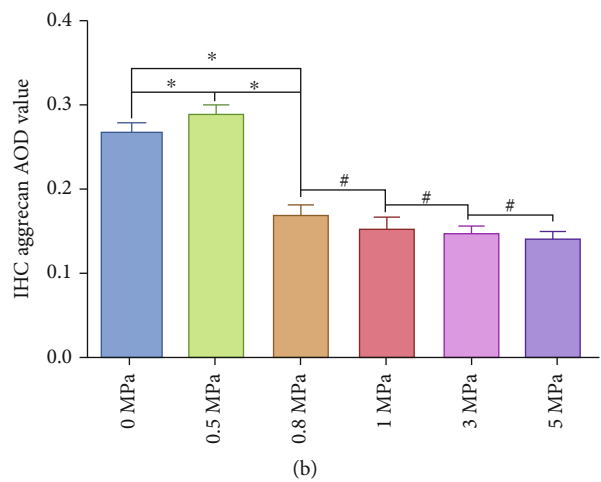
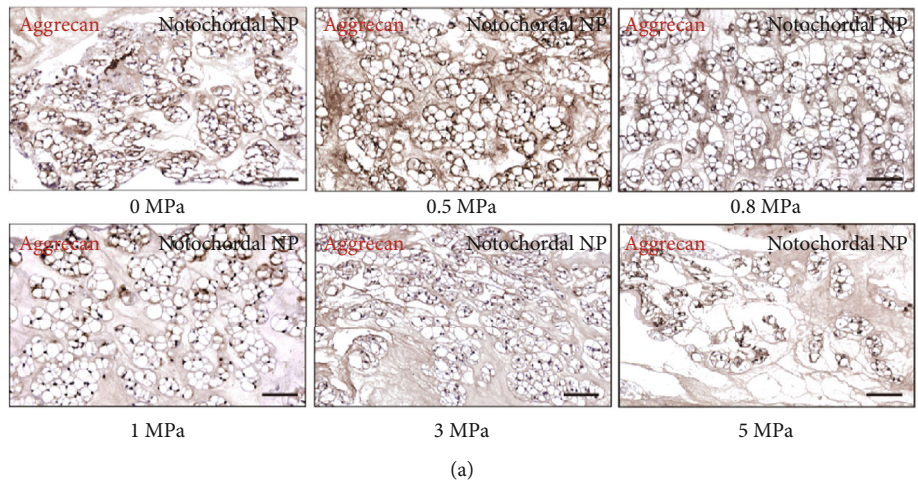


FIGURE 3: Continued.

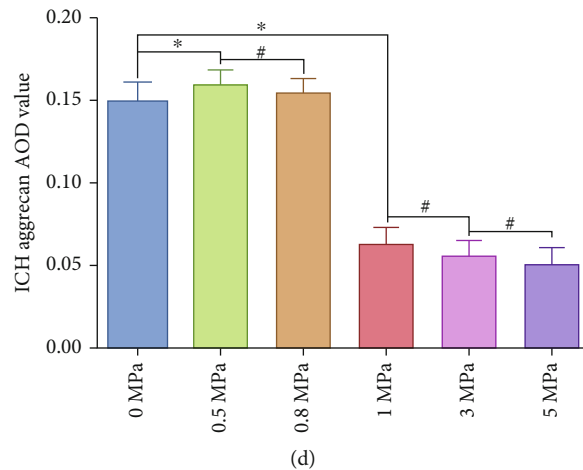


FIGURE 3: Effect of hydrostatic pressure on synthesis of aggrecan of the rabbit notochordal NP and fibrocartilaginous inner AF: (a) aggrecan IHC staining of the notochordal NP under graded hydrostatic pressure (200x); (b) statistic analysis of IHC aggrecan AOD value of the notochordal NP under graded hydrostatic pressure; (c) aggrecan IHC staining of the fibrocartilaginous inner AF under graded hydrostatic pressure (200x); (d) statistic analysis of IHC aggrecan AOD value of the fibrocartilaginous inner AF under graded hydrostatic pressure. * $P < 0.05$. # $P > 0.05$. Scale bar = 100 μm .

provide a novel hydrostatic pressure-based IVD regeneration strategy and potential regulating target to treat compressive loading-related IVD degeneration.

2. Materials and Methods

2.1. Source of Animals. Mature male New Zealand white rabbits (160-week-old, weighing 3.5-3.8 kg) were used in the current study. The lumbar spines were obtained aseptically from the rabbits after euthanasia by an excess dose of sodium pentobarbiturates.

2.2. Tissue Dissection and Culture. The spine motion segments were sharply cut at the proximal and distal vertebrae in the axial parallel plane close to the adjacent endplates and washed with phosphate-buffered saline (PBS) five times in the tissue culture dishes (Jet Biofil, China). Then, the cartilage endplates of the IVDs were sharply cut to expose the NP and inner AF tissues. After that, the treated IVDs were moved to the culture chamber of our self-developed dynamic hydrostatic loading organ culture bioreactor. The tissues were cultured in the chamber with complete culture medium (DMEM/F-12 (Gibco, USA) containing 10% fetal bovine serum (FBS, Gibco, USA) and 1% penicillin/streptomycin (Gibco, USA)) and incubated (5% carbon dioxide, 37°C) for four days before exerting hydrostatic pressure. Culturing media were replaced every four days.

2.3. Hydrostatic Pressure Exerting Protocol. During the pressure performing regime, culture chambers were transferred to our custom-made dynamic hydrostatic pressure bioreactor. We set the pressure apparatus to provide intermittent hydrostatic pressure. Briefly, every dynamic hydrostatic pressure exerting cycle contained a 30 seconds pressure exerting phase and a 30 seconds pressure releasing phase. The samples were assigned into the following groups: the control group (hydrostatic pressure = 0 MPa) and the gra-

dient dynamic hydrostatic pressure exerting groups (hydrostatic pressure = 0.5 MPa, 0.8 MPa, 1.0 MPa, 3.0 MPa, 5.0 MPa). Each group was exerted dynamic hydrostatic pressure for 2 hours per day and then transferred to the incubator (5% carbon dioxide, 37°C). The culture medium was replaced every four days. IVD specimens were collected for further experimental testing after 30 days of culture.

2.4. Histological Haematoxylin and Eosin (HE) Staining. The treated samples were harvested and fixed with 4% paraformaldehyde, embedded in paraffin, and then cut into 5 μm per section. Then, the tissue sections were stained with haematoxylin and eosin. The stained sections were observed and scanned under an optical microscope (Olympus, Japan).

2.5. Alcian Blue Staining. Alcian blue staining was used to detect the ECM glycosaminoglycan deposition. Briefly, each tissue section was incubated in the 0.2% alcian blue solution before rinsing with deionized water. Then, the stained cells were mounted and observed under an optical microscope (Olympus, Japan).

2.6. Sulfated Glycosaminoglycan (sGAG) Quantification. For quantitative analysis of ECM, the sGAG content of each group was quantified by the dimethyl methylene blue chloride (Sigma-Aldrich, USA). Total sGAG was precipitated by the 0.98 mol/L guanidinium chloride solution. After that, the optical density (OD) was detected at 595 nm. The sGAG contents were determined according to the OD value and the standard curve.

2.7. Fluorescent TdT-UTP Nick End Labeling (TUNEL) Assays. TUNEL assays were performed to detect apoptosis of target cells with the One Step TUNEL Apoptosis Assay Kit (Beyotime, China) according to the manufacturer's instructions. Tissue sections were firstly treated with Triton X-100 (0.3%) for 5 minutes at room temperature. Then, the cells were treated with TUNEL for 1 hour at 37°C at the dark.

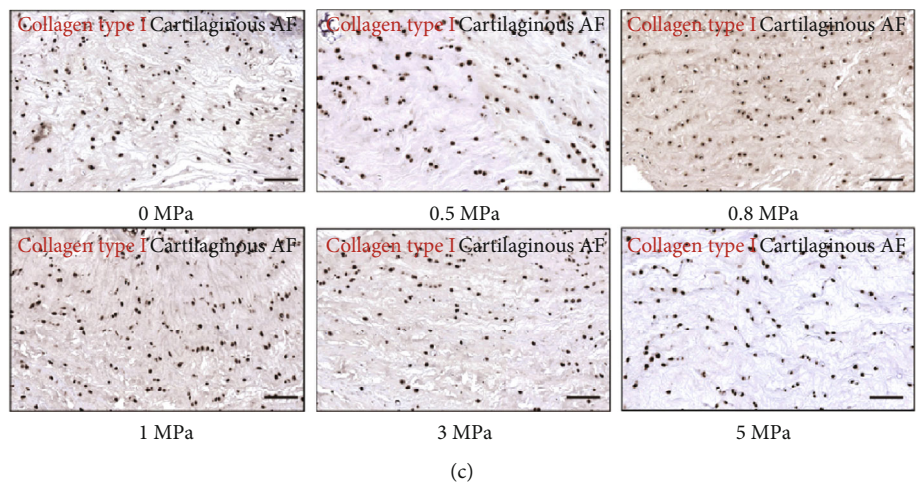
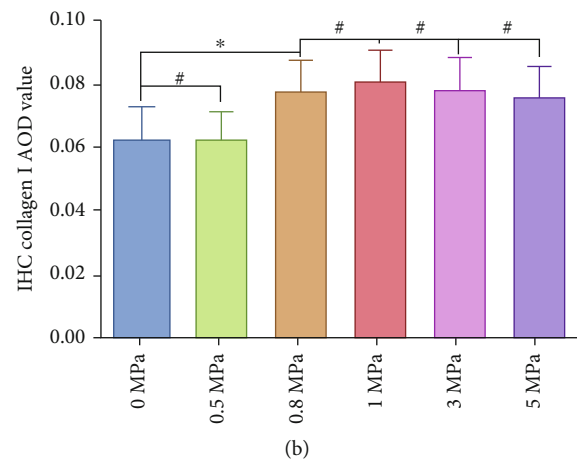
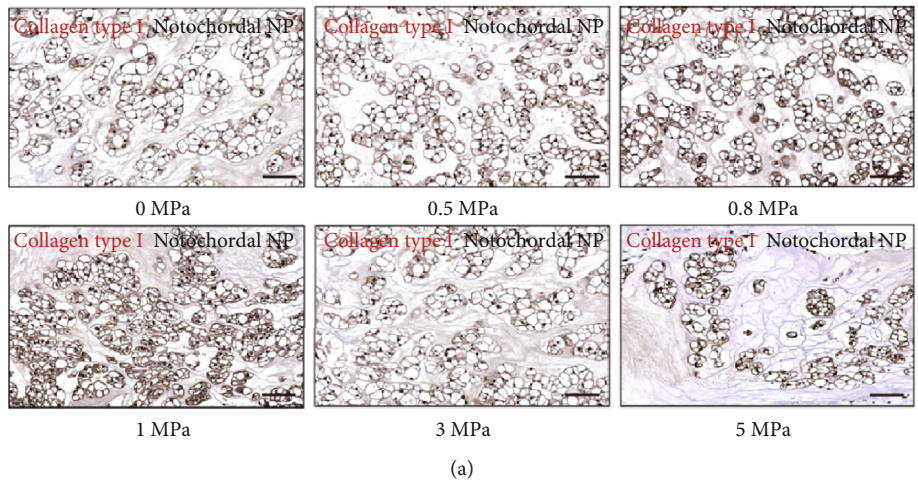


FIGURE 4: Continued.

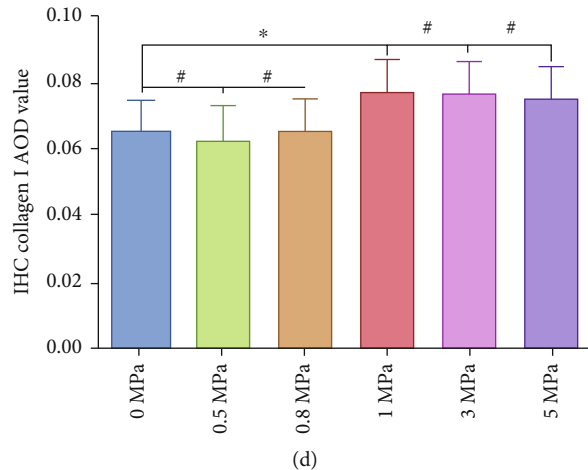


FIGURE 4: Effect of hydrostatic pressure on synthesis of collagen type I of the rabbit notochordal NP and fibrocartilaginous inner AF: (a) collagen type I IHC staining of the notochordal NP under graded hydrostatic pressure (200x); (b) statistic analysis of IHC collagen type I AOD value of the notochordal NP under graded hydrostatic pressure; (c) collagen type I IHC staining of the fibrocartilaginous inner AF under graded hydrostatic pressure (200x); (d) statistic analysis of IHC collagen type I AOD value of the fibrocartilaginous inner AF under graded hydrostatic pressure. * $P < 0.05$. # $P > 0.05$. Scale bar = 100 μm .

The sections were imaged via fluorescence microscopy (Leica, Germany) after the DAPI staining.

2.8. Immunohistochemistry (IHC). To further assess the synthesis of the ECM, IHC staining was utilized to detect the aggrecan, collagen type I and II content. After rehydration, tissue sections were blocked by goat serum, treated with hyaluronidase (0.8%) for 20 minutes at 37°C, and then incubated with aggrecan, type I and II collagen antibody (1:100, Abcam, UK) for 60 minutes. After washing in PBS, biotinylated secondary antibody (1:100, Dako, Denmark) was applied for 30 minutes, washed in PSB, and treated with avidin-biotin complex reagents. Colour was developed using 3,3-diaminobenzidine reagents (Dako, Denmark), and the sections were counterstained with Harris's haematoxylin. The average optical density (AOD) of five randomly selected visual fields (per immunohistochemical slice) under high magnification (400x) was measured using the Image-J analysis system.

2.9. Immunofluorescence Staining. After rehydration, tissue sections were blocked by goat serum, treated with hyaluronidase (0.8%) for 20 minutes at 37°C, and then incubated with N-CDH antibody, integrin β 1 antibody (1:100, Abcam, UK), and YAP-TAZ antibody (1:100, Santa Cruz, USA) overnight at 4°C. Next, after an additional wash step, the sections were incubated with the fluorescent secondary antibody (1:1000; Proteintech, China) for 2 hours at room temperature, protected from light. The sections were then stained with DAPI and imaged using fluorescence microscopy (Leica, Germany).

2.10. Tissue Protein Extraction and Western Blotting. After being ground in liquid nitrogen, the tissues were lysed with RIPA lysis buffer containing 1% PMSF (Beyotime, China) for 30 minutes at 4°C. Then, the lysates were centrifuged at 12000 \times g for 8 minutes at 4°C. The protein samples were

subjected to SDS-polyacrylamide gel electrophoresis and transferred by electroblotting to PVDF membranes. The bands were then incubated with the primary antibodies (anti-N-CDH, anti-integrin- β 1 (1:1000; Abcam, UK), anti-YAP (1:1000; Santa Cruz, USA), anti-Caspase3, and anti-GAPDH (1:500; Proteintech, China)) overnight at 4°C. After the bands were washed with TBST thrice, they were incubated with the secondary antibody for 80 minutes at room temperature. Being washed with TBST thrice, the intensity of the blots was detected by the Image Lab software (Bio-Rad, USA).

2.11. Statistical Analysis. All data were analyzed using GraphPad Prism (version 6.0, GraphPad Software, USA), and presented as mean \pm standard deviation with $n = 3$. Two-tailed Student's t -test was used to assess the statistical significance of results ($P < 0.05$).

3. Results

3.1. Effect of Hydrostatic Pressure on Histomorphology and Glycosaminoglycan Synthesis of the Rabbit Notochordal NP and Fibrocartilaginous Inner AF. According to the study's design, we need to use the IVD simultaneously contains notochordal NP and fibrocartilaginous inner AF as our researching subject. We harvested IVD from twelve mature rabbits of same age and sex, and five of the rabbits maintained entire notochordal NP with many vacuoles of various sizes. The occurrence rate of the notochordal NP in mature rabbits and its tissue gross and histological morphology was consistent with the previous studies [12, 23]. Next, the IVD tissues cohesively with notochordal NP and fibrocartilaginous inner AF were divided into six groups and cultured in chambers with different levels of hydrostatic pressure exerted by our self-developed bioreactor (Figures 1(a) and 1(b)). After 30 days in vitro culture, the histological morphology of the NP and inner AF tissue revealed evident diversity. As

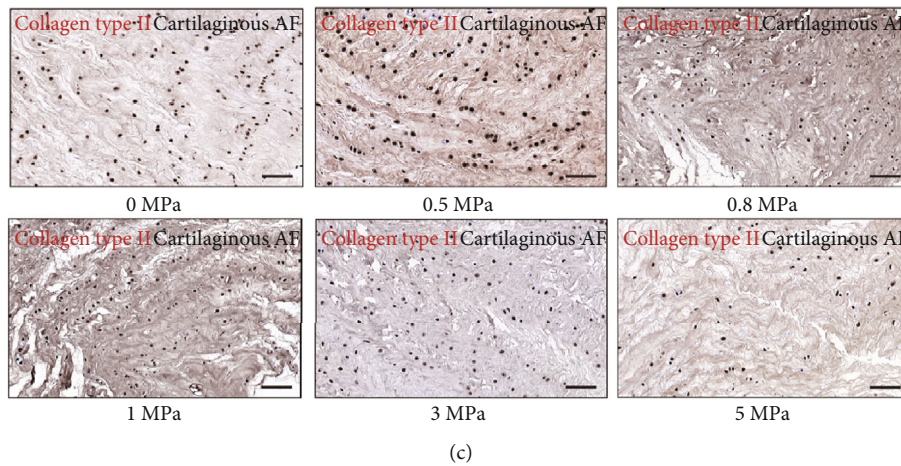
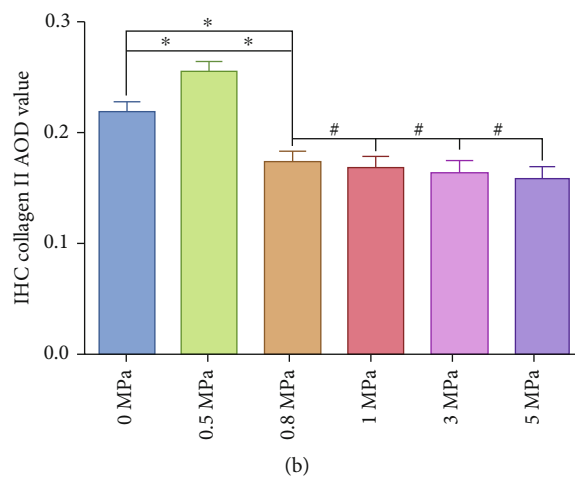
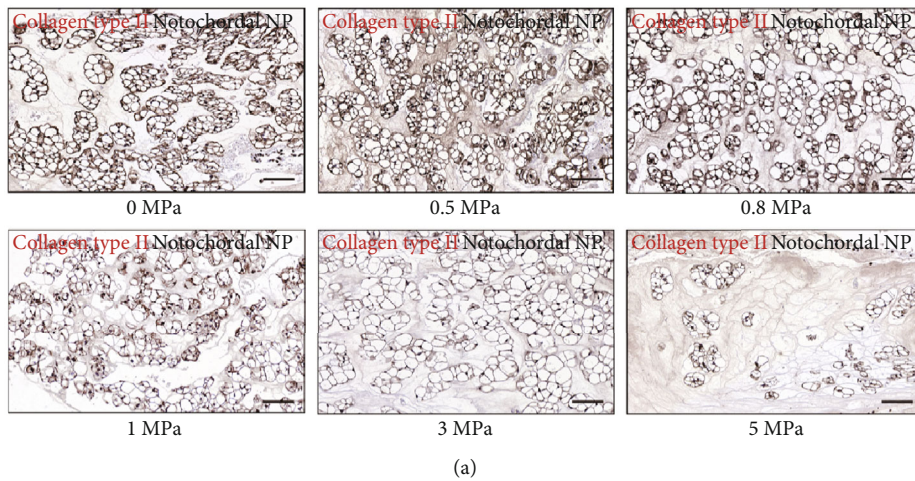


FIGURE 5: Continued.

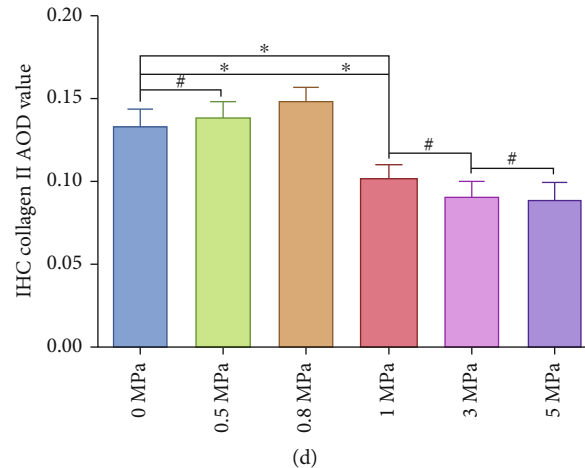
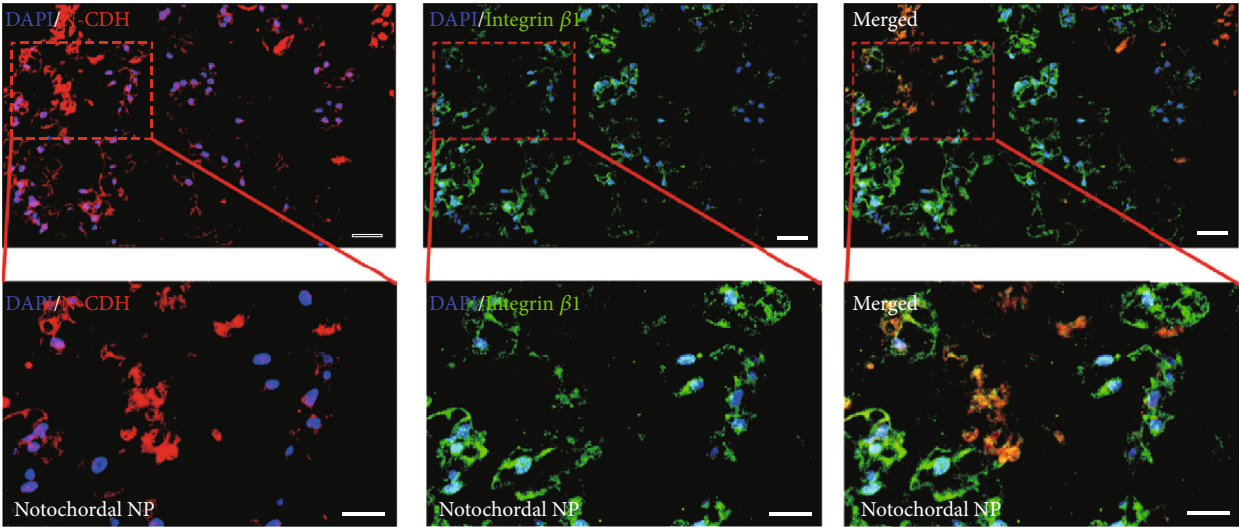


FIGURE 5: Effect of hydrostatic pressure on synthesis of collagen type II of the rabbit notochordal NP and fibrocartilaginous inner AF: (a) collagen type II IHC staining of the notochordal NP under graded hydrostatic pressure (200x); (b) statistic analysis of IHC collagen type II AOD value of the notochordal NP under graded hydrostatic pressure; (c) collagen type II IHC staining of the fibrocartilaginous inner AF under graded hydrostatic pressure (200x); (d) statistic analysis of IHC collagen type II AOD value of the fibrocartilaginous inner AF under graded hydrostatic pressure. * $P < 0.05$. # $P > 0.05$. Scale bar = 100 μm .

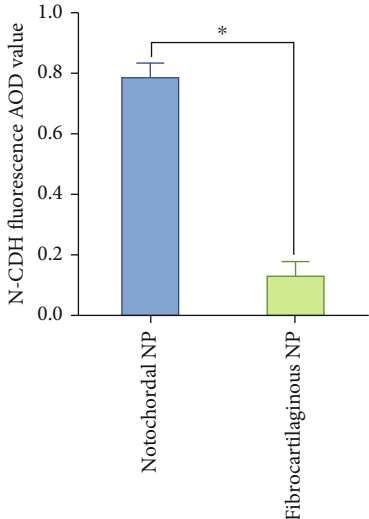
is shown in Figure 1(d), the notochordal NP appeared as a bubbled island consisted of a cell-vacuole complex in the homogeneous basophilic ECM. The inner AF exhibited a fibrocartilaginous morphology, with cells smaller in size than those of the notochordal NP tissue but larger in size and more rounded than those of the outer AF (Figure 1(d)). Moreover, HE staining results indicated that the morphology of the notochordal NP and inner AF cells was relatively normal in groups of tissues under ≤ 1.0 MPa hydrostatic pressure (Figure 1(d)). However, when the grade of hydrostatic pressure was raised to ≥ 3 MPa, the cytoplasm of the cells in NP and inner AF became shrunken, and staining of the ECM began subtly to lighten (Figure 1(d)). Alcian blue staining intensity can reflect the content of glycosaminoglycans in cartilage or cartilage-like tissue [24–26]. As is shown in Figure 1(e), both the NP and inner AF exerted 0.5 MPa hydrostatic pressure had the highest intensity of alcian blue staining. When the pressure level increased over 0.8 MPa, the staining intensity was declined gradually with the rise of pressure loading (Figure 1(e)). Additionally, quantificational sGAG assessment further proved that both the NP and inner AF under 0.5 MPa hydrostatic pressure had the highest content of sGAG (Figures 1(f) and 1(g)). When pressure level reached ≥ 0.8 MPa, the content of sGAG decreased gradually in the NP tissues (Figure 1(f)). However, 0.8 MPa hydrostatic pressure did not decline the content of sGAG compared with the group of tissue exerted 0.5 MPa hydrostatic pressure in inner AF (Figure 1(g)). The results above indicated that low-loading physiological hydrostatic pressure was beneficial for glycosaminoglycans synthesis of notochordal NP and fibrocartilaginous inner AF. However, high-magnitude hydrostatic pressure markedly attenuated the matrix sGAG synthesis in both notochordal NP and fibrocartilaginous inner AF. Noticeably, the diversity of cell morphology was more evident in NP tissues, whereas the diversity of glycosaminoglycans content was more significant in inner AF tissues under different levels of hydrostatic pressure.

3.2. Effect of Hydrostatic Pressure on Cellular Survival of the Rabbit Notochordal NP and Fibrocartilaginous Inner AF. Based on the former overall morphology analysis, we further detected the cell survival rate in notochordal NP and fibrocartilaginous inner AF tissues via fluorescent TUNEL staining. The experimental results revealed that ≥ 0.8 MPa hydrostatic pressure significantly increased the cell apoptosis rate in NP tissues (Figures 2(a) and 2(b)), while the apoptosis rate of inner AF cells was markedly aggravated when exerted ≥ 0.5 MPa hydrostatic pressure (Figures 2(c) and 2(d)). However, there was no significant difference in TUNEL positive rate between the 3.0 MPa and 5.0 MPa groups both for the NP and inner AF (Figures 2(b) and 2(d)), which indicated that 3.0 MPa was the ultimate hydrostatic pressure level for the NP and inner AF cell survival.

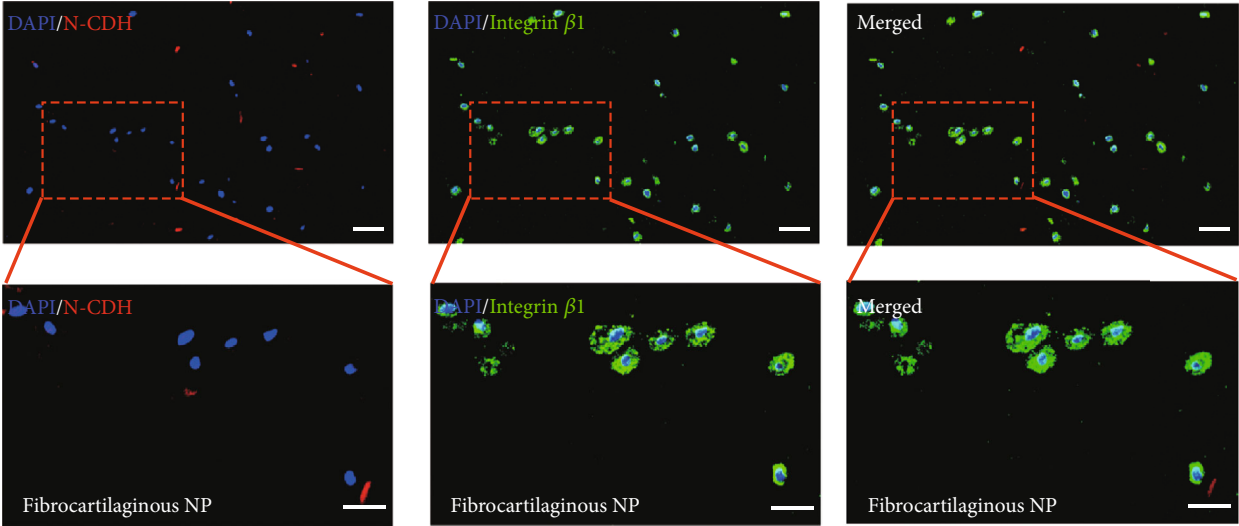
3.3. Effect of Hydrostatic Pressure on the Synthesis of Extracellular Aggrecan of the Rabbit Notochordal NP and Fibrocartilaginous Inner AF. The proteoglycan complex, predominantly aggrecan, is responsible for the hydrophilic nature of the NP, which can exert a mechanical influence upon NP cells through regulating nutrient transport, hydration, and swelling pressure [1, 27]. Additionally, inner AF represents a transitional zone and contains great amounts of aggrecan as it is subjected to compressive loads transferred from NP [1, 28]. Therefore, content of aggrecan is an important indicator to evaluate the degeneration degree of IVD. As is shown in Figure 3, both NP and inner AF under 0.5 MPa hydrostatic pressure had the highest content of matrix aggrecan. When the pressure level reached ≥ 0.8 MPa, the content of aggrecan declined gradually with the rise of pressure loading in the NP tissues (Figures 3(a) and 3(b)). However, 0.8 MPa hydrostatic pressure did not decline the synthesis of aggrecan in inner AF tissues compared with the group of tissues exerted ≤ 0.5 MPa hydrostatic pressure (Figures 3(c) and 3(d)). In contrast, the expression of aggrecan in inner AF was



(a)



(b)



(c)

FIGURE 6: Continued.

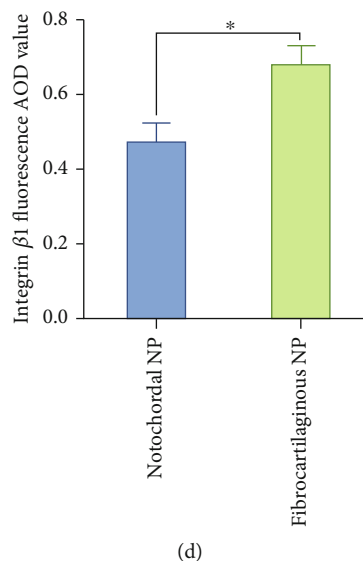


FIGURE 6: Differential expression of N-CDH and integrin $\beta 1$ in the rabbit notochordal NP and fibrocartilaginous inner AF: (a) N-CDH (red) and integrin $\beta 1$ (green) fluorescent staining of rabbit notochordal NP (200x); (b) statistic analysis of fluorescent N-CDH AOD value of the notochordal NP and fibrocartilaginous inner AF; (c) N-CDH (red) and integrin $\beta 1$ (green) fluorescent staining of rabbit fibrocartilaginous inner AF (200x); (d) statistic analysis of fluorescent integrin $\beta 1$ AOD value of the notochordal NP and fibrocartilaginous inner AF. * $P < 0.05$. Scale bar = 100 μm .

significantly attenuated when hydrostatic pressure exceeded 1.0 MPa (Figures 3(c) and 3(d)).

3.4. Effect of Hydrostatic Pressure on the Synthesis of Type I and Type II Collagen of the Rabbit Notochordal NP and Fibrocartilaginous Inner AF. Besides the abundant content of proteoglycans, the NP and inner AF also contain randomly organized collagen, mainly type II, which forms a fibril mesh-like framework to support structures [28]. However, with the development of degeneration, the IVD exhibits more characteristics of fibrous tissues and resembles ligament and tendon with large amounts of type I collagen fibrils [23, 28]. Thus, we further detected the expression level of collagen types I and II via IHC analysis. As is shown in Figure 4, the expression of matrix collagen type I was enhanced when the hydrostatic pressure reached ≥ 0.8 MPa in NP tissues (Figures 4(a) and 4(b)). In inner AF, the expression level of collagen type I was enhanced by ≥ 1.0 MPa hydrostatic pressure (Figures 4(c) and 4(d)). In contrast, the expression of collagen type II in the NP was enhanced by 0.5 MPa hydrostatic pressure but attenuated by ≥ 0.8 MPa hydrostatic pressure (Figures 5(a) and 5(b)), whereas the expression of collagen type II in the inner AF was enhanced by hydrostatic pressure ranged 0.5–0.8 MPa but attenuated by hydrostatic pressure over 1.0 MPa (Figures 5(c) and 5(d)).

3.5. Differential Expression of the N-CDH and Integrin in the Rabbit Notochordal NP and Fibrocartilaginous Inner AF. To further figure out the possible molecular mechanism causing the differential response to the hydrostatic pressure in notochordal NP and fibrocartilaginous inner AF, we detected the expression of N-CDH and integrin $\beta 1$, which are acknowledged mechanosensitive factors in IVD cells [29]. Double fluorescent label of N-CDH (red fluorescence) and

integrin $\beta 1$ (green fluorescence) indicated that the expression of N-CDH was much higher in the notochordal NP than the inner AF (Figures 6(a)–6(c)). However, the expression of integrin $\beta 1$ was relatively higher in the inner AF than the notochordal NP (Figures 6(a), 6(c), and 6(d)).

3.6. Physiological Hydrostatic Pressure Affects the IVD Cell Survival and ECM Homeostasis via YAP/TAZ Pathway. YAP and its paralogue PDZ-binding motif (TAZ) known as the regulator of IVD cell survival were related to N-CDH and integrin-mediated cell-cell and cell-matrix attachment [30]. As is shown in Figures 7(a) and 7(b), the nucleus, cytoplasm proportion of YAP/TAZ was significantly elevated in the 1.0 MPa group compared with the 0.5 MPa group. In addition, the western blots in Figures 7(c) and 7(e) revealed the differential protein expression in the notochordal NP under graded hydrostatic pressure, while the western blots in Figures 7(d) and 7(f) revealed the differential protein expression in the fibrocartilaginous inner AF under graded hydrostatic pressure. As is shown in Figures 7(c) and 7(e), the expression of N-CDH and integrin $\beta 1$ in NP was elevated under 0.5 MPa hydrostatic pressure but declined under ≥ 0.8 MPa hydrostatic pressure. The expression of YAP in the nucleus and Caspase3 was also enhanced by ≥ 0.8 MPa hydrostatic pressure in NP (Figures 7(c) and 7(e)). Correspondingly, the expression of YAP in the cytoplasm was attenuated by ≥ 0.8 MPa hydrostatic pressure in NP (Figures 7(c) and 7(e)). The blots in Figures 7(d) and 7(f) showed that the expression of N-CDH in AF declined under ≥ 0.8 MPa hydrostatic pressure. The expression of integrin $\beta 1$ was enhanced in AF under the hydrostatic pressure ranged 0.5–0.8 MPa but declined under ≥ 1 MPa hydrostatic pressure (Figures 7(d) and 7(f)). The expression of YAP in nucleus and Caspase3 was enhanced by ≥ 1.0 MPa hydrostatic

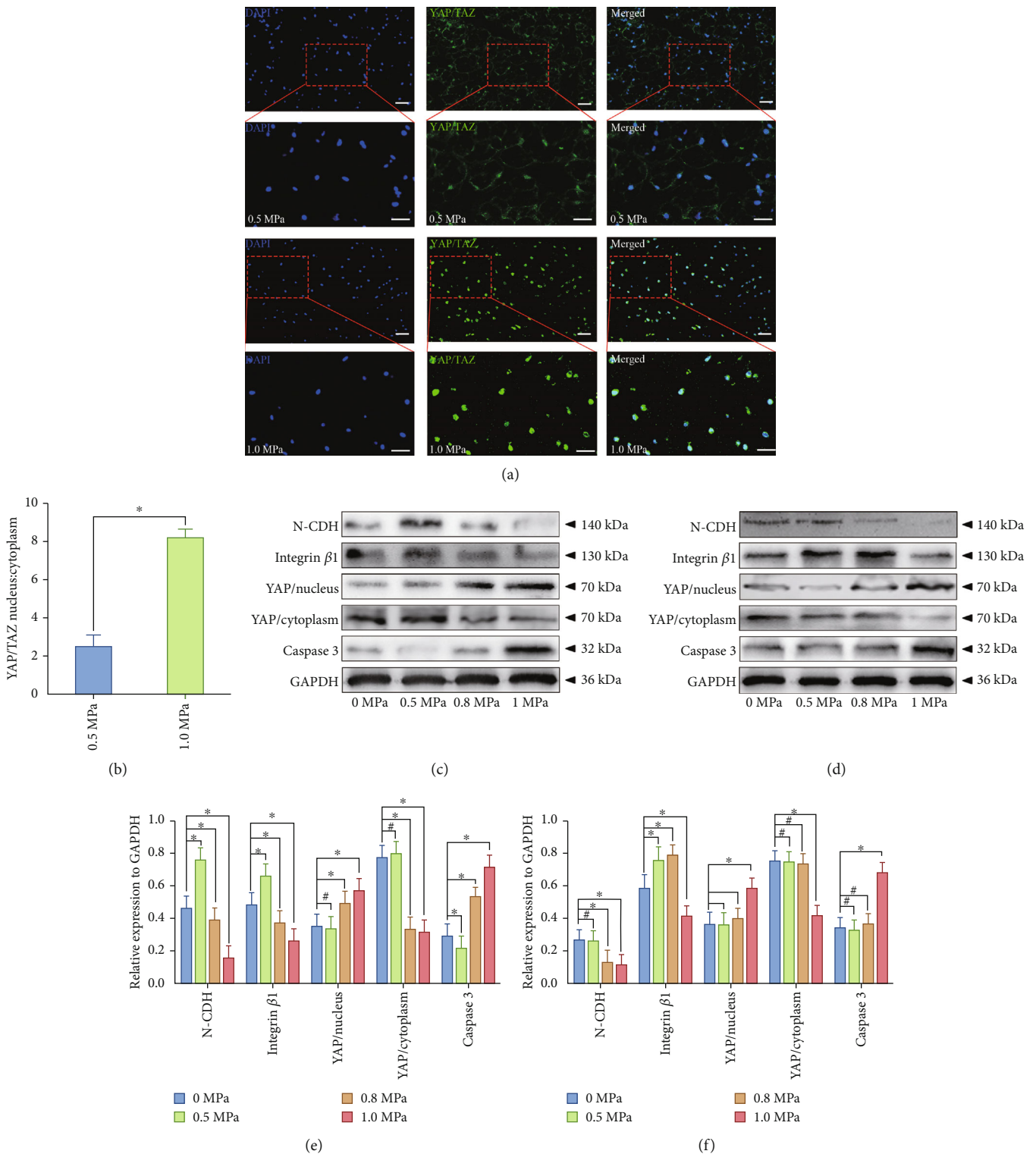


FIGURE 7: Effect of hydrostatic pressure on YAP/TAZ pathway-mediated apoptosis of the rabbit notochordal NP and fibrocartilaginous inner AF: (a) YAP/TAZ complex (green) fluorescent staining of the fibrocartilaginous inner AF under low-loading (0.5 MPa) or high-magnitude (1.0 MPa) physiological hydrostatic pressure (200x); (b) statistic analysis of YAP/TAZ complex nucleus/cytoplasm distribution; (c) western blotting analysis of the expression levels of N-CDH, integrin $\beta 1$, and YAP/TAZ-mediated apoptosis markers (YAP/nucleus, YAP/cytoplasm, Caspase3) of the notochordal NP under graded hydrostatic pressure; (d) western blotting analysis of the expression levels of N-CDH, integrin $\beta 1$, and YAP/TAZ-mediated apoptosis markers (YAP/nucleus, YAP/cytoplasm, Caspase3) of the fibrocartilaginous inner AF under graded hydrostatic pressure; (e) statistic analysis of the western blots of the notochordal NP under graded hydrostatic pressure; (f) statistic analysis of the western blots of the fibrocartilaginous inner AF under graded hydrostatic pressure. * $P < 0.05$. # $P > 0.05$. Scale bar = 100 μm .

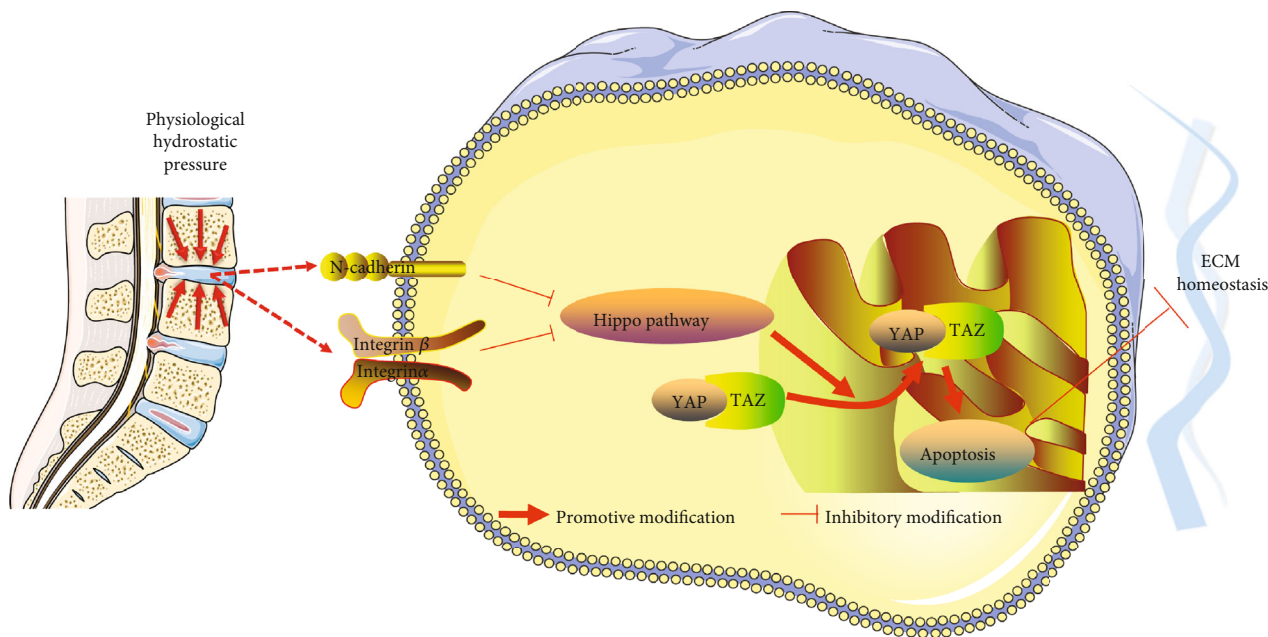


FIGURE 8: Schematic diagram shows the potential mechanism of physiological hydrostatic pressure effects the IVD cell survival and ECM homeostasis: low-loading physiological hydrostatic pressure activates mechanosensitive factors N-CDH and integrin β 1, which inhibit Hippo-YAP/TAZ pathway-mediated cell apoptosis and ECM catabolism.

pressure in AF (Figures 7(c) and 7(e)). Correspondingly, the expression of YAP in cytoplasm was attenuated by ≥ 1.0 MPa hydrostatic pressure in AF (Figures 7(c) and 7(e)).

4. Discussion

It is commonly held that the overloaded compressive force applied to the IVD is one of the causes of IVD degeneration [31, 32], whereas the proper physiological pressure is beneficial for maintaining the cell viability and ECM homeostasis of IVD [1, 2, 10]. There are still some contradictions in the prior studies about the effects of different pressure loading methods or intensities on the biological behavior of the IVD. The majority holds that the cells in NP and inner AF tissues mainly suffered hydrostatic pressure, because when a compressive force is applied to the IVD, the hydrostatic pressure within NP and inner AF is increased [9, 27]. Hence, in the present study, we used the self-developed hydrostatic pressure bioreactor based on a pressure-transmitting mode achieved by a slight deformation of a flexible membrane in a completely sealed stainless steel chamber, to imitate *in vivo* microenvironment for NP and inner AF tissues. And the tissues' responses to the graded hydrostatic pressure were observed via histological and cytologic analysis. The results of our study indicated that low-loading physiological hydrostatic pressure (0.5 MPa) was beneficial for cellular survival and ECM homeostasis both in the notochordal NP and fibrocartilaginous inner AF tissues, whereas high-magnitude dynamic hydrostatic pressure (≥ 1.0 MPa) aggravated cell apoptosis and breakdown of ECM both in the notochordal NP and fibrocartilaginous inner AF. However, there was still some diversity in the sensitivity to the hydrostatic pressure between notochordal NP and fibrocartilaginous inner AF. Specifically, the cell apoptosis rate was markedly increased

in the NP tissue suffered ≥ 0.8 MPa hydrostatic pressure. In contrast, the cell apoptosis in the inner AF tissue was significantly increased by ≥ 1.0 MPa hydrostatic pressure. Additionally, the expression of sGAG, aggrecan, and type II collagen was consistent with the trend of the cell apoptosis rate in the notochordal NP and fibrocartilaginous inner AF. Furthermore, we detected the expression of N-CDH and integrin β 1, two acknowledged mechanosensitive factors in regulating the phenotype and function of NP as well as AF cell. We found that N-CDH was expressed more prominently in NP, while integrin β 1 was expressed more prominently in AF. Our results also revealed that YAP/TAZ localization predominantly transferred to nuclear and triggered cell apoptosis via Hippo-YAP/TAZ pathway when the cells suffered high-magnitude hydrostatic pressure (0.8 MPa for NP; 1.0 MPa for AF). These results indicated that notochordal NP cells were more sensitive to the changes in pressure comparing with the fibrocartilaginous inner AF cells. The potential molecular mechanism was related to the differential expression of mechanosensitive factors and Hippo-YAP/TAZ-associated cell death.

N-CDH was a notochord-associated gene and also regarded as an NP-specific biomarker [33]. Embryonically, the NP originated from the notochord, while the AF arises from the mesenchyme [1, 34]. Thus, the expression of N-CDH was more prominent in notochordal NP. However, notochordal cells are replaced by chondrocyte-like cells of unknown provenance before skeletal maturity in humans [1, 2, 5, 34]. Some studies declared that the lack of hydrostatic pressure or overloaded pressure could induce the disappearance of notochordal cells in the NP tissue [15–17]. The physiological pressure magnitudes in IVD tissue have been estimated to be approximately 0.1 to 0.5 MPa under low-loading conditions and with values as high as 1.0 to 3.0

MPa under extreme loading conditions [35]. Our research further confirmed that the medium-loading degree of hydrostatic pressure (0.8-1.0 MPa) could even induce the degeneration of notochordal NP via attenuating the expression of N-CDH, exacerbating cell death and catabolism of ECM, especially aggrecan and type II collagen fibril. Notochordal cell was reported to have a high potential for proteoglycan production and suppressing cell apoptosis via secreting some functional factors [14, 34, 36]. This is why the time that notochordal NP began to disappear coincided with the occurrence of morphologic signs of disc degeneration [34, 36]. Thus, with the accumulation of compressive loading on the human spine, the degeneration of notochordal NP was unstoppable.

Nevertheless, we also observed that the inner AF exhibited relatively higher expression of integrin $\beta 1$ and greater tolerance to the physiological medium loading degree of hydrostatic pressure. Detailedly, the morphology of the chondrocyte-like cells and the ECM homeostasis of the inner AF under medium loading degree of hydrostatic pressure (0.8-1.0 MPa) revealed no markedly difference comparing with those cultured under atmospheric pressure. However, when the pressure level increased to the high-magnitude degree (>1.0 MPa), the cell death rate was enhanced, and the breakdown of ECM homeostasis was triggered. The characteristic phenotype of the cell in mature human NP displayed a rounded, chondrocyte-like morphology, and secreted ECM macromolecules, which more resembled the typical phenotype of the inner AF cells in nonerect walking animals, such as rabbit or dog [37]. As the human spine suffered more magnitude and frequency of axial compressive loading than the nonerect walking animals, the cell type in human IVD should be more tolerant to compression stress [6]. A previous study indicated that N-CDH and integrin-mediated adhesive interactions modulated YAP-TAZ associated mechanosensing and fate commitment of cells [19]. Noticeably, N-CDH mainly mediated softer cell-cell mechanosensing signal, while integrin-mediated stiffer cell-ECM mechanosensing signal [19]. Our research authenticated that the cell viability and ECM producing ability of the cartilaginous inner AF were superior to the notochordal NP under medium or high loading degree of hydrostatic pressure. The possible molecular mechanism was related to the high expression of integrin and attenuated YAP/TAZ-associated cell death. Although the transition from the notochordal NP to the cartilaginous one was considered as a morphologic sign of IVD degeneration, maintenance of the normal cartilaginous phenotype and matrix producing function was more meaningful for exploring human IVD regeneration strategies.

Although there are some novel findings in the present study, several limitations also exist. Firstly, the tissue samples in the present study were cultured under normoxic conditions, because of the lack of hypoxia-culture settings in our bioreactor. This condition is different from the physiological hypoxic condition in which the NP and inner AF cells live [1]. Our team has been working on updating the devices of our bioreactor and tries to imitate a more bionic microenvironment for the *in vitro* IVD tissue culture. Secondly, the pressure setting precision was relatively rough for the IVD tissue, because this generation of hydrostatic pressure biore-

actor was designed for imitating the *in vivo* condition for all musculoskeletal junctions, such as meniscus and articular cartilage. Thus, the loading device was designed to exert high-magnitude pressure (maximal value = 10 MPa) for the chamber, which limited the accuracy regulating the function of the bioreactor. We have been working on developing a low-pressure loading device with more accurate pressure setting system for NP culture and tries to figure out a more precise data about the effect of hydrostatic pressure on NP biological behavior in future studies.

To conclude, our study reveals that low-loading physiological hydrostatic pressure is beneficial for cell survival and ECM homeostasis in notochordal NP and fibrocartilaginous inner AF. Its possible mechanism is related to the upregulated protective mechanosensing factors (N-CDH and integrin $\beta 1$) under low-loading hydrostatic pressure (Figure 8), whereas high-magnitude hydrostatic pressure aggravates the breakdown of ECM homeostasis in NP and inner AF via downregulating N-CDH and integrin $\beta 1$, which attenuated the inhibitory action of YAP/TAZ-mediated cell apoptosis and ECM catabolism. Moreover, inner AF exhibits a more prominent expression of integrin $\beta 1$ and tolerance to the medium-loading degree of physiological hydrostatic pressure than the notochordal NP. This study may provide a better understanding of the regulatory role of hydrostatic pressure on the cell survival and matrix metabolism of the IVD and more substantial evidence for using hydrostatic pressure bioreactor in exploring the disc degeneration mechanism as well as regeneration strategies.

Data Availability

The data used to support the findings of this study are available from the corresponding author upon request.

Conflicts of Interest

All authors declare no competing financial interests.

Acknowledgments

We sincerely thank Dr. Yujie Hua, Dr. Erji Gao, Dr. Xintong Zhao, Dr. Zheng Ci, Dr. Tao Wang, Dr. Wei Xu, and Dr. Xiaodi Wu from the National Tissue Engineering Center of China for their generous technical assistance. This work was supported by grants from the National Key R & D Program of China (No. 2018YFC1105803); the Natural Science Foundation of China (No. 81772378, No. 81974346); the Natural Science Foundation of Chongqing, China (No. cstc2020jcyj-msxmX0148); the Basic Research and Frontier Exploration Project of Yuzhong District, Chongqing, China (No. 20200121); the Project of Innovative Science Research for Postgraduate of Chongqing Municipal Education Committee, Chongqing, China (CYB20168, CYS20226); and the Basic Research Incubation Project of the Third Affiliated Hospital of Chongqing Medical University, Chongqing, China (No. KY20077).

References

- [1] S. Williams, B. Alkhatib, and R. Serra, "Development of the axial skeleton and intervertebral disc," *Current Topics in Developmental Biology*, vol. 133, pp. 49–90, 2019.
- [2] S. Roberts, "Disc morphology in health and disease," *Biochemical Society Transactions*, vol. 30, no. 6, pp. 864–869, 2002.
- [3] L. J. Smith and N. L. Fazzalari, "The elastic fibre network of the human lumbar annulus fibrosus: architecture, mechanical function and potential role in the progression of intervertebral disc degeneration," *European Spine Journal*, vol. 18, no. 4, pp. 439–448, 2009.
- [4] B. Christ, R. Huang, and M. Scaal, "Formation and differentiation of the avian sclerotome," *Anat Embryol (Berl)*, vol. 208, no. 5, pp. 333–350, 2004.
- [5] L. Lawson and B. D. Harfe, "Notochord to nucleus pulposus transition," *Current Osteoporosis Reports*, vol. 13, no. 5, pp. 336–341, 2015.
- [6] M. T. Bayliss, B. Johnstone, and J. P. O'Brien, "1988 Volvo award in basic science. Proteoglycan synthesis in the human intervertebral disc. Variation with age, region and pathology," *Spine (Phila Pa 1976)*, vol. 13, no. 9, pp. 972–981, 1988.
- [7] M. Kasra, V. Goel, J. Martin, S. T. Wang, W. Choi, and J. Buckwalter, "Effect of dynamic hydrostatic pressure on rabbit intervertebral disc cells," *Journal of Orthopaedic Research*, vol. 21, no. 4, pp. 597–603, 2003.
- [8] C. Neidlinger-Wilke, K. Würtz, J. P. Urban et al., "Regulation of gene expression in intervertebral disc cells by low and high hydrostatic pressure," *European Spine Journal*, vol. 15, Suppl 3, pp. 372–378, 2006.
- [9] J. Zvicar and B. Obradovic, "Bioreactors with hydrostatic pressures imitating physiological environments in intervertebral discs," *Journal of Tissue Engineering and Regenerative Medicine*, vol. 12, no. 2, pp. 529–545, 2018.
- [10] W. C. Hutton, W. A. Elmer, L. M. Bryce, E. E. Kozlowska, S. D. Boden, and M. Kozlowski, "Do the intervertebral disc cells respond to different levels of hydrostatic pressure?," *Clinical Biomechanics*, vol. 16, no. 9, pp. 728–734, 2001.
- [11] J. Oda, H. Tanaka, and N. Tsuzuki, "Intervertebral disc changes with aging of human cervical vertebra. From the neonate to the eighties," *Spine*, vol. 13, no. 11, pp. 1205–1211, 1988.
- [12] K. W. Kim, T. H. Lim, J. G. Kim, S. T. Jeong, K. Masuda, and H. S. An, "The origin of chondrocytes in the nucleus pulposus and histologic findings associated with the transition of a notochordal nucleus pulposus to a fibrocartilaginous nucleus pulposus in intact rabbit intervertebral discs," *Spine (Phila Pa 1976)*, vol. 28, no. 10, pp. 982–990, 2003.
- [13] T. Hansen, L. A. Smolders, M. A. Tryfonidou et al., "The myth of fibroid degeneration in the canine intervertebral disc: a histopathological comparison of intervertebral disc degeneration in chondrodystrophic and nonchondrodystrophic dogs," *Veterinary Pathology*, vol. 54, no. 6, pp. 945–952, 2017.
- [14] R. Cappello, J. L. Bird, D. Pfeiffer, M. T. Bayliss, and J. Dudhia, "Notochordal cell produce and assemble extracellular matrix in a distinct manner, which may be responsible for the maintenance of healthy nucleus pulposus," *Spine (Phila Pa 1976)*, vol. 31, no. 8, pp. 873–882, 2006.
- [15] T. Saggese, A. Thambyah, K. Wade, and S. R. McGlashan, "Differential response of bovine mature nucleus pulposus and notochordal cells to hydrostatic pressure and glucose restriction," *Cartilage*, vol. 11, no. 2, pp. 221–233, 2020.
- [16] H. Hirata, T. Yurube, K. Kakutani et al., "A rat tail temporary static compression model reproduces different stages of intervertebral disc degeneration with decreased notochordal cell phenotype," *Journal of Orthopaedic Research*, vol. 32, no. 3, pp. 455–463, 2014.
- [17] Y. Kanda, T. Yurube, Y. Morita et al., "Delayed notochordal cell disappearance through integrin $\alpha 5 \beta 1$ mechanotransduction during ex-vivo dynamic loading-induced intervertebral disc degeneration," *Journal of Orthopaedic Research*, 2020.
- [18] J. Chen, Z. Yuan, Y. Liu et al., "Improvement of in vitro three-dimensional cartilage regeneration by a novel hydrostatic pressure bioreactor," *Stem Cells Translational Medicine*, vol. 6, no. 3, pp. 982–991, 2017.
- [19] B. D. Cosgrove, K. L. Mui, T. P. Driscoll et al., "N-cadherin adhesive interactions modulate matrix mechanosensing and fate commitment of mesenchymal stem cells," *Nature Materials*, vol. 15, no. 12, pp. 1297–1306, 2016.
- [20] P. Li, Z. Liang, G. Hou et al., "N-cadherin-mediated activation of PI3K/Akt-GSK-3 β signaling attenuates nucleus pulposus cell apoptosis under high-magnitude compression," *Cellular Physiology and Biochemistry*, vol. 44, no. 1, pp. 229–239, 2018.
- [21] T. Kurakawa, K. Kakutani, Y. Morita et al., "Functional impact of integrin $\alpha 5 \beta 1$ on the homeostasis of intervertebral discs: a study of mechanotransduction pathways using a novel dynamic loading organ culture system," *The spine journal: official journal of the North American Spine Society*, vol. 15, no. 3, pp. 417–426, 2015.
- [22] C. L. Le Maitre, J. Frain, J. Millward-Sadler, A. P. Fotheringham, A. J. Freemont, and J. A. Hoyland, "Altered integrin mechanotransduction in human nucleus pulposus cells derived from degenerated discs," *Arthritis and Rheumatism*, vol. 60, no. 2, pp. 460–469, 2009.
- [23] N. A. Scott, P. F. Harris, and K. M. Bagnall, "A morphological and histological study of the postnatal development of intervertebral discs in the lumbar spine of the rabbit," *Journal of Anatomy*, vol. 130, Part 1, pp. 75–81, 1980.
- [24] Y. Zhang, F. He, Z. Chen et al., "Melatonin modulates IL-1 β -induced extracellular matrix remodeling in human nucleus pulposus cells and attenuates rat intervertebral disc degeneration and inflammation," *Aging (Albany NY)*, vol. 11, no. 22, pp. 10499–10512, 2019.
- [25] H. Zhou, J. Shi, C. Zhang, and P. Li, "Static compression down-regulates N-cadherin expression and facilitates loss of cell phenotype of nucleus pulposus cells in a disc perfusion culture," *Bioscience Reports*, vol. 38, no. 1, 2018.
- [26] S. Chen, P. Fu, H. Wu, and M. Pei, "Meniscus, articular cartilage and nucleus pulposus: a comparative review of cartilage-like tissues in anatomy, development and function," *Cell and Tissue Research*, vol. 370, no. 1, pp. 53–70, 2017.
- [27] M. D. Humzah and R. W. Soames, "Human intervertebral disc: structure and function," *The Anatomical Record*, vol. 220, no. 4, pp. 337–356, 1988.
- [28] Z. Q. Zhang, C. S. Wang, P. Yang, and K. Z. Wang, "Mesenchymal stem cells induced by microencapsulated chondrocytes on repairing of intervertebral disc degeneration," *Orthopaedic Surgery*, vol. 10, no. 4, pp. 328–336, 2018.
- [29] B. V. Fearing, P. A. Hernandez, L. A. Setton, and N. O. Chahine, "Mechanotransduction and cell biomechanics of the intervertebral disc," *JOR Spine*, vol. 1, no. 3, p. e1026, 2018.
- [30] B. V. Fearing, L. Jing, M. N. Barcellona et al., "Mechanosensitive transcriptional coactivators MRTF-A and YAP/TAZ

- regulate nucleus pulposus cell phenotype through cell shape,” *FASEB Journal: official publication of the Federation of American Societies for Experimental Biology*, vol. 33, no. 12, pp. 14022–14035, 2019.
- [31] Y. Wang, H. Wang, Y. Zhuo et al., “SIRT1 alleviates high-magnitude compression-induced senescence in nucleus pulposus cells via PINK1-dependent mitophagy,” *Aging (Albany NY)*, vol. 12, no. 16, pp. 16126–16141, 2020.
- [32] P. Li, G. Hou, R. Zhang et al., “High-magnitude compression accelerates the premature senescence of nucleus pulposus cells via the p38 MAPK-ROS pathway,” *Arthritis Research & Therapy*, vol. 19, no. 1, p. 209, 2017.
- [33] S. Chen, Z. J. Hu, Z. J. Zhou et al., “Evaluation of 12 novel molecular markers for degenerated nucleus pulposus in a Chinese population,” *Spine*, vol. 40, no. 16, pp. 1252–1260, 2015.
- [34] T. Tsuji, K. Chiba, H. Imabayashi et al., “Age-related changes in expression of tissue inhibitor of metalloproteinases-3 associated with transition from the notochordal nucleus pulposus to the fibrocartilaginous nucleus pulposus in rabbit intervertebral disc,” *Spine (Phila Pa 1976)*, vol. 32, no. 8, pp. 849–856, 2007.
- [35] I. A. Stokes and J. C. Iatridis, “Mechanical conditions that accelerate intervertebral disc degeneration: overload versus immobilization,” *Spine (Phila Pa 1976)*, vol. 29, no. 23, pp. 2724–2732, 2004.
- [36] N. Boos, S. Weissbach, H. Rohrbach, C. Weiler, K. F. Spratt, and A. G. Nerlich, “Classification of age-related changes in lumbar intervertebral discs: 2002 Volvo Award in basic science,” *Spine (Phila Pa 1976)*, vol. 27, no. 23, pp. 2631–2644, 2002.
- [37] H. A. Horner, S. Roberts, R. C. Bielby, J. Menage, H. Evans, and J. P. Urban, “Cells from different regions of the intervertebral disc,” *Spine (Phila Pa 1976)*, vol. 27, no. 10, pp. 1018–1028, 2002.